

**Modulating Photochromism of Acylated Anthocyanins by Ultraviolet-Visible
Excitation and Acylation Patterns for the Expansion of Color Diversification**

Dissertation

Presented in Partial Fulfillment of the Requirements for the Degree Doctor of Philosophy
in the Graduate School of The Ohio State University

By

Ellia Hyeseung La

Graduate Program in Food Science and Technology

The Ohio State University

2022

Dissertation Committee

Dr. M. Monica Giusti, Advisor

Dr. Emmanuel Hatzakis

Dr. Rafael Jimenez-Flores

Dr. Luis Rodriguez-Saona

Copyrighted by
Ellia Hyeseung La
2022

Abstract

As natural colorants get more attention in the food industry, efforts on anthocyanin (ACN) stabilization and color expression have increased for their incorporation in food products. Studies show enhancement of ACN color performance and resistance to degradation by stabilizing the pigment via intramolecular copigmentation. This reaction occurs between the ACN chromophore and its covalently bound acyl group on the glycoside. In plants, most acylating groups exist in the *trans*-isomeric configuration but can undergo excitation under ultraviolet and visible light to induce the *cis*-conformation. The applied radiant energy affects the isomerization barrier, causing the molecule to adopt its excited state, and producing a molecule with different chemical characteristics. Photochromism, defined as “light-induced, reversible change in color,” is the reaction that occurs when photoisomerization of molecules lead to a change in color. Relatedly, *cis*- and *trans*-acylated ACN have been known to exhibit differences in color expression and stability, but details on the factors affecting photochromism has not been well studied. The *overall objective* of this study was to investigate the conditions that influence photochromism of acylated ACN and compare the *cis-trans* isomers’ spectroscopic characteristics, colorimetry, and stability in various pHs.

In the first objective, the effects of irradiation time and excitation energy on ACN *cis-trans* isomerization and color expression were studied. East Asian eggplants were chosen as the source of the pigment, due to their simple ACN profile that contained the *trans*-isomer necessary to induce isomerization. Delphinidin-3-(*trans-p*-coumaroyl)-rutinoside-5-glucoside, delphinidin-3-(*cis-p*-coumaroyl)-rutinoside-5-glucoside, and a semi-crude extract containing both isomers were characterized, standardized, and subjected to excitation (UV chamber at 254 nm, 365 nm, visible light with D65 lamp, and F2 lamp) for up to 20 hours. All four radiant energies induced photoisomerization of *trans-to-cis* and *cis-to-trans* photoisomerization, but to varying extents, equilibria, and under different exposure times. Visible energy induced greater *trans-to-cis* isomerization while UV induced greater of the reverse reaction. *Cis*-acylated delphinidin showed a more saturated color and stability in pH 1 compared to its *trans*-counterpart and exhibited a greener hue (h^*_{ab} 130°) in pH 8, compared to a bluer hue of the *trans*-isomer (h^*_{ab} 188°).

The second objective explored differences in photoisomerization reactivity of mono- and di-acylated ACN with varying hydroxycinnamic acylation patterns. For this objective, red cabbage was selected for its ACN profile with high abundance of varying mono- and di-acylated compounds. Three monoacylated and three diacylated derivatives of cyanidin-3-sophoroside-5-glucoside (Cy-3-soph-5-glu) with different hydroxycinnamic acids— *p*-coumaric acid (pC), ferulic acid (fer), and sinapic acid (sin)— all in the *trans*-configuration – were isolated and reconstituted in acidified methanol, then subjected with visible light (F2 lamps) for 20 hours. Pigment isomerization was monitored and quantified with

uHPLC-PDA-ESI-MS/MS. Greater extent of photoconversion was observed for mono-acylated pigments than di-acylated pigments. Cy-3-*trans-pC*-soph-5-glu produced the greatest amount of the *cis*-isomer at 53.5% total peak area under the curve (at 510 – 540 nm under LCMS), followed by Cy-3-*trans-sin*-soph-5-glu (47.1%), then Cy-3-*trans-fer-soph*-5-glu (40.0%). When comparing among the diacylated pigments, Cy-3-*trans-sin-sin-soph*-5-glu produced the greatest amount of the *cis*-conformation at 45.6% AUC, in comparison to Cy-3-*cis-sin-fer-soph*-5-glu and Cy-3-*cis-pC-sin-soph*-5-glu that produced less than 30% of the *cis*-isomer. Lastly, regioisomers of Cy showed contrasting behavior. Acylation at the C₆ glycosidic position isomerized extensively (47.1%), but not at the C₂ glycosidic position (0%).

The third objective was to evaluate the *cis*-, *trans*-, and a mixture of the two isomers' spectroscopic characteristics, color expressions, and degradation kinetics at a pH range that's relevant for the food industry. The sinapic acid family—containing Cy-3-(2''-*trans*)-*sin-soph*-5-glu, Cy-3-(6''-*trans-sin*)-*soph*-5-glu, Cy-3-(6-*trans-sin*)-(2-*trans-sin*)-*soph*-5-glu were extracted from red cabbage extract. These *trans*-acylated ACNs were irradiated to produce two mixtures of *cis-trans* acylated ACNs for both mono- and di-acylated Cy. The mixtures were further isolated to produce two *cis*-acylated ACNs: Cy-3-(6'-*cis-sin*)-*soph*-5-glu and Cy-3-(6'-*cis-sin*)-(2'-*trans-sin*)-*soph*-5-glu. Spectrophotometry and colorimetry were analyzed using UV-visible absorbance spectra and converted to CIELAB coordinates using ColorBySpectra software. Cy mono-acylated on glycosyl position C₆' had greater spectral absorbance than Cy mono-acylated on glycosyl position C₂' in pH 4

and pH 6, whereas the di-acylated Cy with acylation on both position C_{6''} and C_{2''} had greater absorbance than the two mono-acylated regioisomers in pH 4 and pH 6. In pH 2 and 8, negligible differences were observed in $\lambda_{vis-mix}$, absorbance at $\lambda_{vis-mix}$, as well as their hue and chroma. *Cis*-acylated Cy had greater spectral and colorimetric differences from their *trans*-counterpart for monoacylated pigments rather than diacylated pigments. *Cis*-monoacylated Cy had a shorter half life and greater degradation rate than its *trans*-isomer, while both isomers of the diacylated Cy degraded at comparable rates, though the *trans*-diacylated Cy was slightly more stable. Mixture of the monoacylated isomers exhibited behavior that lied between the two isomers, but the mixture of diacylated isomers did not; which suggested that isomeric configuration could make less of an impact on chemical characteristics when greater number of acylations are involved. This dissertation shows the ways in which scientists can manipulate photochromism of ACN to produce colorants with varying chemical characteristics—including color expression and stability in various pH matrices.

Dedication

This dissertation is dedicated to all the people that supported me through graduate school.

It wouldn't have been possible without you all.

Acknowledgments

First, I would like to express my gratitude to my advisor, Dr. M. Monica Giusti, for pushing my critical thinking, showing me patience, and allowing me the freedom to explore what I want, beyond anthocyanins. She made me realize the amount of work and dedication that goes into becoming as established and incredibly knowledgeable as she is in the field. To this day, she never fails to amaze me with all her talents and hobbies, even when I have been her student for over 4 years. There's always something to learn from her.

I thank Dr. Emmanuel Hatzakis, Dr. Rafael Jimenez-Flores, and Dr. Luis Rodriguez-Saona for posing the right questions for me to reflect and ponder—both in research and personal life. They offered guidance (and challenging questions, I must add!) on not only experiment design, analysis, and interpretation, but also on being an individual thinker.

In addition, I must acknowledge other teachers and collaborators that helped me in my academic career. I thank Dr. Gregory Sigurdson for teaching me the basic techniques and training me on big instruments that seemed so daunting when I was a young first year PhD student. I also thank soon-to-be Dr. Jennifer Janovick for collaborating with me on NMR elucidation of acylated cyanidins. Lastly, Dr. Kerry Ard, Dr. Shoshanah Inwood, Dr. Jeffrey Jacquet, and Dr. Linda Lobao taught me alternative ways of critically thinking

about my research that deviated from the chemical training I had been used to. I'm forever grateful to have been exposed to new theories, perspectives, analytical approaches, and thousands of papers that showed me the importance of sociological application on natural science.

Of course, I can't end acknowledgements without all my friends and family. Words cannot express the amount of support I received from my dearest friends, roommates, lab mates, department friends, therapists, and family. Thank you all for the snacks and facetime (and real time) work-alongs. Truly. Thank you all for being patient with me when I was in my PhD bubble, unable to process the outside world. It definitely took a village to get me where I am.

Vita

February 20, 1996..... Born, Seoul, South Korea

2014 – 2018..... B.S., Chemistry & Biochemistry
University of California, Santa Barbara

2018 – 2022..... Ph.D., Food Science & Technology
The Ohio State University

Publications

- Shaum, JB; Nikolaev, A; Steffences, HC; Gonzalez, L; Walker, S; Samoshin, AV; Hammersley, G; **La, EH**; Read de Alaniz, J (2022). Copper-Mediated Single Electron Approach to Indoline Amination: Scope, Mechanism, and Total Synthesis of Asperazine A. *Journal of Organic Chemistry*, 87(15): 9907-9914.
- La, EH**; Giusti, MM (2022). Ultraviolet–Visible Excitation of cis– and trans-p-Coumaric Acylated Delphinidins and Their Resulting Photochromic Characteristics. *ACS Food Science and Technology*, 2(5): 878–887.
- Rios-Villa, KA; Bhattacharya, M; **La, EH**; Barile, D; Bornhorst, GM (2020). Interactions between whey proteins and cranberry juice after thermal or non-thermal processing during in vitro gastrointestinal digestion. *Food & Function*, 11: 7661–7680.
- Selig, MJ; Celli, GB; Tan, C; **La, E**; Mills, E; Webley, AD; Padilla-Zakour, O; Abbaspourrad A (2018). High pressure processing of beet extract complexed with anionic polysaccharides enhances red color thermal stability at low pH. *Food Hydrocolloids*, 80: 292–297.

Fields of Study

Major Field: Food Science & Technology
Minor Field: Rural Sociology

Table of Contents

Abstract	ii
Dedication	vi
Acknowledgments	vii
Vita	ix
List of Tables	xiv
List of Figures	xv
Chapter 1. Introduction	1
Chapter 2. Review of Literature	5
2.1. Role of Colorants in the Food System	5
2.1.1. Synthetic Colorants	6
2.1.2. Natural Colorants	9
2.2. Acylated Anthocyanins	14
2.2.1. Anthocyanin Structure and Types of Substitutions	14
2.2.3. Hydroxycinnamic Acylations	17
2.2.4. Stability by Intramolecular Copigmentation	18
2.3. Anthocyanin Photochemistry	19
2.3.1. Flavylium Photochromism	19
2.3.2. Photoisomerization of Hydroxycinnamic Acylation in Anthocyanins	21
2.3.3. Borrowing from Organic Photochemistry – Factors Impact Photoisomerization	23
2.4. Unintended Consequences of Scientific Innovation	25
2.4.1. Actors of the Global Food System	25
2.4.2. Scientific Innovation in the Food System	26
2.4.3. Agricultural University Science and the Industry	29
2.4.4. Sociological Analyses of Notable Agricultural Innovations	31
2.4.5. Potential Methods of Comprehensive Social Impact Assessment	35

Chapter 3. Ultraviolet-Visible Excitation of <i>Cis</i> - and <i>Trans-p</i> -Coumaric Acylated Delphinidins and Their Resulting Photochromic Characteristics	38
3.1. Abstract	38
3.2. Introduction	39
3.3. Materials and Methods	42
3.3.1. Materials	42
3.3.2. Anthocyanin Extraction, Purification, and Identification	42
3.3.3. Anthocyanin Isomerization and Isolation	44
3.3.4. Monomeric Delphinidin Quantitation	45
3.3.5. Determination of Radiant Light Exposure Time: Preliminary Tests	46
3.3.6. Ultraviolet-Visible Irradiation	47
3.3.7. Visible Spectrophotometry and Colorimetry	48
3.3.8. Statistical Evaluation of Data	49
3.4. Results and Discussions	49
3.4.1. Determination of Isolate Purity	49
3.4.2. Selected Times for Radiant Light Exposure – Preliminary Tests	51
3.4.3. Monitoring Photoisomerization with UV-Vis Spectroscopy	52
3.4.4. Equilibrium of <i>Trans</i> ↔ <i>Cis</i> and <i>Cis</i> ↔ <i>Trans</i> Photoisomerization	54
3.3.5. Isomerized Extract Spectral Characteristics and Color Expression	58
3.4.6. Isomerized Extract Color Stability	63
3.5. Conclusions	64
Chapter 4. Photoisomerization Reactivity of <i>Trans</i> -Acylated Cyanidins with Varying Mono- and Di-acylation Patterns	65
4.1. Abstract	65
4.2. Introduction	66
4.3. Materials and Methods	68
4.3.1. Materials	68
4.3.2. Anthocyanin Purification and Identification	68
4.3.3. Monoacylated and Diacylated Anthocyanin Isolation	70
4.3.4. Monomeric Cyanidin Quantitation and Standardization	71
4.3.5. Photoisomerization with Visible Light	72
4.3.6. Rapid Monitoring of Cyanidin Excitation with Ultraviolet-Visible Spectrophotometry	73

4.3.7. Comparison of <i>Trans</i> -Acylated Cyanidin and Delphinidin's Isomerization Reactivity	73
4.3.8. Statistical Evaluation of Data.....	74
4.4. Results and Discussions	75
4.4.1. Acylated Cyanidin-3-sophoroside-5-glucoside Derivatives Isomerized under Fluorescent Light	75
4.4.2. Impact of Acylation Position on Photoisomerization and Photodegradation .	79
4.4.3. Ultraviolet Excitation of Peak B to Further Explore its Photoisomerization..	81
4.4.4. Comparison of Mono- and Di-acylations	84
4.5. Conclusion	90
Chapter 5. Spectral Characteristics and Color Expression of <i>Cis</i> , <i>Trans</i> , and Isomerically Equilibrated Acylated Cyanidins and Their Degradation Kinetics.....	92
5.1. Abstract.....	92
5.2. Introduction.....	93
5.3. Materials and Methods.....	94
5.3.1. Materials	94
5.3.2. Acylated <i>Trans</i> -Cyanidin Semi-Purification and Isolation.....	95
5.3.3. Acylated <i>Trans</i> -Cyanidin Characterization and Standardization	96
5.3.4. Production of <i>Cis-Trans</i> Mixtures of Mono- and Di-acylated Cyanidins	97
5.3.5. Production and Isolation of <i>Cis</i> -Acylated Cyanidins.....	98
5.3.6. Buffer and Storage Conditions for Cyanidin Degradation	98
5.3.7. Spectrophotometry and Colorimetry of Cyanidin Isomers	99
5.3.8. Calculation of Cyanidin Isomers' Half-Lives and Statistical Analysis of Data	100
5.4. Results and Discussions.....	100
5.4.1. Spectrophotometric Properties of <i>Trans</i> -Sinapic Acylated Cyanidin Isolates	103
5.4.2. Colorimetric Characteristics of <i>Trans</i> -Sinapic Acylated Cyanidin Isolates .	108
5.4.3. Analysis of <i>Trans</i> -Isolates' Color Stabilities by Degradation Kinetics and Half Lives Calculations.....	110
5.4.4. Spectrophotometric Characteristics of <i>Cis</i> -Isolate and <i>Cis-Trans</i> Equilibrated Mixtures of Sinapic Acylated Cyanidins	112
5.4.5. Colorimetric Characteristics of <i>Cis</i> -Isolate and <i>Cis-Trans</i> Equilibrated Mixtures of Sinapic Acylated Cyanidins	115

5.4.6. Degradation Kinetics and Half Lives Calculations of <i>Cis</i> -Isolates and Mixture	119
5.5. Conclusions.....	120
Chapter 6. Overall Conclusion and Future Research.....	121
Bibliography	124

List of Tables

- Table 3.1** Colorimetric analysis of semi-crude extract (SCE) after irradiation with 254 nm, D65, and F2. CIELAB values were acquired immediately after equilibration and after 24 hours of storage in the dark at 20 °C. ΔE was calculated for difference between irradiated SCE and *cis*-Dp isolate. L*: lightness; a*: red (+) to green (-); b*: yellow (+) to blue (-); c*_{ab}: chroma; h*_{ab}: hue angle..... 62
- Table 4.1** HPLC-PDA chromatogram of red cabbage extract powder semi-purified in 0.01% HCl in MeOH from which the 7 isolates of interest were purified, along with their chemical structures, abbreviated name, and % purity. 78
- Table 5.1** Composition of *trans*- and *cis* mixture in seven different cyanidins acylated with sinapic acid. % of each isomer is quantified by the area under the curve of the chromatogram monitored at absorbance of 510 – 540 nm max plot..... 102
- Table 5.2** Cyanidins *trans*- and *cis*-acylated with sinapic acid and their mixtures at absorbance values of their respective λ_{max} and the retention of the absorbance over storage in the dark at 4 °C. (n = 3, duplicate plating per replicate)
* % retention of absorbance after 42 days of storage for *cis*-acylated and *cis-trans* mixtures were not indicated in this table because it has not been 42 days since the date of initial color expression..... 106
- Table 5.3** CIELAB (Commission International de l'Eclairage and L*, a*, b*) values of *trans*- and *cis*-sinapic acylated cyanidins under pH 2, 4, 6, and 8 (n = 3, duplicate plating, 380 – 700 nm at 1 nm and 5 nm increment measurements converted to colorimetry values..... 107
- Table 5.4** Delta E of the *cis*- and *trans*-isomers of mono- and di-acylated Cy compared to each other and the isomeric mixture..... 117

List of Figures

- Figure 2.1** Anthocyanin aglycone structure with possible substitution sites and their corresponding numbers associated with the substitution position..... 14
- Figure 2.2** Energy diagram of 4',7-dihydroxy-3-methoxyflavylium at equilibrium. Excitation energy arrows are not drawn in scale. Ct represents *trans*-chalcone, Cc represents *cis*-chalcone. The figure was adopted from Gago et al., (2015)..... 19
- Figure 2.3** Potential energy diagram of photoexcited *trans*- and *cis*-alkene, which represents potential routes of excitation, conversion, and relaxation into isomerization... 22
- Figure 2.4** Categorization of consequences of innovation by intentionality, desirability, and anticipation according to Sveiby (2009), adopted from Rogers (1983) and Merton (1936).....29
- Figure 3.1** Reversible isomerization of *trans*-Dp and *cis*-Dp as a result of excitation with light. The two differing sizes of the arrows represent the favoring of the chemical equilibrium dominated by *trans*-Dp..... 41
- Figure 3.2** HPLC-PDA chromatogram of Semi-Crude Extract (SCE) from East Asian eggplants after semi-purification with a C18 cartridge. Cis- and *trans*-Dp isolates represent the PDA chromatograms of the peaks isolated from SCE. Individual peak % was calculated as % of the total area under the curve when peaks were detected at 520 nm..... 50
- Figure 3.3** Absorbance spectra of a) *cis*-Dp over time of exposure to 254 nm, and b) *trans*-Dp under the same treatment condition. Both compounds were dissolved in 0.01% HCl in MeOH..... 53
- Figure 3.4** Ultraviolet-visible energies impact on isolates' and semi-crude extract (SCE)'s photoisomerization. The time of radiant energy exposure selected for each energies were kept constant. SCE represents a mixture of 86% *trans*-Dp and 14% *cis*-Dp..... 54
- Figure 3.5** Absorbance spectra of a) *trans*-Dp and b) *cis*-Dp under pH 1-10 with corresponding color swatch indicating the two isolate's color comparison at initial (0 h) and final (after 25 h storage for pH 1, 2 and 1 h storage for pH 3—10)..... 59

Figure 3.6 Comparison between a) <i>trans</i> -Dp isolate, b) <i>cis</i> -Dp isolate, and c) SCE irradiated with 254 nm for 15 min at t = 0 (15 minutes after equilibration in pH buffers) before storage.	60
Figure 3.7 Color characteristics of semi-crude extract irradiated with a) 254 nm for 15 min (cis-Dp: 36% and trans-Dp: 64%) b) F2 lamp for 20 hrs (cis-Dp: 51% and trans-Dp: 49%), and c) D65 for 3 hrs (cis-Dp: 47% and trans-Dp: 53%). Isomerized samples were expressed in the pHs with the greatest difference from comparison of the cis- and trans-Dp—pH 1, 2, 6, 7, 8, and 9.	63
Figure 4.1 Typical HPLC chromatogram of monoacylated and diacylated pigments before and after visible light excitation and their resulting photoisomerization.....	76
Figure 4.2 Extent of photoisomerization and degradation of cyanidin-3-(2'-sinapoyl)-sophoroside-5-glucoside (Peak B) with cyanidin-3-(6'-sinapoyl)-sophoroside-5-glucoside (mono-sin). AUC stands for area under the curve under LCMS chromatogram absorbing at 510 – 540 nm. ** represents statistical significance p < 0.01.....	80
Figure 4.3 Absorbance spectra of a) <i>Cy-trans-sin</i> and b) Peak B during excitation with UV chamber at 254 nm for up to 10 h.....	81
Figure 4.4 Absorbance spectra of cyanidin-3-(6''- <i>trans</i> -sinapoyl)-sophoroside-5-glucoside (<i>Cy-trans-sin</i>) and its <i>cis</i> -isomer (<i>Cy-cis-sin</i>).....	82
Figure 4.5 Difference in acylation structure of <i>Cy-trans-sin</i> and Peak B.....	83
Figure 4.6 Extent of photoisomerization and photodegradation by comparison of acylation numbers. ** represents statistical difference at significance p < 0.01 and * at p < 0.05.....	85
Figure 4.7 Extent of photoisomerization and photodegradation as compared by the type of hydroxycinnamic acylations with <i>p</i> -coumaric (pC), ferulic (fer), and sinapic (sin) acids. ** represents statistical significance p < 0.01 and * at p < 0.05.....	87
Figure 4.8 Cyanidin (Cy) and delphinidin (Dp) under photoisomerization and photodegradation. ** represents statistical significance p < 0.01 and * at p < 0.05.....	89
Figure 5.1 Absorbance spectral measurements of cyanidin-3-(2''- <i>trans</i> -sinapoyl)-sophoroside-5-glucoside (Peak B), cyanidin-3-(6''- <i>trans</i> -sinapoyl)-sophoroside-5-glucoside (<i>Cy-trans-sin</i>), and cyanidin-(6''- <i>trans</i> -sinapoyl)-(2''- <i>trans</i> -sinapoyl)-sophoroside-5-glucoside (<i>Cy-trans-sin-sin</i>) in 0.01% HCl in H ₂ O in 380 – 700 nm range. Standardization was done at pH 1 (spectra not shown).....	103

Figure 5.2 Color swatches of cyanidin-3-(2''- *trans*-sinapoyl)-sophoroside-5-glucoside (Peak B), cyanidin-3-(6''- *trans*-sinapoyl)-sophoroside-5-glucoside (Cy-*trans*-sin), and cyanidin-(6''-*trans*-sinapoyl)-(2''-*trans*-sinapoyl)-sophoroside-5-glucoside (Cy-*trans*-sin-sin) in pH 2, 4, 6, and 8 over the course of 84 days in 4 °C storage, in the dark..... 108

Figure 5.3 Degradation kinetics of Peak B, Cy-*trans*-sin, and Cy-*trans*-sin-sin at pH 8, fitted to one phase decay indicating significance at $p < 0.05$ 110

Figure 5.4 Spectral measurements of *cis*-isolates and mixtures of *cis-trans* isomers of mono- and di-acylated Cy in 380 – 700 nm after 1 h of equilibration. Standardization was done at pH 1 (spectra not shown)..... 113

Figure 5.5 Color expression and stability of Cy-*cis*-sin, mixture of Cy-sin isomers, Cy-*cis*-sin-sin, and mixture of Cy-sin-sin isomers after 1 h of equilibration in the dark (H0) and up to 14 days of storage in 4 °C (n = 3)..... 118

Figure 5.6 Degradation of *cis*-isolate and mixtures of *cis-trans* isomers best fitted under one phase decay and line after 14 days of storage in the dark at 4 °C..... 119

Chapter 1. Introduction

Consumers use visual cues to determine the healthiness or tastiness of food (He & Giusti, 2010). Color serves as one of these visual indicators for food quality and acceptability. As consumers and the food industry's interests grow toward the use of natural colorants, anthocyanins (ACNs) have received attention for their role in replacing synthetic colorants. ACNs are great candidates as suppliers of versatile color characteristics from plant sources—such as fruits, vegetables, and in some cases, edible flowers. Under different conditions and sources, ACNs have been one of the most widely used colorants for aqueous applications. Thus, producing various shades of color is crucial and necessary for reaching the full potential of applications with ACNs.

ACNs have the potential to express a wide variety of colors—ranging from orange to blue on the color wheel (Sigurdson et al., 2017). However, their color stability is limited when compared to their synthetic dye counterparts. Researchers have used colloidal complexation or copigmentation to retain ACNs' color with a variety of biopolymers, phenolic compounds, and metals (Boulton, 2001; Cortez et al., 2017; Selig et al., 2018). Although combining these strategies can help to stabilize the product's color characteristics, the use of colloids or copigments may alter the solubility of the matrix or

the flavor of the product (Carocho et al., 2014). Therefore, stabilization of ACN via chemical structural manipulation is a novel and promising strategy.

With over 700 molecular structures, ACNs can vary by the type of glycosylation, methoxylation, hydroxylation, and acylation patterns (Wallace & Giusti, 2015). In general, greater attachments of acylation on the aglycone backbone has been associated with greater pigment stability and color expression. More specifically, among ACN derivatives, molecules acylated with hydroxycinnamic acids have higher color stability in comparison to molecules without acylation (Giusti & Wrolstad, 2003). Both aliphatic and aromatic acids have been known to attach to the glycoside at the C_{6''} position, although C_{2''}, C_{3''}, and C_{4''} positions are also possible (Bakowska-Barczak, 2005). Within these glycosyl acyl positions, the acylation can exist as either a *cis*-isomer or a *trans*-isomer. Studies have shown that *cis*-acylated pigments exhibit increased color strength and stability than their *trans*-counterparts. Unfortunately, *trans*-isomers are highly prevalent in nature, but the exact reasoning for this occurrence is unknown (Sigurdson et al., 2018). Production of the rare *cis*-isomers have been possible by irradiation with UV light, but research has been limited to delphinidins in pH buffers, solvents, and under 365 nm tungsten lamp (Yoshida et al., 1990, 2002). Thus, there is much more to be explored with isomerization of ACN hydroxycinnamic acids, considering that there are myriads of ACNs with conjugated double bonds in their acylated glycosides and even more factors to uncover when the direction of this reversible reaction is accounted for.

Photoisomerization, or inducing isomerization by light irradiation, has been long-discussed and well-researched in the field of photophysics and photochemistry (Liu et al., 2018; Waldeck, 1991). However, its application in food science is sparsely seen. Thermodynamic and kinetic calculations of *cis-trans* isomerization of acylated ACN and their impact on color stability and characteristics have been studied by George et al. (2001) and Sigurdson et al. (2018). Additionally, theoretical framework of isomerization on ACN have been studied in flavylium cation's (ACN aglycone) energy diagram under their pH-dependent multistate and their related energy barriers (Basílio & Pina, 2016). However, the isomerization from *cis*-chalcone to *trans*-chalcone cannot be equated to isomerization of hydroxycinnamic acids attached to a glycoside moiety on the aglycone. In addition, the occurrence of color change via photoisomerization is known, but the factors that contribute to this reaction are under-studied.

The findings from the **first research chapter** of this dissertation addressed the reversibility of *cis-trans* isomerization reaction and related the photoreactants' reactivity with the excitation energy necessary to reach the photostationary equilibria. Industry-accessible light sources were used to determine the photostationary equilibria associated with the excitation energy, along with the duration of exposure necessary to reach the photostationary state. Often, experimental conditions used in photoisomerization involve light sources that are expensive and often limited to academic or research institutions, such as tunable UV lasers. Thus, the efficacy of broad spectrum under accessible light chambers were important to determine.

The **second research chapter** of this dissertation work addressed the effect of acylation patterns (type, number, and position) on ACN photoisomerization reactivity. The position of these acyl group attachment has been shown to play a role in colorimetric characteristics, but research has seldom related the complexities of hydroxycinnamic acylation on photoisomerization (Ahmadiani et al., 2016). To understand variability in chemical characteristics such as color, it is crucial to relate it back to the chemical structure of a pigment, along with its respective chemical reactivity and trends in behavior.

In the **third research chapter**, *cis*, *trans*, and a mixture of the two isomers' color characteristics in food-relevant pHs and their degradation kinetics were modeled. The isomeric comparisons were made for both mono- and di-acylated ACN, which added on an additional factor of complexity. The differences in *cis-trans* isomers' color expression have been mostly discussed in the literature for delphinidins mono-acylated with *p*-coumaroyl units (Sigurdson et al., 2018). The findings of this chapter added onto the growing body of literature of ACN color expression, by comparison isomeric color expressions for both mono- and di-acylated cyanidins.

Chapter 2. Review of Literature

2.1. Role of Colorants in the Food System

Colorants are an integral part of product identification, consumer acceptability, and judgment of quality. Due to its wide versatility, colorants are globally used in the textile, food, paper, cosmetic, and pharmaceutical industries, including the United States (Marmion, 1991). Historically, colorants were derived from sources found in nature—minerals, flowers, vegetables, and animals. However, as technology advanced, industries started using synthetic colorants due to their affordability and reproducibility. Furthermore, artificial dyes can be mass produced with starting materials that cost less than the sources that are required for extracting colorants from plant materials. To add on even more, artificial colorants last longer than natural colorants, because they are synthesized with yield and purity that has been optimized since the 1800s (Mulliken, 1916). Despite these favorable characteristics, artificial dyes are slowly losing their status in industries as their consumer perception becomes increasingly negative. Markets are regulated by consumer behaviors—thus, industries are shifting gears to welcome more natural colorants.

2.1.1. Synthetic Colorants

According to the Code of Federal Regulations (21 CFR §74), there are 7 synthetic color additives that are approved for usage in food (Burdock, 1997). They are: **1.** FD&C Blue No. 1; **2.** FD&C Blue No. 2; **3.** FD&C Green No.3; **4.** FD&C Red No. 3; **5.** FD&C Red No. 40; **6.** FD&C Yellow No. 5; **7.** FD&C Yellow No. 6. These colorants must be certified by the batches produced, to ensure that minimal impurities are present and that all synthesized compounds meet the regulations. Many food companies use combinations of these 7 synthetic additives for products such as confectionaries and beverages, due to their accessibility, economic feasibility, as well as pigment stability.

The Code of Federal Regulations exist to ensure that artificial colorants are safe to eat. The U.S. Food and Drug Administration conducts short and long-term effects of consumption, compositional analyses, and other plethora of analytical methods to ensure that they are safely applied to foods (U.S. Food & Drug Administration, 1977). However, consumers have been driving the market to explore the use of colorants derived from nature in the recent years, and the following sections will discuss some of the reasons facilitating this trend (Wrolstad & Culver, 2012).

2.1.1.1. Potential Concerns on Environmental Impact

The extensive use of synthetic colorants involves production of effluents that have detrimental environmental impacts. For example, the wastewater from the textile industry has been demonstrated to generate the most amount of pollution due to the chemical

stability of recalcitrant organic pollutants, surfactants, and chlorinated compounds that sustain in the environment (Bharagava et al., 2018; K. A. Mansour et al., 2021). Once the synthetic dyes elute into the water streams, it can affect the aquatic plant's photosynthesis and transmit carcinogens to the aquatic life (Weisburger, 2002). Specifically, azo-dyes—one of the most commonly found compounds in dyestuffs—are known to induce high carcinogenic risk in animal studies (Anliker, 1979). Azo dye toxicity arises after the cleavage of the aromatic amines, resulting in a reactive species that can induce carcinogenicity. This process is catalyzed by anaerobic bacteria or oxidation, which are highly likely to be found nature (Brown et al., 1993). Once released, the chances of the proliferation of these toxins are guaranteed, since approximately 10 to 15% of dyes used by varying industries end up in the environment (de Campos Ventura-Camargo & Marin-Maroles, 2013; O'neill et al., 1999) In some cases, research has shown anaerobic, aerobic, and bio-degradative processes that are effective in removing toxins from synthetic dyes, before elution into the environment (H. ben Mansour et al., 2012; Robinson et al., 2001). However, these methods are retroactive, rather than preventative, which means that the toxins have already been produced. In addition, the toxins in synthetic colorants may be removed from the physical environment, but it is unclear what kind of long-term consequences could arise from their production.

2.1.1.2. Effect on People's Health

Artificial dyes could also impart some adverse health effects on select group of people, especially those with sensitivities to these compounds or children who are prone to

hyperactivity (McCann et al., 2007). Consumption of synthetic colorants, such as tartrazine, Pigment Yellow 83, and Allura Red AC has been assigned specific doses of accepted daily intakes (ADI) that could lead to intoxication upon a certain amount of consumption. For example, tartrazine has been known to damage human lymphocytes at high concentrations, resulting in carcinogenetic effects (Amchova et al., 2015). Undoubtedly, since these health concerns occur at high concentrations, the toxic potentials of synthetic dyes are not always observed from moderate food ingestion. Thus, they are deemed safe for consumption under the Federal Food, Drug, and Cosmetic Act by the U.S. Food and Drug Administration; however, it is worth noting that scientific policies depend on the current knowledge, priority of issue, and ever evolving scientific findings. For example, Coca Cola contained coke in its beverages and it was consumed by the public until 1906, when the Pure Food Act was passed. It is also important to be aware of the industries that fund these scientific studies, as well as the leadership in charge of regulatory agencies. Lastly, toxins have the ability to bioaccumulate. Although both hydrophilic and lipophilic colorants have been known to be unlikely in undergoing bioaccumulation, there was only one study conducted, and its model system was fish—which are anatomically dissimilar to the human body (Anliker et al., 1988).

Synthetic dyestuffs have been known to have adverse effect on children (Amchova et al., 2015; Wiles et al., 2009). Aforementioned artificial colorants – tartrazine and Allura Red AC are two colorants out of six that have been closely associated with hyperactivity in children. Due to the prevalence of synthetic dyes in beverages and sweets that are high in

sugar, children are more susceptible to consuming these foods, since their bright colors are attractive and the sugar content often in these confectionaries are addictive. Furthermore, since artificial colorants are economical for food industries to produce, these chemical compounds will be found in cheaper foods, often more unhealthy and often highly processed. Thus, populations of lower socioeconomic class, especially the children within this population are the most impacted. “Junk-food” are foods with low nutritional value with high amounts of sugar, sodium, and calories, but low in fiber, protein, and other nutrients. These foods have also been known to have behavioral effects on people besides hyperactivity; lack of essential nutrients and consumption of junk-food has been associated with violent tendencies amongst high school students (Gesch et al., 2002). Violent tendencies can lead to aggression and crime, as well as an impairment to children’s academic success due to a detriment on health effects (Rasberry et al., 2015).

2.1.2. Natural Colorants

One way to combat the adverse effects of synthetic colorants is replacing them with natural colorants, but this comes with its own set of challenges. Dyes sourced from nature are not naturally shelf stable, due to their chemical instability. Amongst these natural pigments, anthocyanins have one of the widest ranges of color expression. In order to preserve chemically unstable compounds such as anthocyanins, numerous chemical and physical approaches can be used. Often, researchers use methods of colloidal complexation, copigmentation, or processing techniques to retain the vibrant color expression of the pigment (Selig et al., 2018). However, chemical processes such as colloidal complexation

and copigmentation requires the addition of compounds that could alter the solubility of the matrix, thereby altering the flavor and texture of the final product. Physical processing methods encompass both thermal and non-thermal techniques. Thermal pasteurization is the conventional method of preserving the quality of fruits and vegetables, such as canned fruits. However, thermal pasteurization leads to nutritional loss due to the denaturation of active enzymes, as well as color discoloration. Thus, non-thermal processing techniques such as high pressure processing has been used to stabilize nature-derived colorants, without affecting the color, nutrition, and flavor of the final product (Bogahawaththa et al., 2018). The drawback to high pressure processing is that it is an expensive equipment and it can only be used for food matrices with ample amount of free water (Muntean et al., 2016). Thus, stabilization of anthocyanins via structural method is essential, since it is non-destructive and perhaps more economical in that additional compounds are not necessary.

As expected, no single system is completely devoid of potential harm. As the development in scientific manufacturing currently stands, it is difficult to use natural colorants at the same scale and rate as artificial colorants. The process of extraction, purification, and application in food-safe medium is still an underdeveloped area. In addition, the additional costs that companies use to develop natural colorant alternatives may not even provide the exact shade they desire. Furthermore, even when initial color shade is achieved, their stability to light, water, and other atmospheric conditions are low. With that said, research in natural colorants still expanding because of the benefits that outweigh these challenges. The following sections will discuss the strengths of natural colorants.

2.1.2.1. Nutritional Benefits

In comparison to all the aforementioned potential adverse effects of synthetic colorants, anthocyanins provide health benefits that can be applied to food deserts. Food deserts are areas with limited accessibility to nutritive whole foods that also meet cultural needs (Gottlieb, 2009). Food accessibility is not only dependent on socioeconomical factors, but also on physical access to infrastructure that incorporates culturally-acceptable nutrition (Hamm & Bellows, 2003). Geographical environment has an impact on both economical and physical accessibility, as well as race, as race is often related to residential neighborhoods (Taylor & Ard, 2015b). In modern day U.S., residential segregation is observed via urban housing market discrimination, which causes spatial discrepancy in access to nutritive food (Massey, 2001). Low-income families have less exposure to grocery stores and more exposure to fast food stores, gas stations, and liquor stores (Taylor & Ard, 2015a). Studies have shown that socioeconomic class is a strong contributor to behavioral choices regarding health such as chronic illnesses and exposure to toxicity (E. Chen, 2004; E. Chen et al., 2002; Hasselberg et al., 2005; Koster et al., 2005; Starfield & Shi, 2002). Adolescents in lower socioeconomic class has been known to have diets of high-fat intake and show more frequent signs of obesity, in comparison to the affluent group (O’Dea & Caputi, 2001; Wardle et al., 2003). Specifically, people of color face the brunt of this detriment, because they often live in areas of geographical and economical disadvantage (Adelman, 2004; Pulido, 2015). This is supported by the fact that even within the same socioeconomic class, Africa American families are 1.1 mi farther away from access to fresh produce in comparison to White families in Detroit, Michigan (Taylor &

Ard, 2015b). As a model system for neighborhoods without food access, Detroit displays the relationship between racial inequalities and food apartheid—which can also be observed in other U.S. metropolitan cities (Block et al., 2004). Synthetic food dyes are prevalent in confectionaries, jams, beverages, just to name a few (Marmion, 1991). Since these colorants are more likely to be found in so-called “junk foods,” the low-income population will have more opportunities to interact with these compounds, since gas stations and convenience stores are more common in their neighborhoods. Unlike these artificial dyes, dietary anthocyanins contain polyphenolic compounds, which have antioxidative properties, with their consumption associated with reduction in the risk of cardiovascular disease, neuronal disease, inflammation, cancer, and diabetes (Fan et al., 2012; He & Giusti, 2010; Khoo et al., 2017; Saluk et al., 2012; Yousuf et al., 2016).

Another barrier to addressing food insecurity is the uptake of innovative technology by businesses. Since businesses’ main goal is to make profit, employing novel scientific findings can seem costly and unpredictable. However, that is where all scientific findings start—from uncertainty and skepticism. Even innovations such as light bulbs and computers had their fair share of trial and error. Technology can become economical as more people become aware of its possibility. This applies to stabilization efforts to natural colorants as well, as evident in numerous industries’ collaboration with food science departments across United States.

2.1.2.2. Usage of Food Waste

Food insecurity is not the only problem regarding the food system—food waste is also a global problem. Depending on the region, food waste problems can occur in varying areas of the supply chain: food production, post-harvest handling/storage, processing/packaging, distribution, and consumption. This is also attributed to whether the country is developing, intermediate, or developed. In the developed world, food waste is produced at the retail level, in which the consumers play a significant role in the issue (Thyberg & Tonjes, 2016). On the other hand, in developing countries, the problem is mostly attributed to food loss during post-harvest processes, due to the lack of preservation technology that is culturally and economically reasonable (Goletti & Wolff, 2000; Hodges et al., 2011). Food loss can occur due to over-stocking of grocery stores or due to the deformity of the product. Anthocyanins can address food waste at the post-harvest stage, whilst acting as a delivery mechanism of beneficial nutrients. The pigment can be extracted from unused produce items that cannot be sold at the grocery store. Under the Bill Emerson Good Samaritan Food Donation Act, food can be donated in “good faith” to non-profit organizations. Thus, sourcing the starting material for anthocyanins would be cost effective as well. Though, making this ideation into reality requires more practicality, since processing of colorants from food waste materials in grocery stores or farmers would be difficult on a large scale. At the research & development stage in academia, it may be doable, but scaling up would require more logistical planning, organizing, and implementing.

2.2. Acylated Anthocyanins

2.2.1. Anthocyanin Structure and Types of Substitutions

Anthocyanins (ACNs) are dietary flavonoids found in sources derived from nature, such as leaves, flowers, and vegetables. The structure of anthocyanins (ACNs) is built on their aglycones, called anthocyanidins. There are 6 types of anthocyanidins that are classified based on their hydroxy or methoxy substitutions (or the lack of) in the B ring of the chromophore (Fig 2.1). These 6 anthocyanidins are: cyanidin (Cy), delphinidin (Dp), peonidin (Pd), petunidin (Pt), malvidin (Mv), and pelargonidin (Pg) that range from visible colors of magenta, red, and purple, represented by a visible-max ranging in 470 – 550 nm (He & Giusti, 2010).

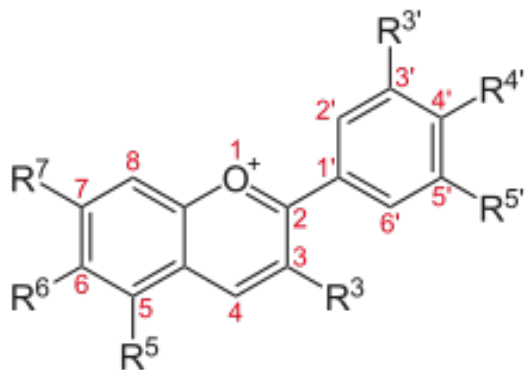


Figure 2.1
Anthocyanin aglycone structure with possible substitution sites and their corresponding numbers associated with the substitution position

When anthocyanidins are substituted with sugars, they are considered ACNs. Glycosylation can occur on the A ring (C₅ or C₇ glycosylation), B ring (C_{3'}), or C ring (C₃ glycosylation) of the chromophore, with C₃ being the most common example of ACN glycosylation (Zhao et al., 2014). The glycosidic bond found are often O-glycosidic with monosaccharides, disaccharides, or even trisaccharides (Zhao et al., 2015). In this

dissertation, disaccharides (rutinose and sophorose) will be the most pertinent. Glycosylation can affect ACN color expression (generally hypsochromic), pigment stability, and the overall chemical reactivity of the ACN, since they change the polarity and hydrophobic effect of the reactant (Farr et al., 2019; Zhao et al., 2014).

ACNs can also be substituted with acids at different positions of the glycosylations—called glycosyl acylations. These acylations are often with organic compounds, specifically aliphatic (such as malonic, acetic, succinic) or aromatic (such as ferulic, sinapic, caffeic, *p*-coumaric) acids (Zhao et al., 2017). In this dissertation, aromatic acids—in particular, hydroxycinnamic acids will be most relevant since isomerization requires conjugated double bonds, as present in hydroxycinnamic acids. The importance of these hydroxycinnamic acylations will be further discussed in a later section.

2.2.2. Plant Sources

ACNs are widely abundant in many fruits and vegetables, thus there are many cultures that already consume them without the knowledge that they're consuming ACNs. They exist in the vacuole of the plant cell and have been hypothesized to have formed as a result of oxidative and environmental stress from light, pests, and droughts (Gould, 2004). ACNs are most commonly found as non-acylated and glycosylated forms, in fruits such as—blueberries (cyanidin-3-glucoside) (Lohachoompol et al., 2004), blackberries (cyanidin-3-glucoside, cyanidin-3-rutinoside) (Fan-Chiang & Wrolstad, 2005), grapes (malvidin-3-arabinoside) (García-Beneytez et al., 2002), strawberries (cyanidin and pelargonidin-3-

glucoside) (Lopes-Da-Silva et al., 2001), mahaleb cherries (cyanidin-3-rutinoside) (Blando et al., 2018), blackcurrant (delphinidin-3-rutinoside), and many more (Vidana Gamage et al., 2022). In vegetables/grains, similar ACNs can be found in black beans (delphinidine-3-glucoside) (Takeoka et al., 1997), American eggplants (delphinidin-3-rutinoside) (Sigurdson & Giusti, 2014), though many vegetable sources are often used to study acylated ACNs. Few examples of monoacylated ACN enriched vegetable sources are—purple carrot (cyanidin-3-xylosyl-glucosyl-galactoside acylated with sinapic, ferulic, *p*-coumaric acid) (E. Gläßgen et al., 1992) and red cabbage (cyanidin-3-sophoroside-5-glucoside acylated with sinapic, ferulic, *p*-coumaric acid) (Ahmadiani et al., 2014). Diacylated ACNs are found in purple sweet potato (peonidin-3-sophoroside-5-glucoside acylated with combinations of caffeic, ferulic and hydroxybenzoic acid) (Sigurdson et al., 2019) and red radish (pelargonidin-3-sophoroside-5-glucoside acylated with *p*-coumaric and malonic acid).

Beyond these mono- an di-hydroxycinnamic acids, triacylation (Tatsuzawa, 2019), or tetraacylation (Goto et al., 1984) could also be found in ACNs, with many of the intricate substitution patterns found in flowers or leaves. In some cases, these sources can be used for food applications—one notable example being Butterfly pea flower – which been used in food and beverages due to their vibrant blue color (Jeyaraj et al., 2021). Selection of plant sources for the desired ACN would depend on the type of aglycone, glycosylation, and acylation of choice, on top of the percent composition the pigment in the total extract.

2.2.3. Hydroxycinnamic Acylations

Acylation has been known to provide stability to the ACN structure (Giusti & Wrolstad, 2003). Common acylating groups found in ACN are hydroxycinnamic acids such as *p*-coumaric and ferulic acids, as well as aliphatic acids such as malonic and malic acids. For the purposes of this dissertation on ACN photoisomerization, hydroxycinnamic acylations will be pertinent. In most monoacylation patterns, the phenolic acid is attached to the C₆' position of sugar on C₃ position of the aglycone (Bakowska-Barczak, 2005). However for diacylation, the acylating group (aliphatic and phenolic) could be either attached to the C₆' or C₂' position of the sugar (Giusti & Wrolstad, 2003). More rare varieties of acylation can be found on C₇ for the A ring and C₃'/C₅' of the B ring, though they have been generally found in blue flowers rather than fruits or vegetables (Saito et al., 2007). Photoisomerization of hydroxycinnamic acids have been mostly discussed in terms of C₆' position of the C₃ sugar (George et al., 2001; Mori et al., 2006; Sigurdson et al., 2018) and there is a gap in literature of photoisomerization on C₂' or other uncommon positions. In general, ACN diacylated have been known to have greater stability than monoacylated ACN due to their increased contribution in stacking of the chromophore-copigment (Malien-Aubert et al., 2001). In addition, studies have shown that ACNs with different phenolic acids could show varying results in their stability due to the effect of copigmentation (Sari, 2016). Thus, position of the acylating group and the type of acid could have an effect on the reactivity of photoisomerization.

2.2.4. Stability by Intramolecular Copigmentation

Copigmentation is a chemical reaction in which a chromophore, such as ACNs react with a molecule that provides a stabilizing effect on the chromophore (Davies & Mazza, 1993). These molecules – called copigments—are often colorless on their own, when they are not complexed with the chromophore. In addition, copigments are able to provide hyperchromic effect on the ACN, which implies that less pigment needs to be used in order to make the same intensity of chromaticity (Brouillard et al., 1989). Furthermore, copigmentation is also associated with bathochromic shifts, though the occurrence of bathochromic and hyperchromic shifts aren't directly correlated (Boulton, 2001). These copigments can be phenolic acids, flavonoids, polyphenols, and metals, and may complex with ACN chromophore to undergo “intermolecular copigmentation.”

Copigmentation can also occur within the molecule, called “intramolecular copigmentation.” In the case of hydroxycinnamic acylated ACN, it is categorized as an intramolecular copigmentation, as the acylglycosylation is covalently bonded to the ACN chromophore. Intramolecular copigmentation occurs due to the acyl moiety that can move in an aqueous medium to form $\pi - \pi$ bonding driven by hydrophobic bonding by conformational folding experiments (Hoshino et al., 1982; Trouillas et al., 2016). As with intermolecular copigmentation, intramolecular copigmentation has also been associated with bathochromic and hyperchromic shifts (Chassaing et al., 2010).

2.3. Anthocyanin Photochemistry

2.3.1. Flavylium Photochromism

Photochromism via isomerization reaction has been long-discussed and well-researched in the field of photophysics and photochemistry (Liu et al., 2018; Waldeck, 1991). However, its application in food science is understudied compared to the plethora of studies done on smaller organic compounds. Among the studies that have been conducted, thermodynamic and kinetic constants of *cis-trans* isomerization of ACN hydroxycinnamic acylation and their impact on ACN color stability and color characteristics have been elucidated (George et al., 2001; Sigurdson et al., 2018). Furthermore, the *cis-trans* isomerization barrier have been determined by kinetic calculations of flavylium multistates with acid-base equilibrium constants (Basilio & Pina, 2016). Flavyliums are related to ACN in that they

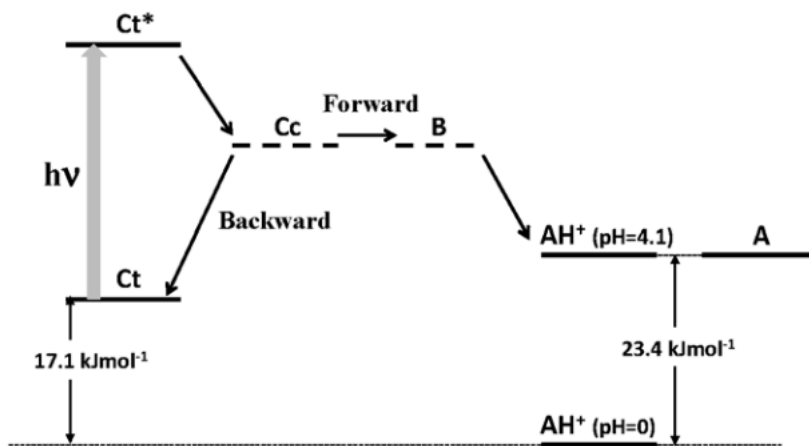


Figure 2.2 Energy diagram of 4',7-dihydroxy-3-methoxyflavylium at equilibrium. Excitation energy arrows are not drawn in scale. Ct represents *trans*-chalcone, Cc represents *cis*-chalcone. The figure was adopted from Gago et al., (2015).

have similar structure of the chromophore backbone, and once the flavylum is substituted with glycosylations, it is categorized from anthocyanidin to ACN (Khoo et al., 2017). Flavylum cation (AH^+) is the state in which the chromophore is able to show its bright red and pink hues. As a pH-dependent multisystem, the flavylum can undergo isomerization from *trans*-chalcone to *cis*-chalcone, after the flavylum undergoes hydration and tautomerization (Gago, Basílio, et al., 2015). Though the chalcones are colorless and thus, less applicable for the purposes of diversifying the expression of food colorants.

Learning from the flavylum chemistry, production of *cis-trans* chalcone is dependent on the direction of the isomerization, because the photoproduct can revert back as the photoreactant. Isomerization barrier and pH was observed to affect this direction of reaction, in which two different wavelengths in pH 4.5 resulted in production of *cis*-chalcone from hemiketal/flavylum cation (275 nm) and production of hemiketal/flavylum cation from *trans*-chalcone is converted to hemiketal/flavylum cation (365 nm). The energy diagram of the necessary electronic transition and direction of the photoreactions are depicted in Fig 2.2 (Gago, Basílio, et al., 2015).

Studies on determining the type of electronic transition was done by laser flash photolysis, in which excitation of the hemiketal at 266 nm increased the absorption of the isomeric chalcones within 50 ns with no absorbance of triplet states, suggesting a singlet excited transition reaction (Costa et al., 2015). Additionally, quantum chemical modeling of

hemiketal resulted in $\pi^1 \rightarrow \pi^*$ transition as the significant transition, which can decay from the conical intersection to the *cis*-chalcone.

However, the isomerization from *cis*-chalcone to *trans*-chalcone cannot be equated to isomerization of hydroxycinnamic acids attached to glycosides on the aglycone. In addition, the occurrence of color change via photoisomerization is known, but the factors that contribute to this reaction is under-studied. The existing body of knowledge on photoisomerization of ACN hydroxycinnamic acylations are detailed in the next section.

2.3.2. Photoisomerization of Hydroxycinnamic Acylation in Anthocyanins

There are limited studies that study the factors that influence photoisomerization of ACN hydroxycinnamic acylation. Yoshida's (1990) work was one of the pioneering studies that isolated *cis*-isomers in purple leaves of *Perilla ocimoides*. In this study, the production of isomerization was varied by the irradiation solvent—methanol, pH 2.0 buffer, and pH 6.0 buffer—which were irradiated under UV and sunlight. The findings suggested that methanol (10^{-2} M) with UV were the most effective in producing the photoproduct. Yoshida further studied the influence of solvation medium by using 0.5% TFA-methanol, 0.5% TFA-H₂O, and phosphate buffer (pH 6.0) for the UV isomerization of gentiodelphin (delphinidin based ACN). Their findings showed that 0.5% TFA-methanol was the most effective out of the three media, elucidating the effect of acidic aqueous solutions on isomerization (Yoshida et al., 2002). From the work of the Giusti Phytochemical Laboratory, the material of the cuvette (glass or quartz) and their dosage response from UV

irradiation were studied (Tang, 2018). Quartz cuvette required less time and energy to trigger the *cis*-isomer, but the final photostationary equilibrium was lower than the plateau phase in the glass cuvette, perhaps because the amount of pigment degradation is exacerbated by the intensity of UV transmitting through quartz cuvettes. Furthermore, Zhou (2021) studied the optimization process of UV irradiation on cyanidins, while modulating the amount of water in the irradiation solvent (ethanol) and the concentration of the pigment (100 – 300 μM). This study determined that 90% ethanol and lower concentration were the most favorable in yielding a high *cis/trans* ratio. These studies offered insight on the importance of irradiation solvent, type of cuvette, and concentration

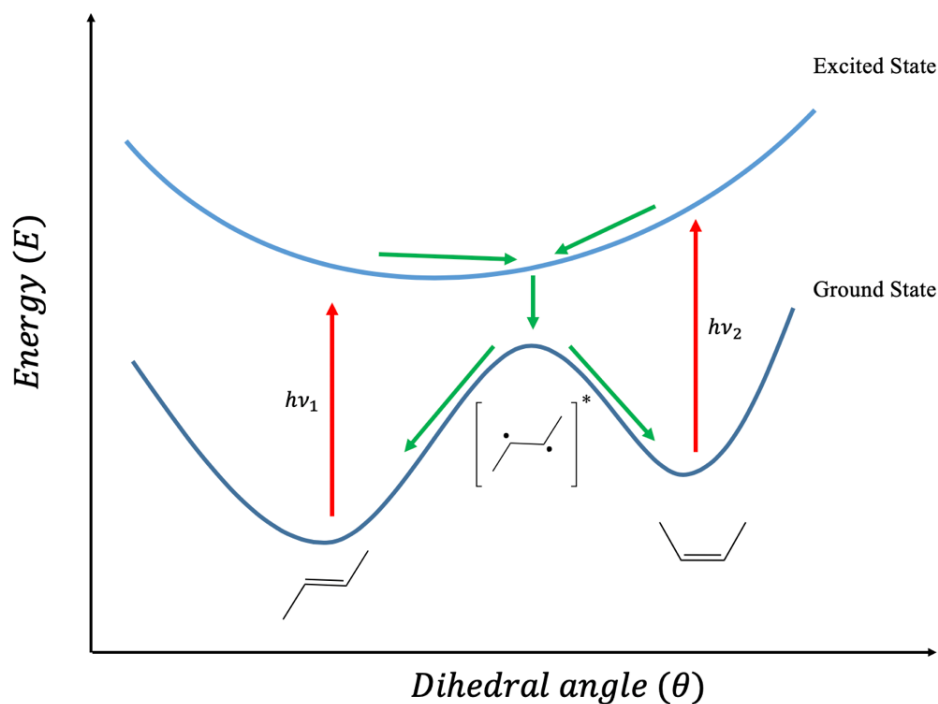


Figure 2.3 Potential energy diagram of photoexcited *trans*- and *cis*-alkene, which represents potential routes of excitation, conversion, and relaxation into isomerization.

of the pigment. However, as the foundation of excitation is the light source itself, the role that radiant energy ($h\nu_1$ or $h\nu_2$) plays in the electronic transition was required (Fig 2.3).

2.3.3. Borrowing from Organic Photochemistry – Factors Impact Photoisomerization

Though the body of knowledge on ACN photoisomerization is lacking, photoisomerization of organic compounds have been well studied in the early 1900s. Mechanism of photoisomerization has varied depending on the molecule in question and the most commonly understood mechanisms are: a) internal conversion (singlet transition), b) intersystem crossing (triplet transition), and c) Hula-Twist (Diau, 2004; Schultz et al., 2003).

The first possible mechanism of *trans*-to-*cis* photoisomerization is an internal conversion that involves singlet state transition from the first excited state to a lower electronic state, which occurs during vibrational relaxation ('CRC Handbook of Organic Photochemistry and Photobiology, Volumes 1 & 2', 2003). This non-radiative process can induce isomerization as a pathway to dissipate the excited energy. The second mechanism is intersystem crossing, in which the excited singlet state changes the spin multiplicity to an excited triplet state. As the excited electron returns back to the ground singlet state, it can phosphoresce as radiative decay ('CRC Handbook of Organic Photochemistry and Photobiology, Volumes 1 & 2', 2003). The third mechanism revolves twisting of double bond and an adjacent single bond by 180 degrees, called Hula-Twist (Fuß, 2012). According to several studies that have observed the production of *cis*-isomers from *trans*-

configured organic hydrocarbons, this mechanism seems to be the most common mechanism of *trans-cis* isomerization (Zimmerman et al., 1969; Waldeck, 1991).

Keeping in mind of these mechanisms, there are several experimental conditions that could impact the path of an excited electronic state. Since the electronic transition is the effect of photoexcitation, specific ranges of wavelengths are required for the desired isomerization to occur. Consequently, *trans* \rightarrow *cis* isomerization occurs at $\lambda = 320 - 380$ nm, while *cis* \rightarrow *trans* reversion occurs around $\lambda = 400 - 450$ nm for azobenzenes (Merino & Ribagorda, 2012). In addition, the wavelength of photoexcitation is often dictated by the substituents of the aryl group (Merino & Ribagorda, 2012). Therefore, radiant energy is a crucial factor that contributes to electronic transitions that produces isomerization. Furthermore, photochemical reactions have been known to be wavelength-dependent, meaning, that the irradiation wavelength affects the efficiency in the formation of the photoproduct (Protti et al., 2019). Wavelength-dependent reactions occur when the photoreactant involves one chromophore, therefore the photoproduct depends on the absorbance of the photoreactant. Thus, carefully selecting the electromagnetic spectra of the radiant energies are critical when investigating the extent of photoisomerization of ACNs.

Second, the bulkiness of the substituent can impact the potential energy surface of the photoreaction (Waldeck, 1991). The size of the substituents can affect the angle of twisting during Hula-Twist, and these constraints are influence by the position of the alkyl

substitution on phenyl rings as well, because of steric effects that may push the molecule out of its geometric planarity (Saltiel et al., 1971). The effect of substituents on ACN hydroxycinnamic acylation has yet to be related in the literature. More specifically, the hydroxycinnamic acid used in photoisomerization of acylated ACN has been *p*-coumaric acid, which little to no exploration on other phenolic acyl groups on this photoreaction.

Other factors that have been discussed in the literature as contributors in photochemical reactions are the solvent/medium of the photoreaction, the direction of reversible reactions, presence of other compounds in the photoreactant matrix, and temperature of the solvated molecules (Horspool & Lenci, 2003; Quant et al., 2019; Turro et al., 1978). As these factors have been studied in either solid state or representative organics such as azobenzene and stilbene, it requires further research to confirm the effect of these factors on the acyl groups of the ACN.

2.4. Unintended Consequences of Scientific Innovation

2.4.1. Actors of the Global Food System

In any given food commodity chain, there are various stakeholders that participate in a piece of the process—from growers, exporters, buyers, retailers, consumers, and many more roles in between those roles. When categorizing the plant sources of pigments as a small player within the macrocosm of the global food system, it is important to consider the role that each stakeholder (including the scientists) plays in the commodity chain. Most

often the middle of the commodity chain hold more power, a concept that is described as an “hourglass hanging by a thread,” by Carolan (2016). Scholars in rural sociology have stated that as global food systems become more consolidated, the processors and retailers will hold more power (Lobao & Meyer, 2003). The growers hold less power than exporters, because exporters “use social status, market accessibility... to discipline growers,” especially in countries in the Global South (Freidberg, 2004). This power imbalance is only more exacerbated between growers and the importers. The importers not only buy the crops, but also finance the growing season. Therefore, the growers often have little fiscal and logistically control over their practices. Friedburg explains that only certain types of suppliers can gain the title of ‘category leader’ of a crop—usually they are suppliers who can acquire paperwork and transparency that the retailers require. Expectedly, these suppliers tend to be linked with white-owned farms in a Global South country, such as Zambia. And Zambian suppliers do not have the material footing that white-owned farmers in Zambia do. To the world outside commodity networks, these inequities may go unnoticed but Friedberg and others clearly highlights how pervasive and deep-seeded these oppressive power structures are (Carr et al., 2016; Selwyn, 2015).

2.4.2. Scientific Innovation in the Food System

Science and innovation have been framed as the answer to many global challenges with dire need for solution. As the global economy celebrates technological advancement and automatization, people living in these societies have adopted superiority of science and engineering over other disciplines. Regardless of the intentions behind perpetuating this

culture, natural and physical scientists have a role to play in how their innovation truly affects the system its designed for. In this literature review, current scholarship on the unintended and undesirable consequences of innovation will be highlighted.

Innovation is defined as “the multi-stage process whereby organizations transform ideas into new/improved products, service or processes, in order to advance, compete and differentiate themselves successfully in their marketplace” (Baregheh et al., 2009). Scholarship around innovation science has directly alluded to its implementation and success via business ventures. This conceptualization could be a product of Westernized view-point of development, since theorization and research stems from scholars with their own opinions and biases. Thus, the direct relationship between innovation and economic development has been the established assumption.

Sveiby and other’s review on the consequences of innovation relates intentionality, desirability, and anticipation in relation to the type of consequences, agents, and affected stakeholders (Sveiby et al., 2009). The authors claim that innovations can cause ‘disruptions in the economy’ by creating new industries and changing the trajectory of old industries. Meaning, innovations can vastly impact not only products’ success in the market, but also, the formation or eradication of the market itself. If markets change, then the people embedded in it will also be impacted. This is explained by the diffusion theory, which states that innovation will be communicated by the adopters in different parts of a commodity chain; thus, innovation impacts not only the direct adopters, but also the population of potential adopters and the communication between the two groups (Palloni,

2001). The categorization of consequences into intentionality, desirability, and anticipation allows for the tailoring of the problem, and hopefully a guide to its solution. Sveiby and others have elucidated the limiting factors of undesirable consequences, irrespective of its intentionality or anticipation (Fig 2.4). These undesirable consequences are framed in perspective of both agents and adopters of the innovation, by the stakeholder theory—which states that there is an inherent bias that innovation is good and desirability between stakeholders, such as agents, adopters, consumers, employees, etc., differ greatly. Therefore, conclusions on undesirable consequences of innovation must be discussed in specifics, by addressing the type of stakeholder and the power that these stakeholders have.

Ostensibly, the driving force of the innovation is its usage among adopters in a free market structure. However, the imbalance of power held among the different adopters in the commodity chain is discussed as an integral piece in the commodity chain analyses (Essabbar et al., 2020). While innovations can bring desirable consequences to one adopter, it could bring detriment to another. In addition, the agency that an adopter has in their choice to resist or adopt an innovation also influences their power in the commodity chain. For example, while advancement in scientific knowledge can bring ease and efficiency to a retailer like Amazon that owns large scale warehouses, other small scale retailers cannot keep up with Amazon's scale, production (by exploitative means), and social/financial capital—consequently leading to the monopolization of online retailers by businesses such as Amazon (Alimahomed-Wilson & Massimo, 2020).

In this way, natural scientists have a responsibility in understanding where their innovation helps and hurts. Too often, the social impact of technological innovation is theorized at the conceptual stage of the project, such as during the writing grant proposals. When in reality, the hypothesized social impact is seldom confirmed nor further analyzed. Ergo, in the following sections, landmark scientific innovations will be juxtaposed between the perspective of both physical and social scientists.

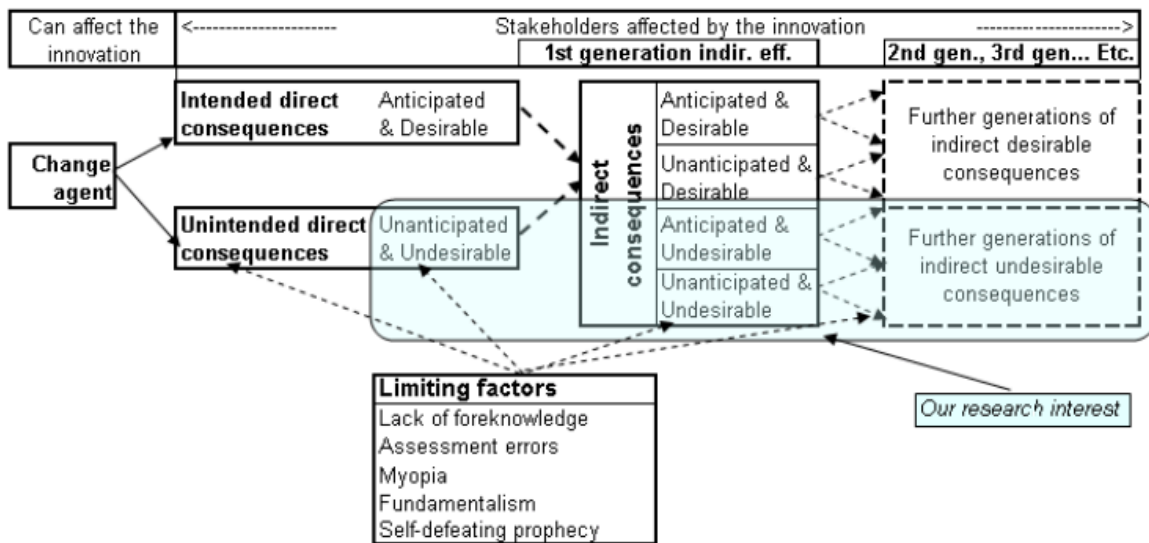


Figure 2.4 Categorization of consequences of innovation by intentionality, desirability, and anticipation according to Sveiby (2009), adopted from Rogers (1983) and Merton (1936).

2.4.3. Agricultural University Science and the Industry

Collaboration between university's research laboratories and business has been extensively done, so much so that industry funding can be the backbone of the research done in some disciplines—particularly, in science and engineering. In fact, this collaboration is seen as a proud merit to be shared, as research fellowships and awards are also often funded by

companies. This brings up the question: how is university science's research findings impacted by their funders?

Under capitalism, commercialization of science promotes university scientists to hold hands with private industries to acquire intellectual property, which is, at its core, privatization of knowledge (Blumenthal et al., 1997; Louis et al., 2001). With funding, it is most likely that production of research would increase, which could be beneficial for the university institution. However, it is also important to consider if marketization of innovation has a role in perpetuating inequity that stems from a) discrepancies among individual research group's sources of funding, b) exposure, status, and endowment from research institution's rankings, and c) countries' power, policies, and resources that influences university science (Glenna et al., 2015; Hottenrott & Thorwarth, 2011).

In some cases, commercialization of science could also impact actors in the food system. Agricultural science could impact small producers because they cannot compete in markets that require a specific standard of quality and safety (Thompson & Scoones, 2009). For free-market enthusiasts, this may be accepted as an inevitable outcome. However, lack of technological implementation or lack of certification does not automatically mean that the product is low quality. One solution to level the playing field is by including farmers and smallholder producers in the conversation around commodification of food and science. For example, in the case of Dutch dairy farmers, the government gave farmers the option to choose their own strategies for nutrient flows necessary in farming scientists (Eshuis &

Stuiver, 2005). This allowed for a shared framework in which varying farmers' styles and priorities, as well as social and soil scientists perspectives given equal consideration.

As such, sociological analyses and critiques on natural colorants and the impact of extraction/stabilization of pigments on different actors in the food system is necessary. The current gap in the literature could be filled by analyses of a) vegetable and fruit sources of pigments and their respective commodity chains, b) intellectual property of extraction methods and pigment formations, and c) impact of novel natural pigment commercialization on various stakeholders in the food system.

2.4.4. Sociological Analyses of Notable Agricultural Innovations

2.4.4.1. Genetically Modified Organisms

One specific scientific innovation that has impacted the US food system greatly is genetically modified organisms (GMOs). GMOs are produced by genetic engineering of identifying and inserting desired genes that produce favorable (higher shelf stability, phenotypically attractive, etc) characteristics (Rótolo et al., 2015). This technique can be done by a gene gun, which uses helium to transfer the desirable genes into the receptor cell of interest (Feldmann et al., 2000). Another technique uses bacteria to transfer its DNA with desired genes into a specific receptor cell. The idea of manipulating genes and inducing genetic recombination has caused consumers to consider GMOs as 'unnatural' or 'unhealthy.' Along with this, there has been a lot of information, some of which are misinformation, on the use of GMOs in all types of products. There are 10 crops that are

currently GMO-approved, such as potatoes, apples, and squash, to name a few. However, labels of “Non-GMO” are often plastered on products as a way to market the perception of health.

In the perspective of food scientists and biotechnologists, GMOs have provided more benefit than harm. The most well-known benefit of using GMOs is its ability to increase its crop yield. As the human population increases and the problem of global hunger remains yet to be solved, increasing the food production in the farming sector has been welcomed. In addition, the crops produced can supply nutrients that are lacking in a population. For example, the Golden Rice Project has been well known for its synthesis of bioavailable beta-carotene in vitamin-A deficient populations. According to the World Health Organization, vitamin A deficiency is prevalent in ~250 million children around the world. Lack of vitamin A in the diet has been known to cause blindness and severe illness among children (Mayo-Wilson et al., 2011).

However, sociologists’ perspective on GMOs considers their impact on growers and other populations that could be impacted by GMOs—besides the nutrition of consumers. As Glover (2010) states, GMO has been framed as a pro-poor technology by being introduced to the public as “transgenic crop that addressed world hunger. This type of political framing of the science would not be a problem if it was the entirety of the truth—which is not in this case. Although GMOs have been marketed as a delivery source of vitamin A, it is most often used by biotechnological corporations as inputs for animal feed or ways to increase

seed productivity, all whilst the technology is privatized with judicial barriers (Kloppenburg, 2004; Wield et al., 2010). When GMO technology such as “roundup” started being patented, farming became a large-scale process that standardized crops with decreased biodiversity and increased adversity for smallholder farmers (Glover, 2010; Motta, 2014).

2.4.4.2. Clustered Regularly Interspaced Short Palindromic Repeats

Clustered regularly interspaced short palindromic repeats (CRISPR) is a technique that allows for DNA sequences in the genome to be added, removed, or altered (Ormond et al., 2017). This means that the original base pairs in the plant’s DNA can be changed without transferring foreign genetic material by bacteria or gene-guns, which is done for GMOs.

Recently, a review in food science was published by Brandt and Barrangou, claiming that crop yields need to increase to satisfy the global demands, along with increase in livestock and biofuels (Brandt & Barrangou, 2019). But this is notion formed under the same assumption that overpopulation is the problem of current global problems such as climate change and global hunger. When in reality, it is a lot more complex than just the mere lack of production. At the essence of basic scientific research, understanding methods of gene editing is not problematic. However, when it is hastily implemented without proper assessment at all levels of the system, unintentional but undesirable consequences will inevitably occur.

United States Department of Agriculture (USDA) expressed that CRISPR-edited plants will not need to be regulated. According to Yang, who engineered white button mushrooms that removed one out of 6 genes that encode for polyphenol oxidase, USDA claimed that CRISPR does not need oversight because “it does not contain foreign DNA from viruses or bacteria” (Waltz, 2016). Whether this decision is a scientifically sound or a bureaucratic is unclear. Seeing how the 2020 Nobel Prize in Chemistry went to CRISPR, the innovation was considered revolutionary. As such, this may be an opportune for stakeholders to come together and radicalize systems to match the innovation that broke barriers.

To prevent further perpetuation of inequity, it is important for natural scientists to ask questions such as the following: if and when CRISPR-edited crop seeds are commercialized, who will be able to purchase them? What would happen if/when the technology is patented? How will this impact the smallholder farmers who tend to hold the least power in the food chain? How would this impact biodiversity of crops? One method of answering these questions is by directly asking the actors that will be impacted by the technology. This type of analysis is called “Social Impact Assessment,” in which theoretical and empirical methods are employed to predict the impact of a new program or project on a population or community (Burdge, 2015). More discussion on this can be found in *Potential Methods of Comprehensive Social Impact Assessment*.

2.4.5. Potential Methods of Comprehensive Social Impact Assessment

2.4.5.1. Scoping Existing Socioeconomic Environment

The scoping process is done during the early stages of constructing a Social Impact Assessment and required for environmental impact statements but not for an assessment under the National Environmental Policy Act of 1969 (43 CFR 46.235). In scoping a program/project of interest, preliminary research on geographic extent, economic status (such as earnings or housing costs of the area, and the type of populations (cultural enclaves or indigenous communities) are studied (Burdge & Robertson, 1990). This process is usually interdisciplinary, with government agencies, consulting firms with experts in the field, as well as the public involvement.

2.4.5.2. Data Collection for Additional Existing Socioeconomic Environment

Primary data on the differences in occupation and salary based on ethnicities, current practices of eating habits and whether they differ by ethnicities, rates of immigration, prices of raw goods and their accessibility by varying transportation (bus, train, walking, bike lanes) are considered (Burdge & Robertson, 1990). These additional data refines the baseline information on a proposed project and offers insight on how it could affect different stakeholders.

2.4.5.3. Public Involvement

Scoping would include public participation of different stakeholders to ensure that public concerns are addressed before designing of any new project or policy. Some of the relevant

stakeholders are: people that are part of different socioeconomic groups, cultural backgrounds, age, family structure (grandparents, children, etc), and location of housing. Additional scoping can include different retail and wholesale commodity industries along with government officials at local and regional levels. Surveys with monetary compensation would be a feasible method, to incentivize the public and ensure that as many voices are heard. These surveys can also be available online and distributed at grocery stores and public offices.

2.4.5.4. Policy Design, Construction, and Implementation

When predicting how a policy would impact a population, comparative diachronic model can be used to compare how similar communities in the past have reacted to a similar construction. Comparative diachronic model uses a “comparative study” that entails the same setting as the proposed study, but at a different point in time (Burdge & Robertson, 1990). Then, using the primary and secondary social impact from the comparative subject, the proposed project’s social impact could be hypothesized. Subsequently, construction of the social impact assessment could consider variables such as: a) influx or outflux of temporary workers, b) seasonal/leisure residents, c) change in employment or occupational opportunities, d) presence of outside agency/inter-organizational cooperation in the area, e) disruption in daily living and movement patterns, f) disruption in social networks, g) change in community infrastructure, and h) effects on known cultural, historical, sacred, or archaeological resources (Burdge 2015). After collecting data on these variables by survey methodologies or probability rating (coupled with severity rating), the major and minor

risks and benefits of a proposed project can be determined. These methods can be employed in assessing the sociological impact of agricultural scientific innovations.

Chapter 3. Ultraviolet-Visible Excitation of *Cis*- and *Trans-p*-Coumaric Acylated Delphinidins and Their Resulting Photochromic Characteristics

Published. **La, E. H.**, Giusti, M. M. (2022). Ultraviolet–Visible Excitation of *cis*- and *trans-p*-Coumaric Acylated Delphinidins and Their Resulting Photochromic Characteristics. *ACS Food Science and Technology*, 2(5), 878–887.

3.1. Abstract

Anthocyanins are often acylated with *trans*-hydroxycinnamic acids, but can undergo a structural transformation to their *cis*-isomer. This study investigated the reversible photochromism of *trans*- and *cis*-acylated delphinidin derivatives (Dp) under industry accessible ultraviolet (UV) and visible energies, and their impact on color expression.

Delphinidin-3-(*trans-p*-coumaroyl)-rutinoside-5-glucoside, delphinidin-3-(*cis-p*-coumaroyl)-rutinoside-5-glucoside, and its mixture were subjected to UV and visible light for up to 20 hours. Isomerization was monitored using HPLC-PDA. Color, spectra, and stability were compared using a spectrophotometer and ColorBySpectra software.

All light treatments induced photoisomerization between *trans* and *cis*-acylated Dp, but to varying extents, equilibria, and at different exposure times. Visible energy induced greater *trans*-to-*cis* isomerization, while UV induced greater *cis*-to-*trans* isomerization. *Cis*-Dp

showed greater color intensity and stability in pH 1, and greener hue (h^*_{ab} 130° than *trans*- (h^*_{ab} 188°) in pH 8 after equilibration of 15 minutes.

Keywords: cis-trans isomerization, radiant energies, anthocyanin isolates, pigment degradation

3.2. Introduction

Anthocyanins (ACN) are phytochemical pigments with health-promoting properties that can be used as food colorants (He & Giusti, 2010). ACN come from different plant sources, and have the potential to express a wide variety of colors—ranging from orange to blue, depending on the pH conditions (Wallace & Giusti, 2015). However, their color stability is limited, when compared to its synthetic dye counterparts. Researchers have used colloidal complexation or copigmentation to retain or enhance ACN's color with a variety of biopolymers, phenolic compounds, and metals (Boulton, 2001; Cortez et al., 2017; Selig et al., 2018). Although combining these strategies can help to stabilize the product's color characteristics, the use of colloids or copigments can alter the solubility of the matrix or the flavor of the product (Carocho et al., 2014). Therefore, stabilization of ACNs via chemical structural manipulation such as photoisomerization is a novel and promising strategy.

ACN have a flavylium base structure and a variety of methoxylation, glycosylation, hydroxylation, and acylation patterns that make up over 700 molecular structures

(Sigurdson et al., 2017). In general, greater attachments of glycosylation and acylation on the aglycone backbone have been associated with greater pigment stability and color expression (Giusti & Wrolstad, 2003; Malien-Aubert et al., 2001). ACN can be acylated with aliphatic acids, such as malonic and malic acid, as well as hydroxycinnamic acids, such as *p*-coumaric, ferulic, and caffeic acid. Most studies have alluded to hydroxycinnamic acylation's role in increasing pigment stability as a result of both intramolecular and intermolecular copigmentation (Sigurdson et al., 2019). Hydroxycinnamic acids can exist in either in its *trans*- or *cis*- configuration, however, *trans*-isomers are known to be highly prevalent in nature (Turner et al., 1993). A previous study showed that *cis*-acylated ACN may exhibit increased color strength and stability than their *trans*-counterparts (George et al., 2001; Sigurdson et al., 2018). However, since *cis*-acylated ACN are difficult to find, photoisomerization of naturally abundant *trans*-acylated ACN to form the rare pigment was studied here.

Photoisomerization of ACN is often discussed in terms of the ground state transitions of chalcones as a result of change in pH and light (Gavara et al., 2014; Leydet et al., 2013; Silva et al., 2016; Trouillas et al., 2016). The photoisomerization that occurs during the flavylum multistate of *trans*-chalcone to *cis*-chalcone depends on the isomerization barrier as well as the pH, as postulated by the energy diagram described by Gago *et al.*,¹⁹ which was adopted from the reaction rates and equilibrium constants of the *trans*- and *cis*-chalcone isomerization (Basílio & Pina, 2016; Brouillard & Lang, 1990; Gago, Basílio, et al., 2015; Mazza & Brouillard, 1990; Pina et al., 2012). Photoisomerization of

hydroxycinnamic acylations of anthocyanins have had less attention and there is much more to be discovered. Earlier works by Yoshida et al. and Hayashi et al. showed that delphinidins acylated with *p*-coumaric acid can undergo photoisomerization under various buffers and solvents (Hayashi et al., 1998; Yoshida et al., 1990). Solvation is just one factor that contributes to the photoisomerization reaction, and other conditions such as concentration, excitation energy, and stereochemistry of reagent molecule may also play a role in its reactivity (Lin et al., 2002; Lui et al., 2019; Sakata et al., 2006). Experimental studies on ACN photoisomerization have focused mostly on solvation effects, which provides opportunities for further exploration of light energy and the reagent molecule on

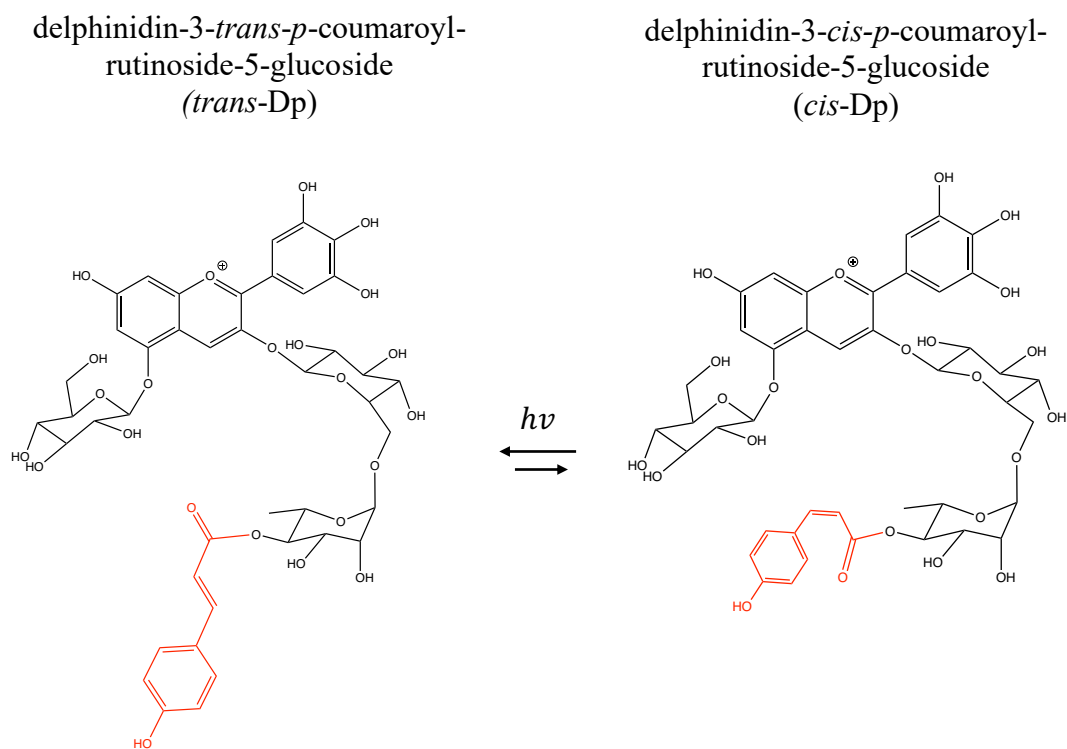


Figure 3.1

Reversible isomerization of *trans*-Dp and *cis*-Dp as a result of excitation with light. The two differing sizes of the arrows represent the favoring of the chemical equilibrium dominated by *trans*-Dp.

this reaction. In order for the findings of this research to be applicable to the food industry, sources of excitation that are easily acquirable and economical were chosen. Thus, the goal of this study was to investigate the effects of industry-accessible ultraviolet and visible energies on the extent, equilibrium, and efficiency of acylated delphinidin's reversible photoisomerization.

3.3. Materials and Methods

3.3.1. Materials

East Asian eggplants (*Solanum melongena* L.) were purchased from a local Chinese grocery store (Sunrise Asian Super Market, Columbus, OH, USA) and used to obtain the anthocyanin extracts. Chemical solvents used for extraction, purification, and analyses were: trifluoroacetic acid (TFA), hydrochloric acid (HCl), formic acid, acetone, chloroform, ethyl acetate (EtOAc), methanol (MeOH), potassium chloride (KCl), citric acid (CA), disodium phosphate (Na_2HPO_4), HPLC-grade acetonitrile, and HPLC-grade water. These chemicals were purchased from either Sigma-Aldrich, Co. (St. Louis, MO, USA) or Thermo Fisher Scientific (Waltham, MA, USA).

3.3.2. Anthocyanin Extraction, Purification, and Identification

Acylated ACN were extracted from East Asian eggplant peels that had been frozen with liquid N_2 , pulverized, and extracted with acidified (HCl and TFA) acetone. The plant material was phase partitioned with chloroform overnight in 4 °C and the solvents in the

aqueous phase were removed by rotary evaporation (Brinkmann Büchi Rotavapor, New Castle, DE, USA). Further purification with solid phase extraction was done by loading the ACN extract onto a Sep-Pak Vac 20cc C18 cartridge (Waters Corporation, Milford, MA, USA) and washing it first with 0.01% HCl in H₂O, then with EtOAc, and finally with 0.01% HCl in MeOH. The acidified water and EtOAc washes were done three times, whereas the acidified MeOH rinse was performed until most of the pigments were recovered from the cartridge. A more detailed procedure is outlined by (Rodriguez-Saona & Wrolstad, 2001). The resulting extract from this procedure will be termed semi-crude extract (SCE) for the rest of this manuscript.

The ACN profile of SCE was characterized by using a Nexera-i-LC 2040C 3D ultra-high performance liquid chromatography with a photo-diode array detector (UHPLC-PDA) coupled to LCMS-8040 triple quadrupole mass spectrometer with electrospray ionization (ESI-MS/MS, Shimadzu, Columbia, MD, USA). Chromatography was done with Kinetex 1.7 μ m F5 column with 100 Å pore size and 100 \times 2.1 mm dimensions (Phenomenex, Torrance, CA, USA). The PDA chromatograms were collected for relative quantitation at 520 nm by % area of the two eluents.

Spectra were analyzed in order to characterize the two eluents by their retention times, fragmentation patterns, and absorbance. The solvents used for gradient-elution chromatography were 4.5% formic acid in MS-grade water for solvent A and MS-grade acetonitrile for solvent B. The UHPLC gradient started from B concentration of 1% for 1

min, 8% for 2 more min, 10% after 13 min, 25% after 2 min, then finally to 45% after 4 min. The column was flushed at 45% then equilibrated down to the starting B concentration. The LC-2040 oven was at 30 °C, collision energy of –35 eV, ESI interface with nebulizer gas flow of 3 L/min, DL temperature 250 °C, heat block temperature 400 °C, and drying gas flow of 15 L/min. The ions were scanned under positive scan under three parameters: Q1 total scan from 100 – 1200 m/z, Q1 Selected Ion Monitoring (SIM) of 773, 919, and 611 m/z, and Q3 SIM 611, 465, and 303 m/z. The injection volume for the runs were 5 μ L. Lab Solutions Software Ver.1 (Released 5.80) was used for data analysis and interpretation (Shimadzu, Columbia, MD, USA).

3.3.3. Anthocyanin Isomerization and Isolation

SCE at a concentration of ~200 μ M were placed in 30 x 10 mm polystyrene petri dishes at 10 mL per iteration and irradiated uncovered with UV light in a chamber (254 nm, Stratagene Stratalinker 1800 UV Crosslinker, La Jolla, CA, USA) for 15 minutes to produce delphinidin-3-*cis-p*-coumaroyl-rutinoside-5-glucoside (*cis*-Dp). The irradiated extract was then concentrated, mixed with acidified water, and passed through a 0.2 μ m syringe filter for semi-preparative HPLC. The reverse phase semi-preparative HPLC system (Shimadzu, MD, USA) was LC-6AD pumps, a CBM-20A communication module, a SIL-20A HT autosampler, a CTO-20A column oven, a SPD-M20A Photodiode Array detector, and a pentafluorophenyl (PFP) column (5 μ m particle size, 100 Å pore size, in a 250 \times 21.2 mm) and ran at a flow rate of 10.0 mL/min (Phenomenex®, Torrance, CA,

USA). LCMS Solution Software Version 3 (Shimadzu, Columbia, MD, USA) was used to monitor the eluting isolates. Both *cis*-Dp and delphinidin-3-*trans*-*p*-coumaroyl-rutinoside-5-glucoside (*trans*-Dp) were fractionated with acetonitrile as solvent A and 4.5% formic acid in HPLC-grade water as solvent B. The gradient for pigment isolation were as follows, with each percentage referring to solvent B—0 min: 18.5%, 2 min: 19%, 5 min: 19.5% and held until 13 min, then flushed out to 30% at 13.01 min and equilibrated to starting conditions. The purity of isolated *cis*- and *trans*-Dp was analyzed on an analytical HPLC-PDA instrument, composed of a DGU-20As degasser, LC-20AD pumps for the same two solvents used during ACN identification, a SPD-M20A diode array detector, and a SIL-20AC auto sampler. The analytical column was a Kinetex EVO C18 column with 5 μ m particle size, 100 Å pore size, and 150 \times 4.6 mm in diameter and length (Phenomenex®, Torrance, CA, USA). The gradient was as follows, in which the percentages refer to the B% concentration—30 min from 10–23%, 2 min from 23–40%, flushed at 40% for 6 min, followed by equilibration to the starting B% concentration. The resulting chromatogram was used for relative quantitation at 520 nm by measurement of the retention times and % area of the two eluents. The purity was quantified by measuring the % area under the curve (AUC) of the pertinent peaks at 520 nm and 260–700 nm, after manual integration.

3.3.4. Monomeric Delphinidin Quantitation

The pH differential method was used to quantify monomeric ACN in SCE. Using 700 nm and λ_{max} of 540 nm under pH 1 and 4.5, the absorbance was measured by SpectraMax 190

Microplate Reader (Molecular Devices, Sunnyvale, CA, USA) and expressed as cyanidin-3-glucoside equivalents with the following equation (1), (Giusti & Wrolstad, 2001):

$$(1) \text{ Monomeric Dp (mg/L)} = \frac{(\text{Abs} \times \text{DF} \times \text{MW} \times 1000)}{\epsilon \times l},$$

in which DF = dilution factor, MW = molecular weight of cyanidin-3-glucoside (449.2 g/mol), and ϵ = molar absorptivity of cyanidin-3-glucoside (26,900 L/mol·cm) in pH 1 buffer.

3.3.5. Determination of Radiant Light Exposure Time: Preliminary Tests

In order to determine the time at which isomerization was maximized and degradation was minimized for each of the four radiant energies, 100 μM of SCE was irradiated in a sealed quartz cuvette (Science Outlet on Amazon, Seattle, WA) with a pathlength of 10 mm and a transmission spectral range of 190–1200 nm under UV chamber at 254 nm, 365 nm, and visible energies of D65 (daylight illuminant), and F2 (fluorescent light). UV chamber at 254 nm emitted 40 W of power within internal dimension of 13.7 cm (l) \times 18.1 cm (w) \times 16.8 cm (h) (UV Stratalinker 1800, Stratagene, La Jolla, CA, USA). Similarly, UV chamber at 365 nm emitted 40 W within 35 cm (l) \times 27 cm (w) \times 16 cm (h) dimensions (61 cm (l) \times 34 cm (w) \times 33 cm (h), UVP Crosslinker CL-3000L, Analytik Jena, Beverly, MA, USA). Lastly, visible light chamber (MiniMatcher MM-2e, GTI Graphic Technology Inc., Newburgh, NY, USA) equipped with both D65 (30 W) and F2 lights (15 W) were used. The time of exposure for each source of radiant energy was determined by irradiating SCE for specific lengths of time, in which the isomerization reached a plateau, signifying a chemical equilibrium. SCE was irradiated up to 120 min with 254 nm, 180 min with 365

nm, 25 hrs with D65 lamp, and finally, 50 hrs with F2 lamp. The resulting isomerization and total delphinidin (Dp) degradation were quantified by the following equations (2, 3, 4):

$$(2) \% \text{ cisDp isomerization} = \% \text{ final transDp} - \% \text{ initial transDp}$$

$$(3) \% \text{ transDp and \% SCE isomerization} = \% \text{ final cisDp} - \% \text{ initial cisDp}$$

$$(4) \% \text{ total Dp degradation} = \% \text{ initial (cisDp + transDp)} - \% \text{ final (cisDp + transDp)}$$

Isomerization by radiant energies were analyzed by analytical reverse phase HPLC, as described in the previous section *Anthocyanin Isomerization and Isolation*. The isomerization and degradation trends were fitted to non-parametric curves (Supporting Information 1 – 4).

3.3.6. Ultraviolet-Visible Irradiation

SCE, *cis*-Dp, and *trans*-Dp in 0.01% HCl in MeOH at 100 μ M were sealed in quartz cuvettes and subjected to four radiant energies for their respective selected irradiation times. Environmental conditions such as temperature inside the laboratory (ranged between 21–23 °C) and placement of the light sources were remained consistent, with the light bulbs above the transparent side of the cuvettes. In addition, the lid of a poly-D-lysine-coated polystyrene 96-well plate was placed under the quartz cuvettes and a white, reflective absorbent pad was used to cover the opening side of the light chamber, in order to maximize the light exposure. Immediately after isomerization for the respective times of each light source, the samples were frozen at -18 °C for up to 7 days before thawing and analyzing on the analytical HPLC-PDA.

3.3.7. Visible Spectrophotometry and Colorimetry

Initial absorbance spectra (from 250–800 nm) of *cis*- and *trans*-isolates in acidified MeOH were compared using a SpectraMax 190 Microplate Reader, under the cuvette setting. Then, both isolates were irradiated with UV chambers (254 nm and 365 nm) for up to 16 min and their shifts in spectra were measured at 2 min increments.

For colorimetry, *cis*-Dp and *trans*-Dp isolates (without irradiation) were placed in buffers pH 1–10 (0.025 M KCl for pH 1, CA–Na₂HPO₄ buffer solutions for pH 2–7, 0.1 M NaHCO₃ for pH 8, Na₂CO₃–NaHCO₃ buffer solutions for pH 9–10) and equilibrated for 15 min on a poly-D-lysine-coated polystyrene 96-well plate (Sigurdson & Giusti, 2014; Zhou et al., 2020). Measurements were taken in triplicates from 250–700 nm in 5 nm intervals under SpectraMax 190 Microplate Reader for 24 hours in the dark, at 20 °C. The two isomers' color characteristics were compared to the irradiated SCE (254 nm, D65, and F2) in acidic (pH 1, 2) and alkaline (pH 6–9) conditions. From pH 3–5, colors were not compared since initial screening of the two isolates' color showed very faint or translucent colors.

CIE 1976 L* a* b* color space, also known as CIELAB, is a quantitative method to characterize color coordinates. L* represents lightness, in which $\pm L^*$ (white/black), $\pm a^*$ (red/green), $\pm b^*$ (yellow/blue), C*_{ab} (chroma), and h*_{ab} (hue angle). The spectral data from 380–750 nm was converted to colorimetric data using ColorBySpectra software, under 10° observer angle, D65 illuminant, and standard 1964 CIE equations.

3.3.8. Statistical Evaluation of Data

Under a randomized split-block design, the statistical significance of the HPLC data (area under the curves of irradiated SCE, *cis*- and *trans*-Dp under 520 nm) was conducted by two-way analysis of variance ($\alpha = 0.05$) and post hoc Tukey's test ($\alpha = 0.05$) with SPSS Statistics software (IBM SPSS Statistics for Macintosh, Version 27.0). The technical software settings were chosen to set the two independent variables (radiant energy and chemical compound) as covariants, for an accurate pairwise comparison.

3.4. Results and Discussions

3.4.1. Determination of Isolate Purity

East Asian eggplants have been previously characterized to have two major peaks absorbing in the 510–540 nm range (Ichiyanagi et al., 2005; Zheng et al., 2011), with *trans*-Dp making up most of the composition (~82%). SCE's PDA chromatogram comprised of 13.8% *cis*-Dp and 80.0% *trans*-Dp within a single run—with the *cis*-isomer eluting before the *trans*-isomer. To characterize these two peaks of the SCE, each of their fragmentation patterns, retention times, and absorbance spectra were compared to the literature. Then, when isolates of *cis*-Dp and *trans*-Dp were produced, the three aforementioned characteristic traits were compared for their identification. The fragmentation patterns of the two isomers were identical to each other. Specifically, 919 M⁺ m/z was detected under Q1 Selective Ion Monitoring (SIM), signifying the intact *p*-coumaroyl acylated Dp. In addition, 303, 465, and 611 M⁺ m/z were detected under MS/MS. These findings are in

congruence with the literature, which states MS/MS fragmentation patterns of 757 (fully intact acylated Dp – one hexose), 611 (intact Dp – one hexose – one deoxy hexose), 465 (intact Dp – one hexose – *p*-coumaric acid), and 303 (delphinidin aglycone) *m/z* (Sadilova et al., 2006a; Yoshida et al., 2003). The absorbance spectra of the two peaks in SCE at 520 nm were compared to the respective isolates' absorbance spectra to use an additional method of characterization. Further information on *cis*-Dp and *trans*-Dp's difference in absorbance spectra will be presented in *Monitoring Photoisomerization with UV-Vis Spectroscopy*.

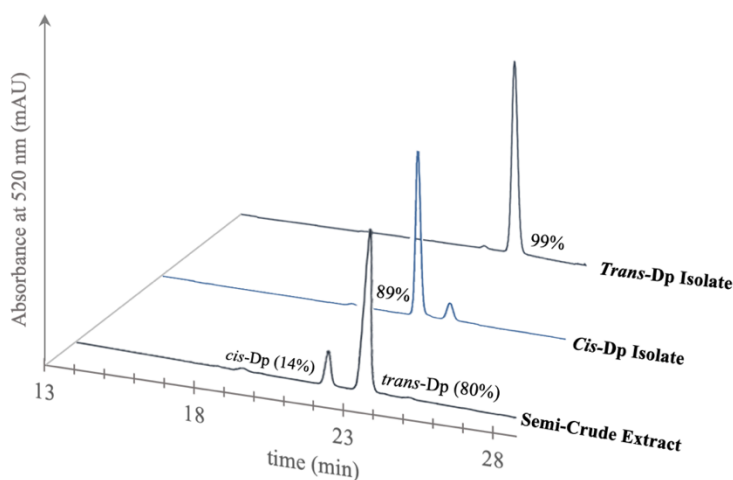


Figure 3.2

HPLC-PDA chromatogram of Semi-Crude Extract (SCE) from East Asian eggplants after semi-purification with a C18 cartridge. *Cis*- and *trans*-Dp isolates represent the PDA chromatograms of the peaks isolated from SCE. Individual peak % was calculated as % of the total area under the curve when peaks were detected at 520 nm.

After semi-prep HPLC isolation, the *trans*-Dp isolate was 92% of the total area under curve (AUC) under max plot absorbance at 260–700 nm and 99% under absorbance at 520 nm (Figure 3.2). Using the same method of quantification, *cis*-Dp represented 80% of the AUC at 260–700 nm and 89% at 520 nm. The impurities detected at 520 nm were the other isomer and 260–700 nm were trace amounts of phenolic acids absorbing at 290 nm and

317 nm. Around 37 min retention time, with solvent B concentration of 40%, a wide peak eluted for both *trans*-Dp and *cis*-Dp isolates that made up 9.7% and 8.9%, respectively. The same wide peak was observed in PDA chromatograms of *trans-p*-coumaric acid in acidified MeOH.

3.4.2. Selected Times for Radiant Light Exposure – Preliminary Tests

Irradiation at 254 nm reached its equilibrium of 37% *cis*-Dp: 63% *trans*-Dp at 30 min, with degradation of $25 \pm 8.1\%$. Though, at 15 min, the extract had photoisomerized to produce 36% *cis*-Dp with $4 \pm 0.9\%$ total pigment degradation. By choosing the exposure parameter to 15 min, pigment degradation was minimized by 6.3 fold, time was saved by 50%, whilst only losing 1% in *cis*- production. Similarly, irradiation was conducted for up to 180 minutes under 365 nm radiant light in order to determine the time in which the isomerization plateau is observed. After 15 minutes of irradiation, 24% *cis*-Dp:76% *trans*-Dp with degradation of 4% is observed. At 30 min, SCE reached its equilibrium of 25% *cis*-Dp:75% *trans*-Dp with degradation of $40 \pm 1\%$, with negligible increase in *cis*-production thereafter. Although equilibrium was observed at 30 min, the chosen time for 365 nm was 15 min because there was only 1% difference in accumulation of *cis*-Dp between 15 min and 30 min, with minimization of 10 fold in total pigment degradation. Since anthocyanins are also prone to degradation under light, general rule of thumb is to select a shorter exposure time. These preliminary tests showed that Dp also follows this rule, thereby saving time with minimal loss in production.

Irradiation with visible radiant energies required longer times to reach equilibrium than it did with UV energies. Photoisomerization with D65 lamp was conducted up to 25 hours, in which equilibrium of 49% *cis*-Dp:51% *trans*-Dp was reached at hour 6, with degradation of $37 \pm 0.5\%$. After the third hour of irradiation, 47% of the total pigment was *cis*-Dp with degradation of $1.1 \pm 0.7\%$ and was therefore chosen as the time parameter for D65. Lastly, irradiation with F2 lamp was conducted for up to 50 hours, in which equilibrium of 52% *cis*-Dp: 48% *trans*-Dp was reached at ~26 hrs, with little increase thereafter. Degradation was approximately 30%. At 20 h, *cis*-Dp production was at 51% with $2.1 \pm 0.2\%$ degradation. Similar to the determination of time for the UV chambers, since 20 h had 1% less *cis*- production while saving 6 hrs, hour 20 was chosen as the F2 time parameter. Determining the acceptable amount of degradation for the amount of isomerization is dependent on the application of the colorant. When isomerization leads to the production of an isomer with greater stability and tinctorial strength at specific pHs, as in the case with *cis*-Dp, less pigment is necessary to produce color. In which case, the consequence of total pigment photodegradation may be neutralized. If further mitigation of degradation is desired, then deoxygenation of photoreactants may be fruitful, though this was not the main purpose of this study.

3.4.3. Monitoring Photoisomerization with UV-Vis Spectroscopy

The behavior of *cis*- and *trans*-Dp under photoisomerization was monitored by ultraviolet-visible (UV-Vis) spectroscopy. Absorbance spectra of the two isomers differ the greatest in their curvatures at 285 nm and 310 nm (Figure 3.3a and 3.3b). While *trans*-Dp had

greater absorbance at 310 nm than 285 nm, its *cis*-counterpart displayed the opposite behavior with greater absorbance at 285 nm than 310 nm. Although irradiation of both isolates under 254 nm for 20 min did not shift the curve patterns of the spectra, the presence of isomerization and degradation was observed as shifts in 285 nm and 310 nm (isomerization) and 540 nm (degradation) occurred. Thus, if the difference:

$$\text{absorbance (285 nm)} - \text{absorbance (310 nm)} = \text{positive (+)},$$

then the mixture is primarily made up of *cis*-isomer; whereas if the difference is a negative number, then the mixture is comprised of majority *trans*-isomer. Although specific numerical values in absorbance comparison at 285 nm or 310 nm was not enough to determine the extent of the photoisomerization reaction, this method of detecting positive

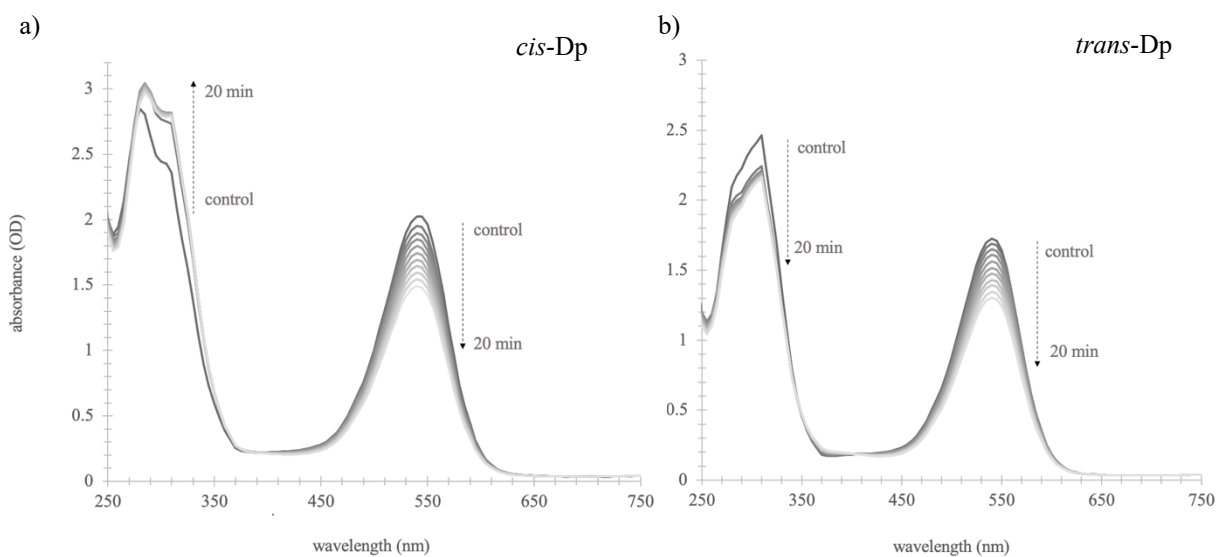


Figure 3.3. Absorbance spectra of a) *cis*-Dp over time of exposure to 254 nm, and b) *trans*-Dp under the same treatment condition. Both compounds were dissolved in 0.01% HCl in MeOH

or negative changes in curvature is a simple way to determine the dominant geometric isomer.

3.4.4. Equilibrium of *Trans* ↔ *Cis* and *Cis* ↔ *Trans* Photoisomerization

Applied radiant energies were not the only factor that affected the photoisomerization reaction of acylated Dp. Three different starting materials—SCE, *cis*-Dp, and *trans*-Dp—resulted in varying extents of isomerization when subjected to light (Figure 3.4). Greatest % isomerization was observed with F2 lamp for SCE, 365 nm for *cis*-Dp, and F2 lamp for *trans*-Dp, showing that the extent of isomerization was dependent on the starting material of the irradiation. UV lamp at 254 nm induced $48 \pm 5.2\%$ for *cis*-Dp, $34 \pm 1.3\%$ for *trans*-

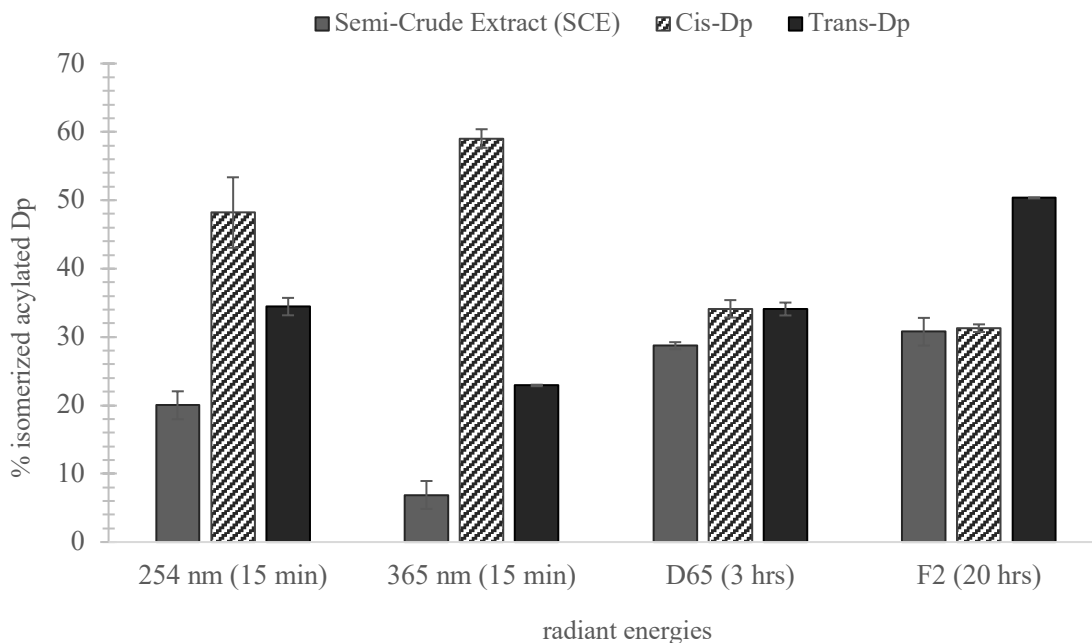


Figure 3.4 Ultraviolet-visible energies impact on isolates' and semi-crude extract (SCE)'s photoisomerization. The time of radiant energy exposure selected for each energies were kept constant. SCE represents a mixture of 86% *trans*-Dp and 14% *cis*-Dp.

Dp, and $20 \pm 2.0\%$ isomerization for SCE. Likewise, UV lamp at 365 nm induced greatest % isomerization for *cis*-Dp at $59 \pm 1.7\%$, *trans*-Dp at $23 \pm 0.1\%$, and SCE at $7 \pm 2.0\%$. This may be attributed to *cis*-Dp absorbing more in the UV region in MeOH, the solvent of isomerization, thereby causing UV to favor *cis* \rightarrow *trans* isomerization rather than *trans* \rightarrow *cis*.

Starting materials' photoisomerization reactivities were different under irradiation with visible energies. Irradiation with D65 lamp yielded comparable conversion for both *cis*- and *trans*-Dp at 34%, with standard deviation of 1.3% for *cis*- and 0.9% for *trans*-Dp. SCE did not isomerize as well as the isolates with 29% photoconversion $\pm 0.5\%$. Irradiation with F2 was unexpectedly the most favorable for isomerizing *trans*-Dp at $50.3 \pm 0.1\%$, while both SCE and *cis*-Dp yielded 31% conversion with standard deviation of 2.0 for SCE and 0.6 for *cis*-Dp. Though these numbers may suggest that SCE's behavior under F2 irradiation was similar to *cis*-Dp rather than *trans*-Dp, the reverse is true based on some simple algebraic calculation. As described by equation (3), % isomerization of SCE was calculated by the subtraction of initial % *cis*-Dp. Consequently, the final % *cis*-Dp accumulation was $\sim 45\%$ AUC, comparable to SCE's 51% *cis*-production by F2 from *Selected Times for Radiant Light Exposure – Preliminary Tests*. Subtraction of $\sim 14\%$ initial *cis*-Dp from 45% is reflected as $\sim 30\%$ isomerization of SCE by F2 in Figure 3.4.

Overall, *cis*-to-*trans* Dp photoisomerization was more efficiently induced by the following radiant energies (from most to least efficient): 365 nm > 254 nm > D65 \approx F2.

Photochemical processes are known to be wavelength-dependent. As illustrated in Figure 3.3, absorption of *cis*-Dp in 0.01% HCl in MeOH occurs the most at ~285 nm, though it also absorbs in the nearby regions—between 260 – 340 nm and 460 – 600 nm. Thus, our experimental finding that UV chamber with spectral peak at 365 nm yields the greatest amount of isomerization is in congruence with theory (details of the spectral distribution is found in Supporting Information 5a-5d). Unlike the broad spectrum that exists for the spectral distribution of UV chamber at 365 nm, UV chamber at 254 nm emits a sharp spectral irradiance that does not overlap in the wavelengths of absorbance for *cis*-Dp. Furthermore, *cis-p*-coumaric acid absorbs at 294 nm, which is red shifted to the *cis*-Dp complex. This bathochromic shift also suggests the presence of intramolecular copigmentation (Rodrigues et al., 2009).

On the other hand, *trans*-Dp to *cis*-Dp photoisomerization was induced in the order of: F2 > D65 \approx 254 nm > 365 nm. Unlike *cis-p*-coumaric acid, *trans-p*-coumaric acid absorbs at an increased wavelength of 309 nm. Visible light's ability to induce excitation of the *trans*-isomer suggests that charge-transfer complexation between *p*-coumaric acid and delphinidin is occurring, followed by non-radiative decay of the complex. Anthocyanin-copigment complex has been understood to excite at low energies, according to theoretical molecular orbital calculations (Ferreira Da Silva et al., 2005). Thus, the exciplex's absorption in wavelengths of visible light supports the order of the light sources favorable for this photoisomerization.

When the samples of irradiated SCE, *cis*-Dp, and *trans*-Dp were analyzed approximately a year later, both *cis*-isomer and *trans*-isomer were present in similar proportions, though in some radiant energy sources, *trans*-isomer's % area decreased more than its *cis*-counterpart did. Further experiments and replications must be done to definitively quantify the stability of each compounds after excitation, since this was not an objective of this study. However, both isomers' presence in samples after a year of storage suggest that the thermal reaction back to *trans*-Dp is not a prominent mechanism.

A comparison between SCE and *trans*-Dp provides an opportunity to explore when it may be desirable to use an isolate versus an extract. The two differ approximately ~20% in their composition, with 80% of SCE comprised of the *trans*-isolate. Additional flavonoids and phenolics in SCE may absorb some of the emitted radiated energy, thereby lessening the total amount of energy absorbed by the chromophore. Thus, irradiation of SCE led to decrease in the extent of isomerization when compared to that of the *trans*-isolate. If the goal is to produce rare *cis*-isomers, then isolates are not required, because the SCE will still isomerize to produce the *cis*-isomer. However, it will not form as much *cis*-isomer as the isomerized *trans*-isomer isolate. The efficiency difference between SCE and *trans*-isomer are as follows, for each spectral energy: D65, 7% (greater for *trans*-isomer); 254 nm, 15%; 365 nm, 16%; F2, 19%. Therefore, if higher quantity of *cis*-Dp is desired, then it would be wise to start with a higher concentration of SCE, rather than using 100 μ M. Contrastingly, if greater rate of photoconversion is desired to produce *cis*-, then using *trans*-isomer isolate as the substrate would yield better results.

3.3.5. Isomerized Extract Spectral Characteristics and Color Expression

Spectral absorbance of *cis*- and *trans*-Dp was compared from 380–700 nm for pH 1–10. In highly acidic pH of 1–2, the patterns of absorbance across the wavelengths were comparable between the two isomers, but *cis*-Dp absorbed slightly greater than *trans*-Dp for both pHs (Figure 3.5). In pH 3–5, both isomers did not absorb, which is supported by the colorless color swatch, indicative of anthocyanins in the hemiacetal form. The greatest difference between the two isomers occurred at pH 8, which is supported by their varying curvature around 380–430 nm (Figure 3.5). In between the aforementioned range of wavelength, *trans*-Dp depicts a clear peak around 370 nm, whereas its *cis*-counterpart behaves closer to a peak around 360 nm, signifying a slight hypsochromic shift. The hypsochromic shift from *trans*- to *cis*-Dp is in congruence with the bluer tone of *trans*-Dp under visual analysis.

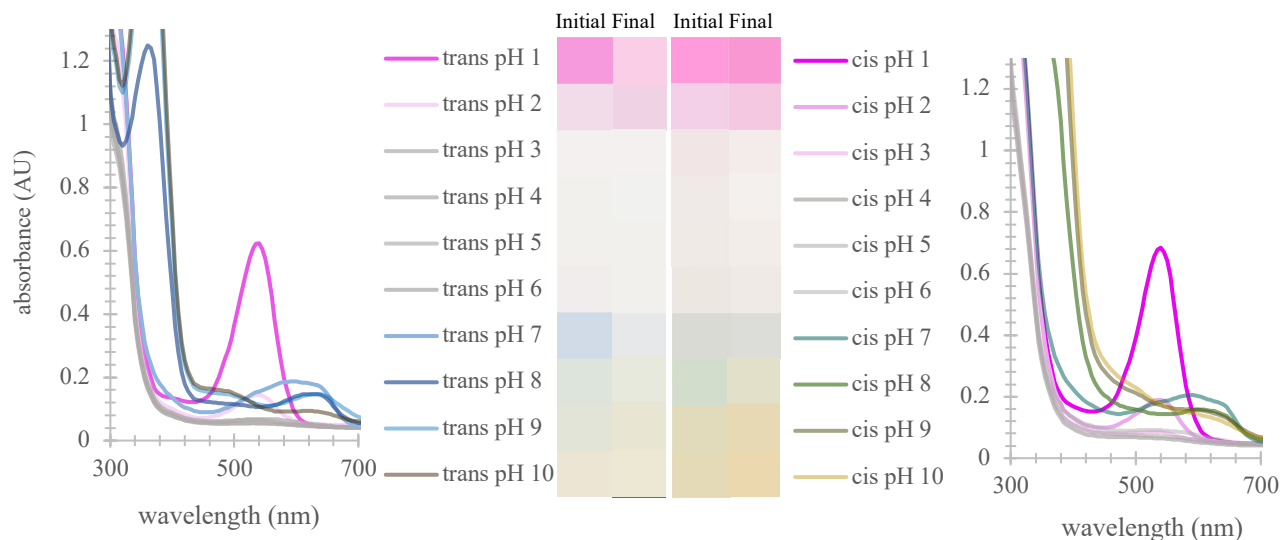


Figure 3.5 Absorbance spectra of a) *trans*-Dp and b) *cis*-Dp under pH 1-10 with corresponding color swatch indicating the two isolate's color comparison at initial (0 h) and final (after 25 h storage for pH 1, 2 and 1 h storage for pH 3-10).

On a previously reported study on *cis*- and *trans*-acylated Dp's color performance, the *cis*-isomer was shown to have greater half-life than the *trans*-isomer in pH 1.¹³ This finding is consistent with the noticeable color vibrance of *cis*-Dp in comparison to *trans*-Dp, after 25 hrs of storage under 20 °C in the dark, especially in the acidic pH range (Figure 3.5). The aforementioned study also reported shorter color half-life for *cis*-Dp at alkaline pH in comparison to its *trans*-counterpart. In this study, the *cis*-isomer in alkaline pH retained its saturation for longer than *trans*-Dp, as depicted by the color swatch (Figure 3.5). The findings could be attributed to the faint starting color at time 0 of the *cis*-isomer.

Irradiation of SCE under 254 nm, D65, and F2 lamp for their selected times resulted in comparable color characteristics to each other, regardless of the source of the radiant energy. Since the final equilibrium of *trans*-Dp-to-*cis*-Dp in irradiated SCE was known to be different for each of the radiant energy, their difference in final color characteristics

were expected. As indicated in *Selected Times for Radiant Light Exposure – Preliminary Tests*, irradiation with 254 nm yielded 36% isomerization and irradiation with F2 lamp yielded the greatest conversion among the radiant energies at 51%. Despite their difference in isomer composition post-irradiation, their similar

color characteristics suggest ~15% difference in isomer composition does not affect color characteristics. It is possible that a greater difference in chemical equilibrium, such as 60% *cis*-Dp vs 30% *cis*-Dp, may show a difference in color. Further studies on the relationship between isomer composition and color characteristics will need to be conducted for definitive conclusions.

Irradiated SCE's colorimetric data were compared to both *cis*- and *trans*-Dp isolates' in acidic pH and alkaline pH, but not from pH 3 to pH 5, since both isomers bleached in this region (Figure 3.5). In acidic pH, irradiated SCE exhibited similar color expression to the *trans*-Dp isolate. Quantitative comparison showed that $\Delta E_{SCE-trans}$ was around 5,

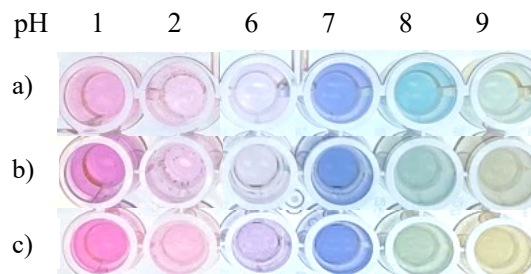


Figure 3.6 comparison between a) *trans*-Dp isolate, b) *cis*-Dp isolate, and c) SCE irradiated with 254 nm for 15 min at t = 0 (15 minutes after equilibration in pH buffers) before storage.

whereas $\Delta E_{SCE-cis}$ was closer to 10. Upon qualitative analysis, irradiated SCE resembled similar hue of *trans*-Dp in pH 1 and 2, but with the color intensity of *cis*-Dp (Figure 3.6). This discrepancy could be due to the fact that the concentration of irradiated SCE was 100 μm whereas the isolates were 90 μm , which would affect c^*_{ab} and L^* . H^*_{ab} values would be unaffected by slight concentration differences, and upon its comparison, irradiated SCE was more similar to *cis*-Dp isolate in acidic pH. However, *cis*- and *trans*-isomers only differed by 1° in hue angle, so this observation may not be detected by consumers or untrained human eyes.

In pH 6 to pH 9, irradiated SCE resembled color expression of *cis*-Dp, as indicated by smaller $\Delta E_{SCE-cis}$ rather than $\Delta E_{SCE-trans}$ (Table 3.1). This quantitative analysis is supported by Figure 3.6, which shows irradiated SCE's greater chromaticity in pH 6 and green hue in pH 8—much like the *cis*-Dp isolate. The color expression of irradiated SCE was expected to be like the dominant isomer, or *trans*-Dp for many of the radiant energies. However, its resemblance to *cis*-Dp suggests that in alkaline conditions where ACN are often unstable, *cis*-Dp was able to persevere—potentially due to an increase in intramolecular copigmentation effect as a result of the *cis*-hydroxycinnamic acid conformation (Eiro & Heinonen, 2002; George et al., 2001).

Table 3.1 Colorimetric analysis of semi-crude extract (SCE) after irradiation with 254 nm, D65, and F2. CIELAB values were acquired after equilibration and after 24 hours of storage in the dark at 20 °C. ΔE was calculated for difference between irradiated SCE and *cis*-Dp isolate. L*: lightness; a*: red (+) to green (-); b*: yellow (+) to blue (-); c*_{ab}: chroma; h*_{ab}: hue angle

		pH 1	pH 2	pH 6	pH 7	pH 8	pH 9
0 h	L*	76.5	87.8	87.5	79.5	85.6	86.2
		(±1.3)	(±1.1)	(±0.9)	(±1.0)	(±0.3)	(±0.8)
	a*	37.1	12.5	3.5	-1.1	-1.7	0.02
		(±2.8)	(±2.1)	(±0.3)	(±0.08)	(±0.1)	(±0.3)
	b*	-11.9	-0.3	2.2	-5.7	16.0	20.9
		(±1.1)	(±0.8)	(±0.3)	(±1.1)	(±0.4)	(±1.1)
	c* _{ab}	39.0	12.9	4.1	5.8	16.1	20.9
		(±2.9)	(±1.7)	(±0.4)	(±1.1)	(±0.4)	(±1.1)
	h* _{ab}	342.4	184.7	32.4	258.7	96.2	90.0
		(±0.5)	(±6.3)	(±5.1)	(±0.9)	(±1.1)	(±0.9)
	$\Delta E_{SCE-cis}$	9.5	7.6	5.2	8.8	10.8	5.6
	$\Delta E_{SCE-trans}$	5.5	5.8	7.0	9.5	17.2	17.6
24 h	L*	79.7	86.2	91.3	90.0	89.7	90.7
		(±1.1)	(±1.1)	(±1.2)	(±0.3)	(±0.2)	(±0.2)
	a*	31.3	16.3	0.1	-0.2	-0.9	-1.4
		(±2.2)	(±2.3)	(±0.2)	(±0.1)	(±0.1)	(±0.04)
	b*	-7.9	-1.5	8.7	12.9	20.3	20.0
		(±0.9)	(±0.5)	(±0.07)	(±0.4)	(±0.7)	(±1.1)
	c* _{ab}	32.2	16.4	8.7	12.9	20.3	20.0
		(±2.3)	(±2.3)	(±0.08)	(±0.4)	(±0.7)	(±1.1)
	h* _{ab}	345.9	354.8	89.4	91.0	92.5	94.1
		(±0.6)	(±1.1)	(±1.6)	(±0.4)	(±0.5)	(±0.4)
	$\Delta E_{SCE-cis}$	36.2	21.2	7.0	1.1	6.0	7.5
	$\Delta E_{SCE-trans}$	7.3	16.0	11.2	10.5	3.9	4.3

3.4.6. Isomerized Extract Color Stability

Color stability of irradiated SCE was measured for up to 24 hours by storage in the dark at 20 °C (Figure 3.7). According to the colorimetric values in Table 3.1, the c^*_{ab} value of irradiated SCE at pH 1 decreased by 6.8 after storage, and still retained much of its color. This is comparable the behavior of *cis*-Dp at pH 1 after 25 hours of storage, which decreased in its c^*_{ab} value by 2.1, rather than the *trans*-isomer, which decreased in saturation by 24.4 after storage. Although the irradiated SCE did not retain its green-blue hue in alkaline pH, its c^*_{ab} increased after 24 hours of storage, just as *cis*-Dp—though, this increase in chromaticity is most likely due to browning. Comparison of the color between irradiated SCE in pH 1 (Figure 3.7) to the color swatch of *trans*-Dp and *cis*-Dp after 25 hours of storage (Figure 3.5) shows that the color intensity of the irradiated mixture remained vibrant like the *cis*-isomer in acidic pH. This allows for the opportunity to achieve favorable color performance using extracts with mixed composition of isomers, without the labor and resource-intensive method of acquiring pigment isolates.

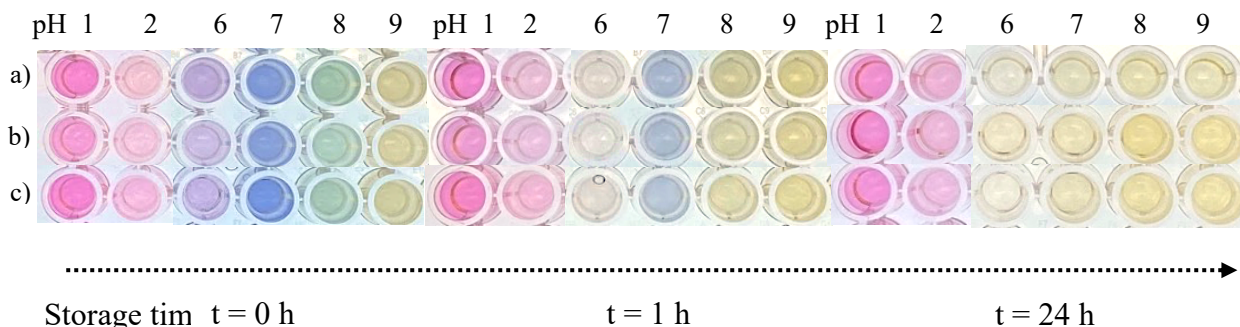


Figure 3.7 Color characteristics of semi-crude extract irradiated with a) 254 nm for 15 min (*cis*-Dp: 36% and *trans*-Dp: 64%) b) F2 lamp for 20 hrs (*cis*-Dp: 51% and *trans*-Dp: 49%), and c) D65 for 3 hrs (*cis*-Dp: 47% and *trans*-Dp: 53%). Isomerized samples were expressed in the pHs with the greatest difference from comparison of the *cis*- and *trans*-Dp—pH 1, 2, 6, 7, 8, and 9.

3.5. Conclusions

Ultraviolet-visible energies induced photochromism of acylated Dp, though at varying yields and efficiencies depending on the starting material. Since specific laser wavelengths are often difficult to acquire and expensive, industry-accessible energies sources were used in this study. Excitation of *trans*-chromophore with visible radiant energy yielded whereas ultraviolet energies produced more isomerization of the *cis*-chromophore. Reactivity of the mixture of *trans*- and *cis*-acylated Dp were distinct from irradiation of isolates when the applied energies were ultraviolet. The resulting color differences between the two isomer pigments were the greatest in pH 1 and alkaline pH, though their stability varied the most in pH 1. The color performance of irradiated extracts were similar, regardless of the wavelengths of the applied energy. Their color characteristics in both the acidic and alkaline pHs were comparable to that of *cis*-isolates, including at pH 1, in which the irradiated extract were deemed as stable as the *cis*-isolate. This study gives insight to the photochromic properties of acylated Dp, as it absorbs ultraviolet-visible light. Production of rare *cis*-acylated Dp with easily acquirable light sources can aid in providing a greater color palette for the food industry.

Chapter 4. Photoisomerization Reactivity of *Trans*-Acylated Cyanidins with Varying Mono- and Di-acylation Patterns

4.1. Abstract

Anthocyanins acylated with hydroxycinnamic acids can undergo ground-state charge transfer to induce photoisomerization. Production of pigment isomers diversifies color intensity and stability since isomers have distinct chemical characteristics. In this study, the photoreaction was triggered by visible light and the quantification of its resulting photoproducts were measured with UV-Vis spectrophotometry and uHPLC-PDA-ESI-MS/MS. Cyanidins mono- and di-acylated with combinations of *p*-coumaric, ferulic, and sinapic acids were evaluated and compared to mono-acylated delphinidin with *p*-coumaric acid. The position of glycosyl acylation made the biggest influence on the occurrence of photoisomerization, in which the *trans*-acid attachment position C₆'' isomerized but the C₂'' did not. The number and type of acylation also affected the photoreaction, though at lesser extents than acylation position. Monoacylated cyanidins produces greater amount of their *cis*-isomers in comparison to diacylated cyanidins. In addition, cyanidins acylated with *p*-coumaric acid isomerized the most, regardless of the number of acid attachments. Manipulation of structural variations can be used to further understand how photoisomerization influences the pigment intramolecular complexation and its potential differences in their resulting expression.

Keywords: *trans* to *cis* isomerization, hydroxycinnamic acid, acylation patterns, isolates, intramolecular copigmentation, pigment degradation

4.2. Introduction

Anthocyanins (ACNs) are polyphenolic pigments that are present in fruits, vegetables, flowers, and their pH-dependent color can be used for a variety of food applications (Sigurdson et al., 2017; Wallace & Giusti, 2015). Their diversity in chemical structure allows for their range of reactivity, color expression, stability, and therefore, application (Castañeda-Ovando et al., 2009). ACN acylation patterns play an integral role in their structural diversity and can possess variations in the position, type, and number of substitutions (Zhao et al., 2017). These acylations are primarily with organic acids, though sometimes it may be inorganic (Giusti & Wrolstad, 2003; Toki et al., 1994). Even within the category of organic acids, there is considerable molecular diversity, with aliphatic or aromatic carboxylic acid moieties substituted most often on C₆' of the C₃ glycosylation, though it is also possible on different positions of the chromophore (ex. C₇ acylation in butterfly pea flower) (Terahara et al., 1989) and different positions on C₅ glycosylation (Giusti et al., 1999). Furthermore, ACNs can also have one or more acylations, making the combination of acylation patterns ever expansive (Vidana Gamage et al., 2022).

An exceptional property of hydroxycinnamic acylation is its ability to photoisomerize, producing a photoproduct that reacts differently than its original isomeric configuration. Intramolecular copigmentation of the anthocyanin flavylum and its covalently-bound copigment can act as electron-donor/acceptor pairs. Studies have shown that

photoisomerization of delphinidin-3-*p*-coumaroyl-rutinoside-5-glucoside can occur with ultraviolet and visible light in various solvents (Yoshida et al., 2002), buffers (Yoshida et al., 1990), and light sources (Yoshida et al., 2003). However, this phenomenon has yet to be applied to hydroxycinnamic acylated cyanidins, the most common ACN aglycone found in fruits and vegetable (Wu et al., 2006). The beauty of glycosyl acylations of cyanidins is its natural variation of pigment composition in commercially relevant edible sources; it can have one or two acylations, *p*-coumaric acid/ferulic/or sinapic acids, or glycosyl acyl position in C₂' or C₆'. Isomerization of di-acylated ACNs have been seldom discussed in the literature, though their increased photostability may suggest the possibility of less occurrence of photoisomerization due to their increased planar stacking between the flavylium and the di-copigment (Gérard et al., 2019; Malien-Aubert et al., 2001; Song et al., 2013). ACN flavylium and colorless molecules such as phenolic acids can react as electron acceptor-donor pairs, thereby producing a greater stability and increased chromic effect—a phenomena known as copigmentation (Brouillard et al., 1989; Trouillas et al., 2016). When this non-covalent interaction happens between a flavylium and hydroxycinnamic acid, it can self-fold in three dimensional space, further known as intramolecular copigmentation (Figueiredo et al., 1999). This interaction may affect isomerization by affecting the stability of chromophore-copigment stacking. Thus, the objective of this study was to compare the reactivity of mono- and di-acylated cyanidin (Cy) under visible light photoisomerization and further understand the influence of acylation patterns on their photoreactivity.

4.3. Materials and Methods

4.3.1. Materials

Red cabbage powders were donated by Mars Wrigley Confectionary (Hackettstown, NJ, USA) and were purified to obtain the following pigments: 1) cyanidin-3-(2'-sinapoyl)-sophoroside-5-glucoside (Peak B), 2) cyanidin-3-(6'-*p*-coumaroyl)-sophoroside-5-glucoside (Cy-pC), 3) cyanidin-3-(6'-feruloyl)-sophoroside-5-glucoside (Cy-fer), 4) cyanidin-3-(6'-sinapoyl)-sophoroside-5-glucoside (Cy-sin), 5) cyanidin-3-(6'-*p*-coumaroyl)-(2'-sinapoyl)-sophoroside-5-glucoside (Cy-pC-sin), 6) cyanidin-3-(6'-feruloyl)-(2'-sinapoyl)-sophoroside-5-glucoside (Cy-fer-sin), and 7) cyanidin-3-(6'-sinapoyl)-(2'-sinapoyl)-sophoroside-5-glucoside (Cy-sin-sin). Chemical solvents used for purification and analyses were: hydrochloric acid (HCl), formic acid, acetone, chloroform, ethyl acetate (EtOAc), methanol (MeOH), potassium chloride (KCl), citric acid (CA), monosodium phosphate (NaH₂PO₄), disodium phosphate (Na₂HPO₄), sodium carbonate (Na₂CO₃), HPLC and MS-grade acetonitrile (MeCN), and finally, HPLC and MS-grade H₂O. These chemicals were purchased from either Sigma-Aldrich, Co. (St. Louis, MO, USA) or Thermo Fisher Scientific (Waltham, MA, USA).

4.3.2. Anthocyanin Purification and Identification

Acylated ACN were purified from powdered red cabbage extract by loading Sep-Pak Vac 20cc C18 cartridges (Waters Corporation, Milford, MA, USA) for solid phase extraction. The loaded extracts were washed with 0.01% HCl in H₂O, then with EtOAc, and finally with 0.01% HCl in MeOH. The first two chemicals were washed three to four times, but

the final elution with MeOH was performed until all remaining pigments were recovered from the cartridge, according to methods described by Rodriguez-Saona and Wrolstad (2001). The semi-purified ACN were characterized by a Nexera-i-LC 2040C 3D ultra-high performance liquid chromatography with a photodiode array detector (uHPLC-PDA) coupled to a LCMS-8040 triple quadrupole mass spectrometer with electrospray ionization (ESI-MS/MS, Shimadzu, Columbia, MD, USA). Chromatographic separation was done with Kinetex 1.7 μm F5 column with 100 Å pore size and 100 \times 2.1 mm dimensions (Phenomenex, Torrance, CA, USA). The PDA chromatograms were collected for relative quantitation at 510–540 nm by % area of 7 desired major peaks.

The separated peaks were characterized by their retention times, fragmentation patterns, and absorbance spectra. The solvents used for gradient-elution chromatography were 4.5% formic acid in MS-grade H₂O for solvent A and MS-grade MeCN for solvent B. The uHPLC gradient had a starting B% concentration of 0% for 2 min, followed by 7% for 8 min, and finally flushed at 30% for 3 min, before equilibrating back down to the starting B concentration. The Nexera-i-LC 2040C oven was at 60 °C, collision energy of -35 eV, ESI interface with nebulizer gas flow of 1.2 L/min, DL temperature 230 °C, heat block temperature 200 °C, and drying gas flow of 12 L/min. The ions were scanned under 5 parameters: Q1 total scan from 100 – 1000 m/z (+), Q1 total scan 100 – 1000 m/z (–), Q1 Selected Ion Monitoring (SIM) 164, 195, 224.80 m/z (+), Q1 SIM 121, 123, 151 m/z (+), Q1 SIM 162.7, 193, 222.8 m/z (–), and Q1 SIM 119, 121, 149 m/z (–). The injection volume for the runs were 5 μL . Gradient conditions were further adjusted for elution of cyanidin-3-(2'-sinapoyl)-sophoroside-5-glucoside: Starting from 0% to 8% for 6 min,

flushed at 8% for 4 min, and finally to 15% for 2 min before equilibrating down to the starting B%. Lab Solutions Software Ver.1 (Released 5.80) was used for data integration, analysis, and interpretation (Shimadzu, Columbia, MD, USA).

4.3.3. Monoacylated and Diacylated Anthocyanin Isolation

Trans-monoacylated and diacylated ACN in the semi-purified red cabbage extract were concentrated, mixed with 0.01% HCl in H₂O, and filtered through 0.2 μ m syringe filter for semi-preparative HPLC. *Trans*-monoacylated and diacylated ACN from the semi-purified extract were loaded onto a reverse phase semi-preparative HPLC system (Shimadzu, MD, USA) with LC-6AD pumps, a BM-20A communication module, a SIL-20A HT autosampler, a CTO-20A column oven, a SPD-M20A Photodiode Array detector, and a pentafluorophenyl (PFP) column (5 μ m particle size, 100 Å pore size, in a 250 \times 21.2 mm) and ran at a flow rate of 12.0 mL/min (Phenomenex®, Torrance, CA, USA). LabSolutions Software (Shimadzu, Columbia, MD, USA) was used to monitor the eluting *trans*-acylated pigments. First fractionation was acquired using a FRC-10A fraction collector (Shimadzu, Columbia, MD, USA), but secondary fraction collection was done manually. Similar to the anthocyanin purification process, isolation required 4.5% formic acid in HPLC-grade H₂O for solvent A and MeCN for solvent B. The gradient for pigment isolation started with a starting B concentration of 16%, then increased to 25% for 15 min, flushed at 25% for 1 min, and brought up to 30% for 4 minutes before equilibrating back to the starting B concentration. After the peaks were collected, the isolates were washed with 0.01% HCl in H₂O and reconstituted in 0.01% HCl in MeOH. Subsequently, the solvent was removed by rotary evaporation (Brinkmann Büchi Rotavapor, New Castle, DE, USA) and the isolates

were stored in minimal amount of acidified MeOH for the determination of their concentration.

The purity of isolated pigments were quantified on uHPLC-PDA-MS/MS by measuring the % area under the curve (AUC) in two max plots: 510–540 nm and 260–700 nm. The % purity quantified under 510–540 nm represented the % of desired pigment out of total amount of anthocyanin pigments. The latter % purity represented the % of desired pigment out of total amount of anthocyanins, phenolics, and flavonoids.

4.3.4. Monomeric Cyanidin Quantitation and Standardization

The concentration of the 7 isolates were determined as monomeric cyanidin-3-glucoside equivalents at pH 1, in reference to Giusti and Wrolstad (2001). The absorbances of the said isolates were measured at 700 nm and their λ_{max} of 540 nm under pH 1, using a SpectraMax 190 Microplate Reader (Molecular Devices, Sunnyvale, CA, USA). Though the pH differential method's standard protocol uses pH 1 and pH 4.5, the latter was not used since one of the monoacylated cyanidins did not bleach in pH 4.5.

The concentrates of isolates were diluted to 100 μ m with 0.01% HCl in MeOH and further standardized to an absorbance of $\approx 1.1 \pm 0.05$ at the $\lambda_{vis-max}$.

4.3.5. Photoisomerization with Visible Light

According to La and Giusti (2022), visible light (with F2 lamp) induced the greatest amount of photoisomerization of acylated delphinidins when accounting for their respective photodegradation as a result of exposure to light. Thus, visible light chamber equipped with 15 W of F2 lights (MiniMatcher MM-2e, GTI Graphic Technology Inc., Newburgh, NY, USA) were used to irradiate 7 selected monoacylated and diacylated cyanidins, according to the methodology used by La and Giusti (2022). The isolates were subjected to irradiation with visible light for 20 hours, in a poly-D-lysine-coated polystyrene 96 well-plate covered with ClearVue adhesive film (Molecular Dimensions, Holland, OH, USA). The light chamber was covered with a white, reflective absorbent pad to ensure the radiant energies are contained as much as possible. After irradiation, aliquots of the isolates were mixed with 0.01% HCl in H₂O and stored in -18 °C for 24 hours before 3 days before uHPLC-PDA-MS/MS analysis.

Isomerization and degradation of isolates were calculated as percentages using the following equations (1, 2):

$$(1) \textit{ Photoisomerization} = (AUC_{510-540 \text{ nm } cis \text{ cyd}})_{t_{20}} / (AUC_{510-540 \text{ nm } cis + trans \text{ cyd}})_{t_{20}}$$

$$(2) \textit{ Photodegradation} = 1 - [(AUC_{510-540 \text{ nm } trans \text{ cyd}})_{t_{20}} / (AUC_{510-540 \text{ nm } trans \text{ cyd}})_{t_0}]$$

In which AUC = area under the curve and cyd = acylated cyanidin pigments

Quantification of the extent of isomerization was done by calculating the area under the curve of the pertinent peaks in max plot 510 – 540 nm as depicted by uHPLC-PDA-ESI-MS/MS chromatograms. The instrumentation and running conditions were the same as

Anthocyanin Purification and Identification. The integrated AUC was compared to the calculated % isomerization and degradation for further interpretation of data.

4.3.6. Rapid Monitoring of Cyanidin Excitation with Ultraviolet-Visible Spectrophotometry

Based on the findings from the methodology detailed in *Photoisomerization with Visible Light*, additional attempts of cyanidin isomerization were conducted using a higher excitation energy with UV Chamber (254 nm), emitting 40 W of power with internal dimension of 13.7 cm (l) × 18.1 cm (w) × 16.8 cm (h) (UV Stratalinker 1800, Stratagene, La Jolla, CA, USA). The standardized Peak B and mono-sin pigments were placed in a poly-D-lysine-coated polystyrene 96 well-plate for each of the following time points: 0 h (control), 1 h, 2 h, 3 h, 5 h, and 10 h and sealed with a clear adhesive film. After the completion of each irradiation time points, aliquots were transferred to a new 96 well-plate and their spectral characteristics from 250 – 650 nm were measured in 2 nm increments, using a SpectraMax 190 Microplate Reader.

4.3.7. Comparison of *Trans*-Acylated Cyanidin and Delphinidin's Isomerization Reactivity

To further understand the reactivity of acylated cyanidin photoisomerization in reference to the pigment described in the literature, delphinidin-3-(*trans*)-*p*-coumaroyl-rutinoside-5-glucoside (Dp-mono-pC) was extracted, purified, isolated, characterized, and quantified according to the methods detailed by La and Giusti (2022). Both Dp-mono-pC and

cyanidin-3-(6'-*p*-coumaroyl)-sophoroside-5-glucoside (Cy-mono-pC) in 0.01% HCl in MeOH were standardized to an absorbance of $\approx 1.1 \pm 0.05$ at the $\lambda_{vis-max}$. Cy-mono-pC treated with 20 h of visible light excitation in a sealed poly-D-lysine-coated polystyrene 96 well-plate. Three replicates were acquired.

Extent of *trans* \rightarrow *cis* photoisomerization and photodegradation under visible light were quantified using uHPLC-PDA-ESI-MS/MS with the same instrumentation as found in 4.3.2. *Anthocyanin Purification and Identification*, but with Pinnacle DB IBD column (1.9 μm , 50×2.1 mm, 140 Å, Restek Corporation, Bellfonte, PA, USA) rather than the previously used Kinetex F5 column.

4.3.8. Statistical Evaluation of Data

One-way analysis of variance (ANOVA) ($\alpha = 0.05$) were performed for pigment's response to the LCMS quantification of isomerization and degradation under 510 – 540 nm. Statistical analyses were done using Graph Prism 9 (GraphPad Software for macOS, Version 9.3.1, San Diego, CA, USA). Multiple comparisons between the means of the independent variable were determined with Tukey's test ($\alpha = 0.05$).

4.4. Results and Discussions

4.4.1. Acylated Cyanidin-3-sophoroside-5-glucoside Derivatives Isomerized under Fluorescent Light

A chromatogram showing the different compounds separated from cabbage is presented in Table 4.1, along with their relative abundance and abbreviated names. When separating semi-purified red cabbage extract, the order of elution on a reverse-phase chromatography involves 8 main pigments—non-acylated cyanidin, and the 7 acylated pigments.

The first pigment, non-acylated cyanidin, is often called Peak A, which leaves the second elution to follow as Peak B. The rest of the mono- and di-acylated pigments in semi-purified red cabbage extract were named after the type of acyl groups – *p*-coumaric (pC), ferulic (fer), and sinapic (sin) acids, which were used once or twice depending on the number of acylations. The nomenclature of Peak B was derived from the precedent literature on hydroxycinnamic acylated cyanidins, which were distinguished due to their difference in acylation pattern from the typical aromatic acylation on C₆ of the C₃ glycosylation (Denish et al., 2021; Fenger et al., 2021). The purities of the 7 acylated pigments were quantified under absorbance at 510 – 540 nm, the wavelength range containing their $\lambda_{vis-max}$. Their absorbance from 260 – 700 nm was also detected to gauge the amount of phenolic impurities. Most of the isolates has purities over 91.0%, with the exception of Cy-fer and Cy-sin-sin. The former consisted of 5.6% of Cy-pC impurity and 16.8% of Cy-sin impurity. It is possible that these impurities play a small part in the photoisomerization of Cy-fer, but the quantification was proportionally calculated with the lower area under the curve of the isolate in mind. Likewise, Cy-sin-sin had impurities of

8.5% and 7.1% of *trans*-acylated Cy that were not Cy-pC-sin nor Cy-fer-sin based on their respective retention times and absorbance spectra. Further identification of these impurities were possible with MS, but unnecessary since the peaks were minor and relative quantifications were used for final calculations.

Photoisomerization was evident a by the production of a new distinctive peak with earlier retention time and unique absorbance spectra, which is suggestive of the *cis*-isomer (Fig 4.1). Cy-*cis*-pC had a greater absorbance at 280 nm than 320 nm, as compared to Cy-*trans*-pC that had a greater absorbance at 312 nm. This behavior was also observed for diacylated isomers, in which Cy-*cis*-pC-sin had less absorbance around 320 nm than Cy-*trans*-pC-sin.

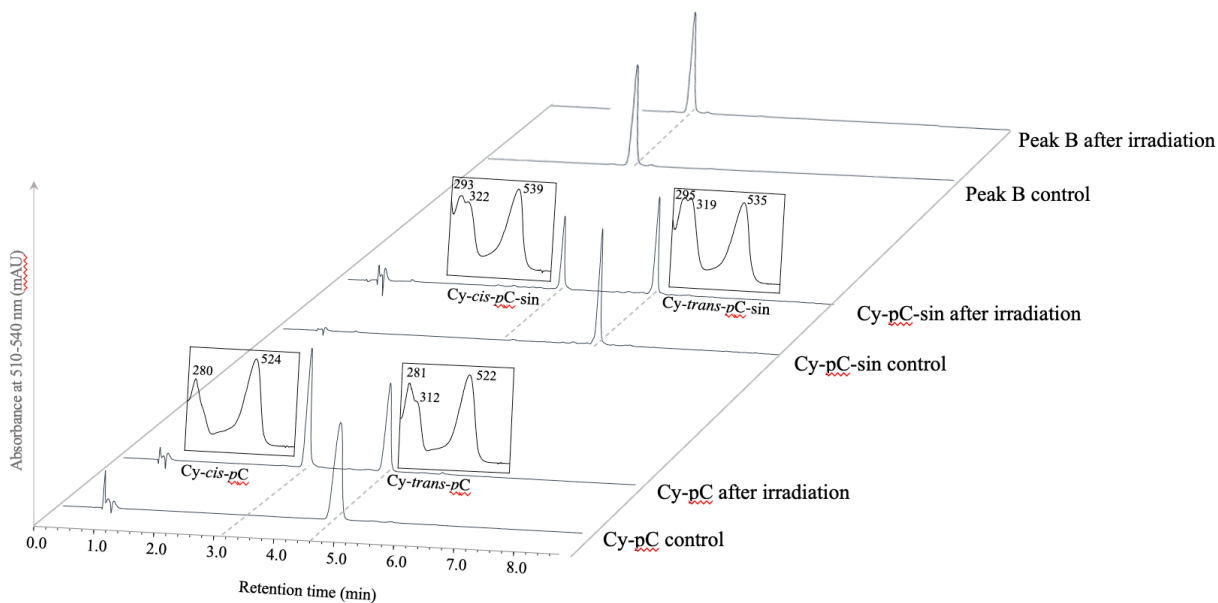
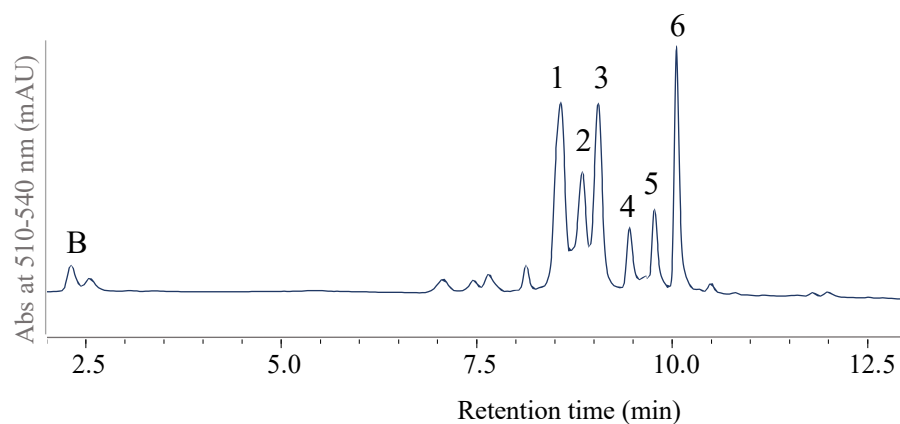
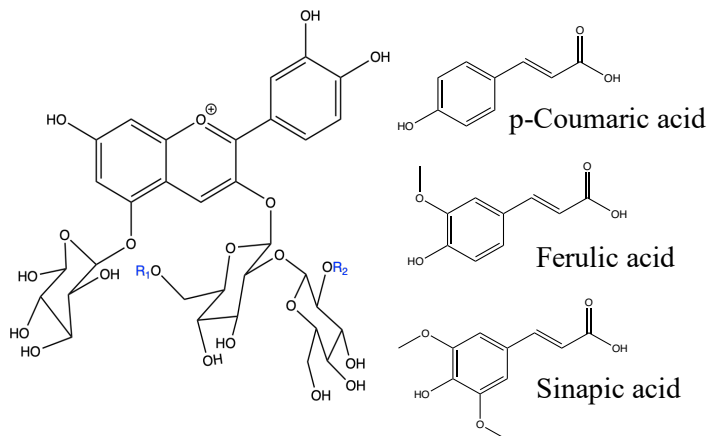


Figure 4.1 Typical HPLC chromatogram of monoacylated and diacylated pigments before and after visible light excitation and their resulting photoisomerization.

Qualitative monitoring of the amount of *cis*- and *trans*-isomers by comparing the absorbance at 280 and 320 nm was a method performed with acylated delphinidins as well (La & Giusti, 2022). Upon further identification of the newly formed peaks, the mass of the *cis*-isomers matched that of the *trans*-isomers, as well as their MS/MS fragmentation (for all mono- and di-acylated Cy).

Additionally, photoisomerization of diacylated *trans*-Cy formed one new peak, as it was observed for monoacylated *trans*-Cy. This was a surprising and exciting finding, because two acid substitutions imply that theoretically, four isomers can exist. Thus, it was hypothesized that three new peaks may form. However, as depicted in Figure 4.1, excitation of diacylated Cy produced one new peak, indicating one new isomer. This finding was in alignment with that lack of *cis*-isomer in Peak B, which showed a resistance to photoisomerization of acylation on C_{2''} of the second glucose. Thus, the C_{2''} acylation in diacylated Cy may also be staying in their *trans*-configuration, thereby only producing a *cis*-isomer of the first glycosylacyl group on C_{6''} position.

Table 4.1 HPLC-PDA chromatogram of red cabbage extract powder semi-purified in 0.01% HCl in MeOH from which the 7 isolates of interest were purified, along with their chemical structures, abbreviated name, and % purity.



Peak #	Identity	Abbreviated Name	R1	R2	% Purity (510 – 540 nm)
B	Cyanidin-3-(2"-sinapoyl)-sophoroside-5-glucoside	Peak B	H	Sinapic acid	99.3%
1	Cyanidin-3-(6"- <i>p</i> -coumaroyl)-sophoroside-5-glucoside	Cy-pC	<i>p</i> -Coumaric acid	H	100.0%
2	Cyanidin-3-(6"-feruloyl)-sophoroside-5-glucoside	Cy-fer	Ferulic acid	H	74.7%
3	Cyanidin-3-(6"-sinapoyl)-sophoroside-5-glucoside	Cy-sin	Sinapic acid	H	91.0%
4	Cyanidin-3-(6"- <i>p</i> -coumaroyl)-(2"-sinpoyl)-sophoroside-5-glucoside	Cy-pC-sin	<i>p</i> -Coumaric acid	Sinapic acid	96.7%
5	Cyanidin-3-(6"-feruloyl)-(2"-sinpoyl)-sophoroside-5-glucoside	Cy-fer-sin	Ferulic acid	Sinapic acid	97.5%
6	Cyanidin-3-(6"-sinapoyl)-(2"-sinpoyl)-sophoroside-5-glucoside	Cy-sin-sin	Sinapic acid	Sinapic acid	82.7%

4.4.2. Impact of Acylation Position on Photoisomerization and Photodegradation

Among the 7 isolated mono- and di-acylated Cy, Peak B was the only pigment that did not produce any of its *cis*-isomers under irradiation with visible light. Under reverse-phase chromatography, *cis*-hydroxycinnamic acids often elute as a distinctive new peak with an earlier retention time and an absorbance spectrum that differs from its *trans*-isomer (Hayashi et al., 1998; Yoshida et al., 1990). This was not observed in the HPLC-PDA chromatogram as illustrated in Fig 4.1. The gradient of the elution was further adjusted to isocratic flow from 6 – 10 min for the irradiated Peak B sample, but once again, only a single peak was observed, indicating the lack of a *cis*-isomer. Fragmentation patterns of both the non-irradiated and irradiated Peak B pigments matched. Under Q1 Selected Ion Monitoring (SIM), 979 m/z [M]⁺ represented the intact Peak B, and MS/MS ions of 449 m/z [M]⁺ and 287 m/z [M]⁺, signifying the fragmentation of cyanidin-3-sophoroside-5-glucoside (Cy-3-soph-5-glu) into Cy-3-glu and Cy aglycone, respectively (Ahmadiani et al., 2014, 2016; Singh et al., 2022). The irradiated Peak B pigment also produced the same fragments of 979 m/z, 449 m/z, and 287 m/z [M]⁺ as non-irradiated Peak B, but also fragmented to 817 m/z [M]⁺, which was the aglycone-glucose (K. A. Mansour et al., 2021). Further examination of Peak B's resistance to isomerization is discussed in *Ultraviolet Excitation of Peak B for Maximal Generation of Photoisomerization*.

When comparing reactivity of irradiated cyanidin pigments acylated with mono-sinapic acid in two different acylation positions—Peak B and Cy-sin—the former yielded no photoisomerization and 26.1±6.6% photodegradation, while the latter yielded 45.2±2.7%

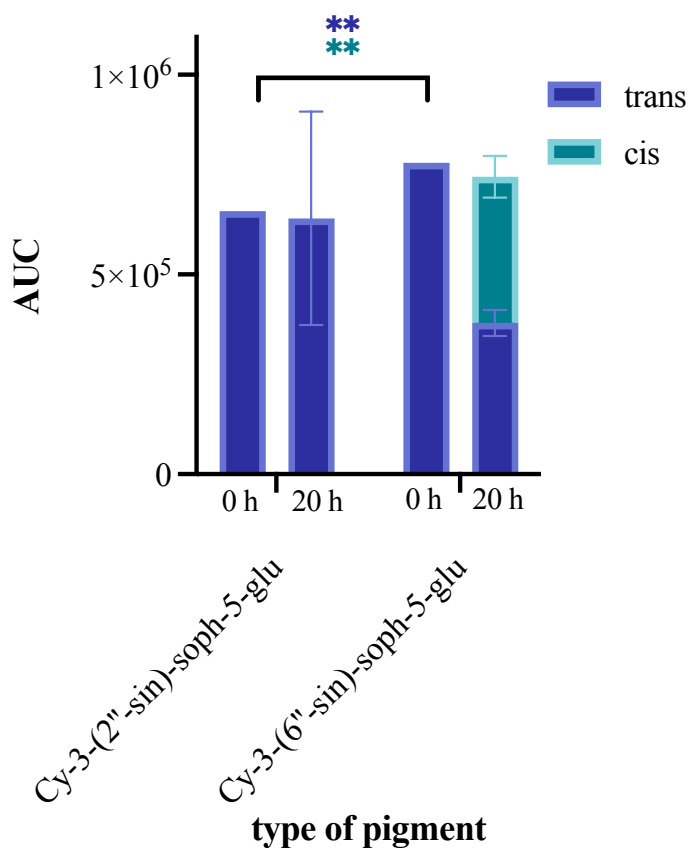


Figure 4.2.

Extent of photoisomerization and degradation of cyanidin-3-(2'-sinapoyl)-sophoroside-5-glucoside (Peak B) with cyanidin-3-(6'-sinapoyl)-sophoroside-5-glucoside (mono-sin). AUC stands for area under the curve under LCMS chromatogram absorbing at 510 – 540 nm. ** represents statistical significance $p < 0.01$

photoisomerization and

51.4 ± 4.2 % photodegradation

(Fig 4.2). Peak B's sinapic acid

acylation is on position C_{2''} of

the second sugar of the C₃-

glucose dimer, whereas mono-

sin consists of acylation on

position C_{6''} of the first sugar of

the sophoroside. The absence of

cis-isomer formation of peak B

and nearly 50% decrease in the

amount of photodegradation

suggest that acylation on

position C_{2''} may impart

substantial amount of stability to

the pigment. Anthocyanin

glycosyl acylations have been

known to affect chemical

reactivity of the anthocyanidin, for example, in polarity, steric hindrance, and hydration

(Bakowska-Barczak, 2005; Figueiredo et al., 1999; Zhao et al., 2017). Though, these trends

in chemical characteristics have been related to aliphatic acylations and substitutions on

the B ring of the anthocyanidin, rather than the C ring. This suggests that it is possible for

intramolecular copigmentation to be further stabilized when the hydroxycinnamic acylation is on a bound sugar of the anthocyanin moiety.

4.4.3. Ultraviolet Excitation of Peak B to Further Explore its Photoisomerization

Based on the peculiar findings of Peak B's resistance to visible light photoisomerization, the comparison of Peak B and Cy-sin's spectral changes were compared over time (Fig 4.3). Previous studies in the literature have shown that UV excitation at 254 or 365 nm for 15 to 30 min resulted in *cis-trans* photoequilibrium (La & Giusti, 2022; Yoshida et al., 1990; Zhou, 2021). According to La and Giusti (2022), the absorbance spectra of *cis*- and *trans*-acylated delphinidins in 0.01% HCl in MeOH show distinct peak shapes, with distinguishable variation in absorbance at 285 nm and 310 nm. Thus, *trans*- to *cis*- photoisomerization could be monitored with UV-Vis spectroscopy. Under this rationale,

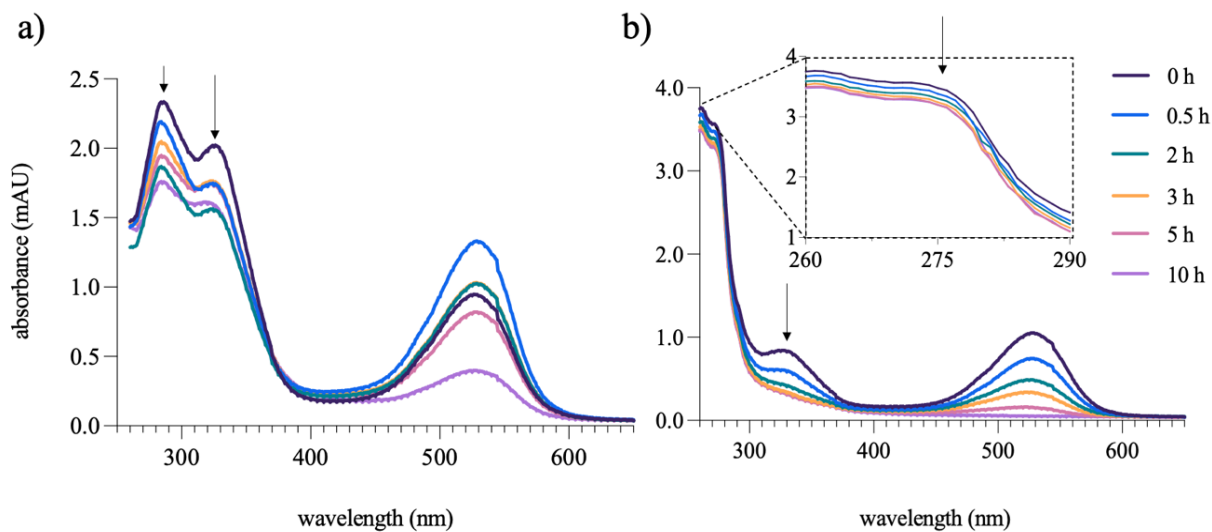


Figure 4.3

Absorbance spectra of a) *Cy-trans*-sin and b) Peak B during excitation with UV chamber at 254 nm for up to 10 h.

Cy acylated with *cis*- and *trans*-sin will have distinct spectral characteristics as well (Fig 4.4). Unlike *trans*-pC acylated delphinidins with absorbance at 310 nm > absorbance at 280 nm, *trans*-sin acylated Cy (Cy-*trans*-sin) had slightly lower absorbance at 330 nm than at 281 nm. The ratio of $abs(281\text{ nm}) / abs(330\text{ nm}) = 1.1$. The same pattern applied to Cy-*cis*-sin, though the ratio of $(abs(281\text{ nm}) / abs(324\text{ nm})) = 1.7$. These pigment-specific spectral characteristics can be further used to monitor the presence of Cy isomerization during irradiation. The measured spectral distribution of Cy-*trans*-sin during irradiation with UV chamber at 254 nm indicated that its *cis*-counterpart was increasing in the mixture as the absorbance at 280 nm was decreasing at a slower rate than absorbance at 320 nm (Fig 4.3a). The initial increase in absorbance at the $\lambda_{vis-max}$ of 524 nm after 0.5 h of irradiation also supported the increase in the *cis*-isomer in the mixture, since *cis*-

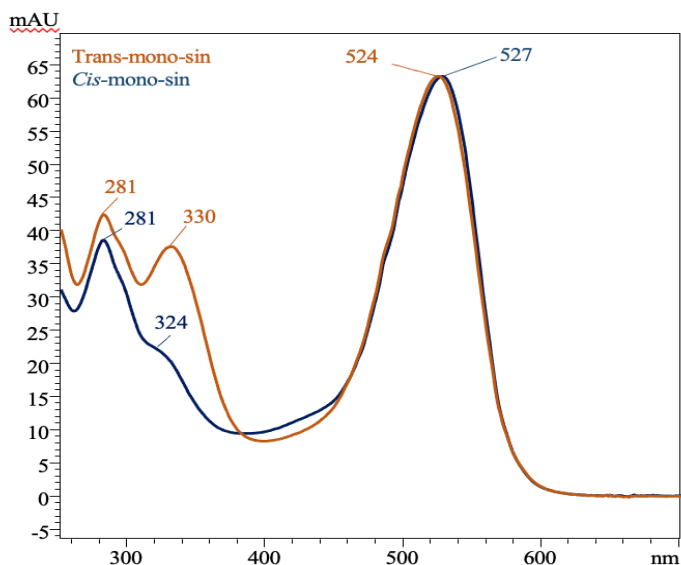


Figure 4.4. Absorbance spectra of cyanidin-3-(6''-*trans*-sinapoyl)-sophoroside-5-glucoside (Cy-*trans*-sin) and its *cis*-isomer (Cy-*cis*-sin).

acylated anthocyanins have been shown to have increased tinctorial strength at $\lambda_{vis-max}$. As expected, the absorbance values at the pertinent wavelengths decreased since photodegradation was bound to occur under irradiation with a high energetic source of excitation.

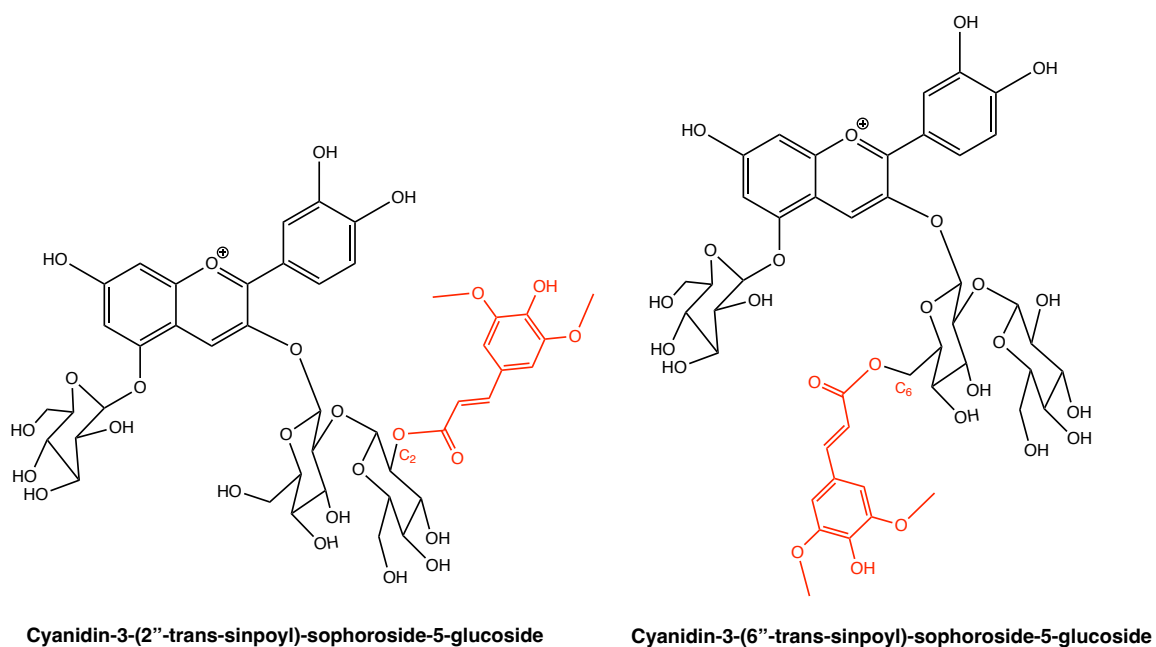


Figure 4.5.

Difference in acylation structures of Peak B and *Cy-trans-sin*

Unlike irradiated *Cy-trans-sin*, irradiated Peak B only showed signs of photodegradation at 285 nm, 320 nm, and at the 524 nm after 10 h of excitation with UV at 254 nm, without changes in absorbance at the regions indication isomerization (Fig 4.3b). The lack of change in the absorbance curvature in below 400 nm suggested that the acylating group, sinapic acid on C_{2''} of the glucose dimer, did not change in spatial configuration. When comparing the structure of mono-sin and Peak B, their biggest difference is on the glycosyl acylation of C_{6''}/C_{2''} of the first/second glycosylation, respectively (Fig 4.5). While isomerization of mono-sin under visible light was observed, the same could not be said for Peak B. The influence of acylation sites on glycosylated anthocyanins have been studied to influence the occurrence of copigmentation, though their extent of stability differs

(Stintzing et al., 2002; Yoshida et al., 1992). The free rotation of single bonds within the anthocyanin structure and the hindrance of free rotation of aromatic moieties influence the strength of copigmentation interaction (Andersen & Fossen, 1995; Sadilova et al., 2006a). Likewise, the free rotation in C₆' acylation of monoacylated sinapic acid may impart less stability of the sinapoylation than the same acid attached to the bound C₂' position of the sugar.

4.4.4. Comparison of Mono- and Di-acylations

Trans-monoacylated cyanidins produced greater amount of the *cis*-isomers when compared to *trans*-diacylated cyanidins, but only by a small margin. *Cy-trans-pC* isomerized by $48.9 \pm 3.9\%$, whereas *Cy-trans-pC-sin* isomerized by $44.7 \pm 1.8\%$. As indicated in Figure 4.6, there was no statistical significance between this comparison under ordinary one-way ANOVA ($p < 0.05$). On the other hand, *Cy-trans-fer* resulted in $43.5 \pm 1.8\%$ isomerization while *Cy-trans-fer-sin* resulted in $33.5 \pm 3.3\%$. This difference was statistically significant with an adjusted p value of 0.005.

Lastly, *Cy-trans-sin* yielded $45.2 \pm 2.7\%$ isomerization and *Cy-trans-sin-sin* yielded $41.5 \pm 3.0\%$ isomerization. Comparison of mono- and di-acylation with ferulic acid was not statistically significant. Despite the lack of statistical significance for *Cy-pC* vs *Cy-pC-sin* and *Cy-sin* vs. *Cy-sin-sin*, the trend of greater isomerization for mono-acylation over di-acylation is clear. One possible explanation of this could be the inverse relationship between concentration of pigment and the extent of isomerization (Zhou, 2021). As the

pigments in the aqueous solution aggregate, the excitation energy has limited reach toward the hydroxycinnamic acids, thus slowing down the production of isomerized photoproducts.

Irradiation of Cy-pC led to $69.7 \pm 12.0\%$ photodegradation while irradiation of Cy-pC-sin resulted in $76.3 \pm 1.9\%$ degradation. In a similar trend, Cy-fer degraded by $60.9 \pm 0.8\%$ while Cy-fer-sin degraded by $66.2 \pm 1.9\%$. Both of these comparisons were not statistically significant under one-way ANOVA ($p < 0.05$), though the pattern of degradation suggests that mono-acylated cyanidins are more prone to degradation than di-acylated cyanidins. Increase in acylation has been associated with lessening the likelihood of nucleophilic

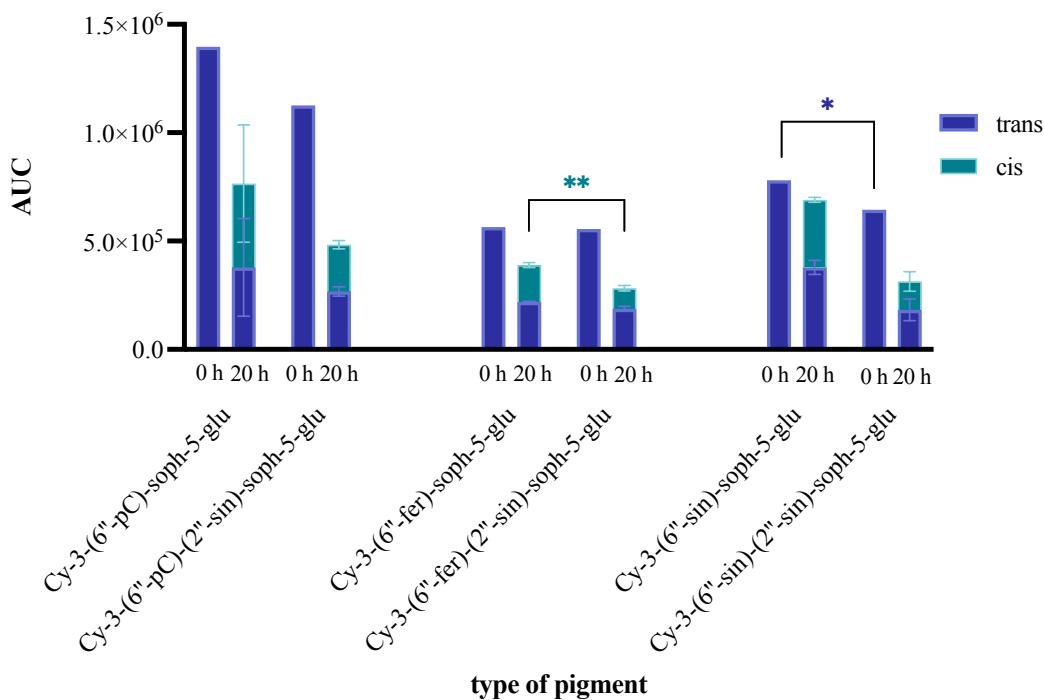


Figure 4.6
Extent of photoisomerization and photodegradation by comparison of acylation numbers. ** represents statistical difference at significance $p < 0.01$ and * at $p < 0.05$

attack of water from causing anthocyanin hydration (Farr et al., 2019; Giusti & Wrolstad, 2003; Mazza & Brouillard, 1987). Thus, structural stability of di-acylated cyanidins decreases the amount of photoisomerization and photodegradation.

Unlike the degradation reactivity of Cy-pC and Cy-fer, Cy-sin's degradation of $51.4 \pm 4.2\%$ was less than Cy-sin-sin's $71.7 \pm 7.8\%$. These values were statistically significant at $p < 0.05$. This was an expected finding since increase in glycosyl acylation has been associated with increased chemical stability (Matsufuji et al., 2007) It is possible that there is a threshold in which phenolic substitutions can affect degradation. Sinapic acids have two methoxy substitutions, and the decreased polarity of di-sinapic acylations may be contributing to degradation more than the steric hindrance of the bulky substituents. As there are often exceptions to the rule, increased number of acylation does not always increase stability, as is observed with patterns of glycosylation on the stability of anthocyanins (Farr et al., 2019).

4.4.5. Impact of Hydroxycinnamic Acylation Type

Between pC, fer, and sin acids, differences in photoisomerization and photodegradation reactivities were minor. Comparison of the three different types of acylation groups categorized within mono-acylation presented favorable isomerization in the following order: Cy-pC > Cy-sin > Cy-fer, though these differences were not statistically significant ($p < 0.05$) (Fig 4.7). When the acylation groups of di-acylated pigments were compared, the same order of isomerization efficiency was observed: Cy-pC-sin > Cy-sin-sin > Cy-fer-sin, with statistical significance. It was hypothesized that polarity of the copigment may be the most influential factor in the efficiency of isomerization since copigmentation effect

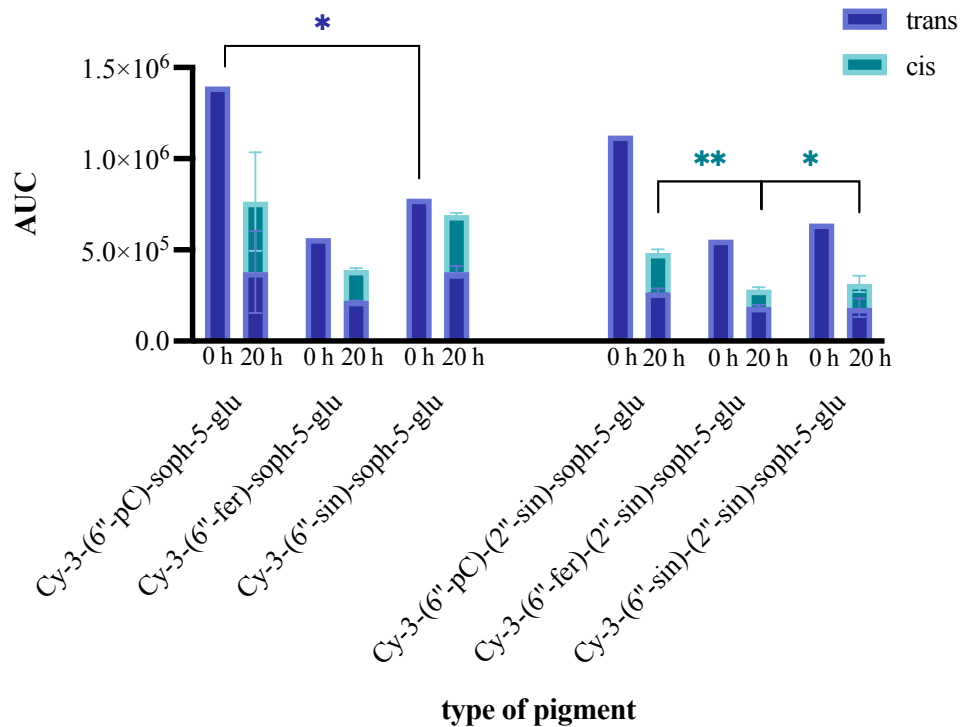


Figure 4.7

Extent of photoisomerization and photodegradation as compared by the type of hydroxycinnamic acylations with *p*-coumaric (pC), ferulic (fer), and sinapic (sin) acids. ** represents statistical significance $p < 0.01$ and * at $p < 0.05$

occurs upon the deprotonation of acidic OH groups, though the results proved otherwise (Galland et al., 2007). Rather than polarity, it may be the polarizability of electron cloud of the hydroxycinnamic acid that affects its reactivity, since the symmetry of *p*-coumaric acid and sinapic acid could contribute to the electronic dispersive forces, while this may dampen the reactivity of ferulic acid.

Photodegradation of Cy-pC was the greatest, followed by Cy-fer, and Cy-sin, in which comparison of Cy-pC and mono-sin resulted in statistical significance but not for the other combinations. This ordering of photodegradation was different from the order of isomerization, though the negligible differences between isomerization of Cy-fer and Cy-sin makes it difficult to claim that photodegradation and photoisomerization of mono-acylation groups behave distinctly. Di-acylated pigments degraded in the same order as isomerization, with Cy-pC-sin degrading and isomerizing the most, followed by Cy-sin-sin, and Cy-fer-sin. This congruence may suggest behavioral characteristics of diacylated cyanidins under light stability.

4.4.6. Comparison of Cyanidin and Delphinidin Photoisomerization and Photodegradation

Cyanidin acylated with *p*-coumaric acid

Cyanidin-3-*p*-Coumaroyl-sophoroside-5-glucoside (Cy-3-pC-soph-5-glu) and delphinidin-*p*-Coumaroyl-rutinoside-5-glucoside (Dp-3-pC-rut-5-glu) differ in their anthocyanin aglycone (cyanidin vs. delphinidin) and type of glycosylation (sophorose vs. rutinose). When the two pigments were treated with visible light excitation for 20 hours, more photoisomerization was observed for Dp-3-pC-rut-5-glu at $60.9 \pm 0.02\%$ than Cy-3-pC-soph-5-glu at $50.6 \pm 0.02\%$ with significance observed at $p < 0.05$ (Fig 4.8). However, comparison of the raw

quantification of the area under the curve suggests that Cy-3-pC-soph-5-glu yielded more total amount of *cis*-isomers, but yielded less total degradation, so the final percentage of *cis*-isomer in the matrix of *cis*- and *trans*- was smaller than that of Dp-3-pC-rut-5-glu.

Meanwhile, greater photodegradation was observed for Dp-3-pC-rut-5-

glu at $79.6 \pm 0.03\%$ than Cy-3-pC-soph-5-glu at $50.6 \pm 0.01\%$ at significance of $p < 0.01$.

Acylated delphinidins were expected to degrade to a greater extent than cyanidins, because

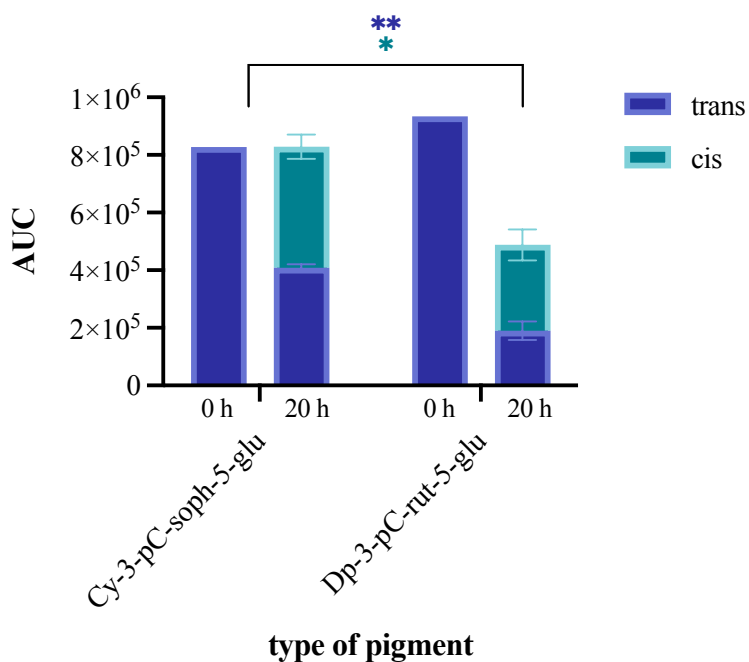


Figure 4.8
Cyanidin (Cy) and delphinidin (Dp) under photoisomerization and photodegradation. ** represents statistical significance $p < 0.01$ and * at $p < 0.05$

the additional hydroxyl ring in the B ring of the aglycone welcomes more nucleophilic attack by surrounding water, thereby leading to hydration (Sadilova et al., 2006). However, theoretically, less stable pigment is expected to yield greater photodegradation and photoisomerization since the molecule with less strength in bonding will undergo both hydrolysis or isomerization. It was unexpected that the findings revealed acylated cyanidins to induce greater amount of isomerization, since Cy-3-pC-soph-5-glu has a 1 → 2 glycosidic linkage, which has been associated with more resistance to hydration, and therefore greater stability (Farr et al., 2019). Ergo, the bonding of glycosidic linkage is not a determinant for photoisomerization, but rather the effectiveness of the anthocyanin-copigment interaction. Examination of the thermodynamic parameters of cyanin and delphin self-association binding suggest that delphin has greater binding constant and a lower Gibbs free energy (Trouillas et al., 2016). If intramolecular copigmentation is a type of self-association, then it is possible that the stronger binding of delphinidin to its copigment lessens the likelihood of isomerization.

4.5. Conclusion

The type of substitution is a crucial factor to consider in most chemical reactions and this applies to acylation for the photoreactivity of Cy as well. Acylated Cy can photoisomerize under visible light, but the yield of photoproduct varies depending on the position, number, and type of the acid attachment. Out of the three factors, glycosyl acyl position made the biggest influence on photoisomerization of acylated Cy—in which, the *cis*-isomer of the *trans*-acylation on position C_{2''} of the second glycosylation was not produced, whereas its

regioisomer with acylation on position C₆' of the first glycosylation underwent isomerization. Monoacylated Cy yielded a greater amount of the *cis*-photoproduct in comparison to diacylated Cy, though this may be related to the lack of photoisomerization on C₂'', since diacylated Cy's second acylation is found on C₂'' of the second glycosylation. Lastly, the type of hydroxycinnamic acid influenced the amount of Cy isomerization, with *p*-coumaric acid producing its isomer most readily. This study contributes to a further understanding of hydroxycinnamic acid photoisomerization of ACN, which have been often studied with Dp. The diversity of ACN acylation patterns opens the doors to further utilizing ACN's behavior under light for their color applications.

Chapter 5. Spectral Characteristics and Color Expression of *Cis*, *Trans*, and Isomerically Equilibrated Acylated Cyanidins and Their Degradation Kinetics

5.1. Abstract

Cyanidins (Cy) are one of the most common anthocyanins that exist in plant sources. Depending on the variety of glycosyl or acyl moieties, cyanidins can show difference in reactivities. In this study, *cis*-, *trans*-, and mixtures of the *cis-trans* isomers are spectrophotometrically and colorimetrically compared. Furthermore, the said measurements were performed on both mono- and di-sinapoylated Cy, allowing for the investigation of isomeric behaviors in relation to the number of acylations. Spectrophotometry was measured with UV-Vis absorbance spectra and converted to colorimetric data with ColorBySpectra software. Degradation kinetics were modeled under best fit of linear, one phase, and two phase decay over the course of 42 days in the dark at 4 °C. The difference between *cis*- and *trans*-isomers were greater for monoacylated Cy than diacylated Cy. *Cis*-mono-acylated Cy had greater absorbance and saturated color performance at pH 4 and 6, compared to their *trans*-counterparts. The color differences in isomers were detected in di-acylated Cy, though at lesser extents. Both *cis*-monoacylated Cy and *cis*-diacylated Cy had shorter half life and greater degradation rate than its *trans*-isomer. Mixture of the monoacylated isomers exhibited behavior that laid in-between the two isomers, but the mixture of diacylated isomers did not. Characterization of *cis*- and

trans-isomeric differences in expression and stability allows for the diversification of the use of anthocyanins in food, particularly in pH ranges that common anthocyanins show limitations in.

Keywords: *cis*-isolate, *trans*-isolate, *cis-trans* mixture, spectrophotometry, CIELAB color space, pigment stability, degradation kinetic model fitting

5.2. Introduction

Colorants are used in the food industry get a food product to match consumers' expectation and acceptance. Depending on the product, it can offer information about product stability, nutritional value, flavor, and more (Sigurdson et al., 2017). Synthetic colorants have been used as food colorants but in the last couple decades, they have been slowly getting replaced by colorants derived from fruits, vegetables, or flowers. However, the challenge lies in natural colorants' limitations in chemical and physical stability when compared to synthetic dyes, which hinders their potential in expression and application (Wallace & Giusti, 2015).

Out of natural colorants that are used for commercial purposes, anthocyanins (ACNs) are often chosen due to their drastically malleable color expression based on the pH of the medium. There are over 700 types of ACNs with variations in chromophore substitutions (e.g. glycosylation, hydroxylation, acylation, methoxylation) (Farr et al., 2019). and even more modifications when these substituents can undergo their own chemical reactions (e.g.

isomerization, tautomerization, hydration, complexation, copigmentation) (Basílio & Pina, 2016; Pina et al., 2012).

Acylated ACNs, in particular, have greater stability than their non-acylated pre-cursors and are thus strong candidates for food applications. Acylation can greatly influence ACN chemical reactivity in many ways, including spectral and colorimetric characteristics (Giusti & Wrolstad, 2003). Previous studies have shown that generally, hydroxycinnamic acylations lead to a bathochromic shift, decrease in L^* , and increase in C^*_{ab} values (Sigurdson et al., 2018). Additionally, these acids can exist in different isomeric forms, in which they present distinguishable chemical reactivity. For example, acylated delphinidins' *cis*–*trans* isomerism can result in their color performance and stability (La & Giusti, 2022; Sigurdson et al., 2018). This geometric rearrangement also occurs in acylated cyanidins. Thus, the objective of this study was to explore the *cis*-, *trans*-, and a mixture of *cis*-*trans* isomers on spectral and colorimetric properties of cyanidins mono- and di-acylated with sinapic acids.

5.3. Materials and Methods

5.3.1. Materials

Commercial red cabbage powders were donated by Bejo Seeds Inc. (Geneva, NY, USA). This was the source of the seven following acylated ACNs: **1.** Cyanidin-3-(2'-sinapoyl)-sophoroside-5-glucoside (Peak B), **2.** cyanidin-3-(6'-*trans*-sinapoyl)-sophoroside-5-

glucoside (Cy-*trans*-sin), and **3.** cyanidin-3-(6'-*trans*-sinapoyl)-(2'-*trans*-sinapoyl)-sophoroside-5-glucoside (Cy-*trans*-sin-sin). These *trans*-acylated ACNs were excited to produce two mixtures of *cis-trans* acylated ACNs: **4.** mixture of Cy-*trans*-sin and its *cis*-isomer (Mixture of Cy-sin isomers), and **5.** mixture of Cy-*trans*-sin-sin and its *cis*-isomer (Mixture of Cy-sin-sin isomers). The mixtures were further isolated to produce two *cis*-acylated ACNs: **6.** cyanidin-3-(6'-*cis*-sinapoyl)-sophoroside-5-glucoside (Cy-*cis*-sin), and **7.** cyanidin-3-(6'-*cis*-sinapoyl)-(2'-*trans*-sinapoyl)-sophoroside-5-glucoside (Cy-*cis*-sin-sin). Further details of the isomerization and isolation procedures are described in a later section. Chemical solvents used for semi-purification, isolation, and characterization were: methanol (MeOH), HPLC and MS-grade acetonitrile (MeCN), HPLC and MS-grade water, formic acid, hydrochloric acid (HCl), ethyl acetate (EtOAc), methanol (MeOH), potassium chloride (KCl), citric acid (CA), monosodium phosphate (NaH₂PO₄), disodium phosphate (Na₂HPO₄), and sodium carbonate (Na₂CO₃). These chemicals were purchased from either Sigma-Aldrich, Co. (St. Louis, MO, USA) or Thermo Fisher Scientific (Waltham, MA, USA).

5.3.2. Acylated *Trans*-Cyanidin Semi-Purification and Isolation

Red cabbage extract was semi-purified in a similar manner to the procedure detailed in *Anthocyanin Purification and Identification*. Peak B, Cy-sin, and Cy-sin-sin were isolated using a reverse phase semi-preparative high performance liquid chromatography (semi-prep HPLC) equipped with LC-6AD pumps, a CBM-20A communication module, a SIL-20A HT autosampler, and a SPD-M20A photodiode array detector. Solvent A was filtered

and sonicated 4.5% formic acid in HPLC-grade water and solvent B was HPLC-grade MeCN. Isolations were done with a pentafluorophenyl (PFP) column (5 μm , 100 Å, 250 \times 21.2 mm) with flow rate of 12 mL/min (Phenomenex®, Torrance, CA, USA). The eluting pigments were monitored on the LC Solution Software Version 3 (Shimadzu, Columbia, MD, USA). The gradient for pigment isolation followed the order of: 15 min from 16% – 25%, 5 more min at 25%, increase to 30% for 1 min and flush for 5 min before equilibrating back to 16%, for a total of 30 min. After isolation, the desired pigments were loaded onto a Sep-Pak Vac 20cc C18 cartridge (Waters Corporation, Milford, MA, USA) and washed with 0.01% HCl in HCl, then 0.01% HCl in MeOH.

5.3.3. Acylated *Trans*-Cyanidin Characterization and Standardization

Trans-acylated Cy were characterized by a Nexera-i-LC 2040C 3D ultra-high performance liquid chromatography (uHPLC) with photodiode array detector (PDA) coupled to an electrospray ionized LCMS-8040 triple quadrupole mass spectrometer (ESI-MS/MS, Shimadzu, Columbia, MD, USA). The instrument was equipped with Nexera-i-LC 2040C oven at 60 °C and conditioned at nebulizer flow of 1.2 L/min, heat block temperature of 200 °C, DL temperature of 230 °C, collision energy of -60 eV, and drying gas flow rate of 12 L/min. The compounds of choice were separated on a Pinnacle DB IBD column (1.9 μm , 140 Å pore size, 50 \times 2.1 mm) (Restek Corporation, Bellefonte, PA, USA). Solvent A was 4.5% formic acid in MS-grade water, and solvent B was MS-grade MeCN. The chromatographic gradient started at 5% starting B% concentration for 18 min, then 25% for 2 min, and flushed for 3.5 min before equilibrating back to the starting B%. The

injection volume was 10 μ L and pump flow rate was 0.3 mL/min. The ions were scanned under 4 parameters: Q1 total scan from 100 – 1000 m/z (+ & –), Q1 Selected Ion Monitoring (SIM) 100, 979, 1185 m/z (+), Q1 SIM 100, 222.8 m/z (–), and Q3 SIM 121, 148.90 (–). All measurements, integrations, and analyses were done on Lab Solutions Software Ver.1 (Released 5.80). The % purity of compounds were determined by relative quantification of the area under the curve of pertinent peaks at the collected chromatograms in 510 – 540 nm.

Samples were standardized to an absorbance of 2 at $\lambda_{vis-max}$ at pH 1 buffer of 0.025 M KCl-HCl in MS-grade water, adjusted with concentrated NaOH. Subsequently, they were allowed to equilibrate for an hour in the dark at 20 °C, and absorbance readings were measured using a SpectraMax 190 Microplate Reader (Molecular Devices, Sunnyvale, CA, USA). The calculated dilution factors for each of the isolates from this step were applied to pH 2, 4, 6, and 8. Further methods on pH buffer preparation can be found in *Buffer and Storage Conditions for Cyanidin Degradation*.

5.3.4. Production of *Cis-Trans* Mixtures of Mono- and Di-acylated Cyanidins

Mixtures of *cis-trans* isomers for both mono- and di-acylated Cy were produced by irradiating *Cy-trans-sin* and *Cy-trans-sin-sin* with UV chamber at 254 nm (Stratagene Stratalinker 1800 UV Crosslinker, La Jolla, CA, USA) for 15 min inside sealed quartz cuvettes (La & Giusti, 2022). The *trans*-isolates were isomerized at standardized concentrations to absorbance of 1 in 0.01% HCl in MeOH. The resulting mixtures

contained *cis-trans* isomers at varying % isomeric composition. Subsequently, the mixtures were concentrated with either a nitrogen evaporator (Sample Concentrator, BT Lab Systems, Saint Louis, MO, USA) for approximately 2-3 h or vacuum centrifuge (Vacufuge Plus, Eppendorf, Enfield, CT, USA) for 3–4 h then stored in $-40\text{ }^{\circ}\text{C}$ until further use.

5.3.5. Production and Isolation of *Cis*-Acylated Cyanidins

Concentrated mixtures of *cis-trans* isomers (mixtures of Cy-sin and Cy-sin-sin isomers) were used as the starting material for isolation of *cis*-isolates. Instrumentation and method conditions found in *Acylated Trans-Cyanidin Semi-Purification and Isolation* was used again to produce *cis*-isolates. Once the eluents were reconcentrated in 0.01% HCl in MeOH, the solvent was evaporated off with a nitrogen evaporator and their purities were analyzed by uHPLC-PDA-ESI-MS/MS under the conditions detailed in *Acylated Trans-Cyanidin Characterization and Standardization*.

5.3.6. Buffer and Storage Conditions for Cyanidin Degradation

Trans-isolates, *cis*-isolates, and mixtures of *cis-trans* Cy isomers were equilibrated in pH 2, 4, 6, and 8 buffers, prepared with MS-grade water. First, pH 2 buffer was prepared with 0.025 M KCl adjusted with concentrated NaOH, pH 4 and 6 were prepared with varying amounts of 0.1 M citric acid and 0.2 M Na_2HPO_4 and adjusted to their respective pHs, further adjusted with concentrated HCl. Lastly, pH 8 was prepared with 0.2 M Na_2HPO_4 combined with 0.2 M NaH_2PO_4 . After each of the pigment of study was placed in the four

pH conditions, the initial spectral reading was measured with SpectraMax 190 Microplate Reader (Molecular Devices, Sunnyvale, CA, USA) an hour after equilibration. Further spectral measurements were taken for day 1 (23 h after initial reading), 2, 3, 5, 7, 14, 21, 28, 42. Between the time points, each of the plates were wrapped in aluminum foil and stored in 4 °C.

5.3.7. Spectrophotometry and Colorimetry of Cyanidin Isomers

Spectrophotometric measurements of 3 *trans*-isolates, 2 *cis*-isolates, and 2 *trans*- + *cis*-mixtures were plated in a poly-D-lysine-coated polystyrene 96-well plates in their respective buffer conditions for absorbance spectral reading in 1 nm increment from 250 – 700 nm for the first replicate, using the same microplate reader as in 5.3.5. *Buffer and Storage Conditions for Cyanidin Degradation*, at 20 °C. Then, the readings were acquired in 5 nm increments from 380 – 700 nm for the second and third replicates. The % retention of absorbance after 84 days of storage in 4 °C in the dark was calculated with the following equation:

$$(1) \quad \% \text{ Absorbance Retention} = \frac{(\text{Absorbance at Day 42})_{pH_n}}{(\text{Absorbance at Hour 0})_{pH_1}} \times 100$$

Colorimetric measurements were based on CIE 1976 L* a* b* color space (CIELAB), which is a quantitative method for color characteristics. Values are represented under the categories of L* a* b*, in which ± L* represents lightness (+light/–dark), ± a* (+red/–green), and ± b* (+yellow/–blue). The spectral data from 380 – 700 nm was converted to discrete

values using ColorBySpectra software, under 10 ° observer angle, regular transmission, D65 illuminant, and calculated by 1964 CIE equations. Graphical depictions of these values were constructed using Adobe Color (San Jose, CA, USA), under the custom LAB mode.

5.3.8. Calculation of Cyanidin Isomers' Half-Lives and Statistical Analysis of Data

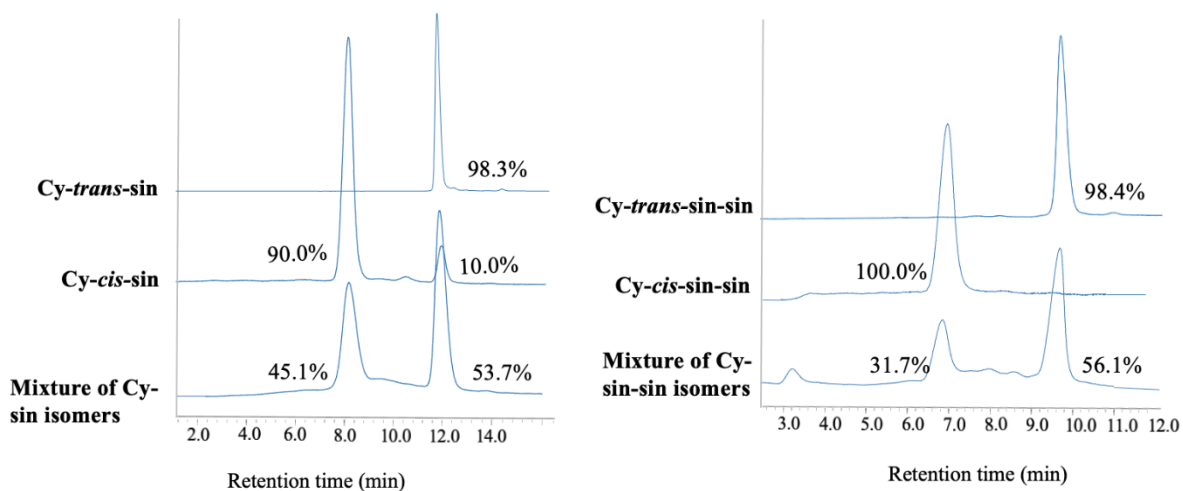
The seven isolates and mixtures were plated under a block randomized design, with duplicate plating, and three replicates. The degradation of these samples in pH 2, 4, 6, and 8 in refrigerated storage were calculated using non-linear kinetic modeling, using a line as the null hypothesis and one phase decay as the alternative hypothesis. In some cases, one phase decay was used as the null hypothesis, with the two phase decay being the alternative hypothesis. Fitting method of least square regression with sum-of-squares F test ($p < 0.05$) was used to determine the model that best suits degradation behavior.

5.4. Results and Discussions

The purity of acylated cyanidins (Cy) were presented in Table 5.1: **1.** Peak B, **2.** *Cy-trans-sin*, **3.** *Cy-cis-sin*, **4.** mixture of *Cy-trans-sin* and *Cy-cis-sin*, **5.** *Cy-trans-sin-sin*, **6.** *Cy-cis-sin-sin*, and **7.** mixture of *Cy-trans-sin-sin* and *Cy-cis-sin-sin*. The % purity of each compound was quantified as the % area under the curve of the individual peak as compared to the total area under the curve under the absorbance of 510 – 540 nm. Under these parameters, Peak B consisted of 99.3% purity, *Cy-trans-sin* consisted of 98.3% purity, and

Cy-*cis*-sin consisted of 90% purity, with the other 10% being the *trans*-isomer. The photostationary mixture of Cy-sin isomers was composed of 45.1% Cy-*trans*-sin and 53.7% Cy-*cis*-sin. Cy-*trans*-sin-sin had 98.4% purity, Cy-*cis*-sin-sin had 100% purity, and lastly, the mixture of Cy-sin-sin isomers was composed of 56.1% of the *trans*-isomer and 31.7% of the *cis*-isomer. The 12.2% impurity was the non-acylated Cy that was most likely produced as a result of photodegradation.

Table 5.1 Composition of *trans*- and *cis* mixture in seven different cyanidins acylated with sinapic acid. % of each isomer is quantified by the area under the curve of the chromatogram monitored at absorbance of 510 – 540 nm max plot.



Identity	Abbreviated Name	<i>Trans</i> -pigment (%)	<i>Cis</i> -pigment (%)
Cyanidin-3-(2''- <i>trans</i> -sinapoyl)-sophoroside-5-glucoside	Peak B	99.3	0.0
Cyanidin-3-(6''- <i>trans</i> -sinapoyl)-sophoroside-5-glucoside	Cy- <i>trans</i> -sin	98.3	0.0
Cyanidin-3-(6''- <i>cis</i> -sinapoyl)-sophoroside-5-glucoside	Cy- <i>cis</i> -sin	10.0	90.0
Cyanidin-3-(6''- <i>trans</i> -sinapoyl)-sophoroside-5-glucoside & Cyanidin-3-(6''- <i>cis</i> -sinapoyl)-sophoroside-5-glucoside	Mixture of Cy-sin isomers	45.1	53.7
Cyanidin-3-(6''- <i>trans</i> -sinapoyl)-(2''- <i>trans</i> -sinapoyl)-sophoroside-5-glucoside	Cy- <i>trans</i> -sin-sin	98.4	0.0
Cyanidin-3-(6''- <i>cis</i> -sinapoyl)-(2''- <i>trans</i> -sinapoyl)-sophoroside-5-glucoside	Cy- <i>cis</i> -sin-sin	0.0	100.0
Cyanidin-3-(6''- <i>trans</i> -sinapoyl)-(2''- <i>trans</i> -sinapoyl)-sophoroside-5-glucoside & Cyanidin-3-(6''- <i>cis</i> -sinapoyl)-(2''- <i>trans</i> -sinapoyl)-sophoroside-5-glucoside	Mixture of Cy-sin-sin isomers	56.1	31.7

5.4.1. Spectrophotometric Properties of *Trans*-Sinapic Acylated Cyanidin Isolates

As depicted in Figure 5.1, the spectral peaks of the *trans*-isolated compounds (Peak B, *Cy-trans-sin*, and *Cy-trans-sin-sin*) had unimodal shapes, with spectral shifts observed as pH increased. As pH increased, the wavelength of $\lambda_{vis-max}$ also increased, with ~100 nm increase in pH 8 compared to ~10-20 nm in pH 4 and pH 6. A remarkable trait of Peak B that was its ability to absorb in low acidic ranges, between pH 4 – 6, which is a difficult

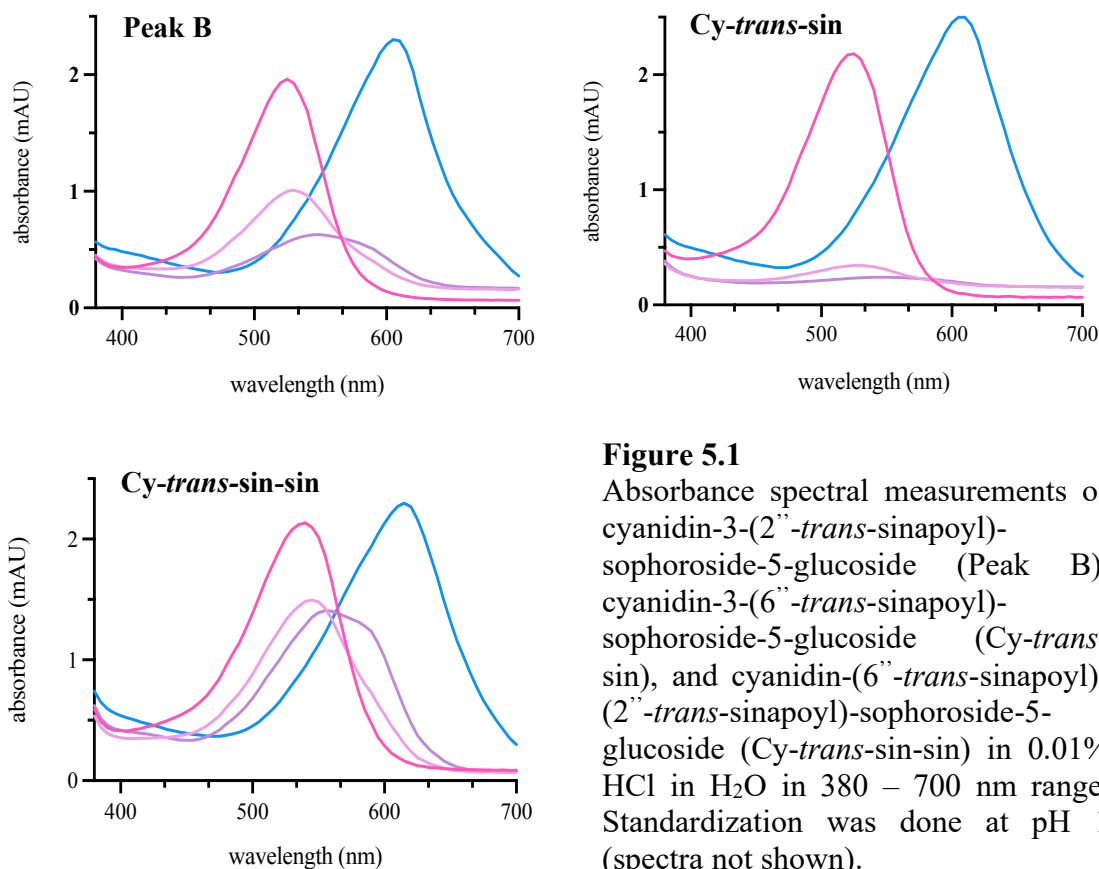


Figure 5.1 Absorbance spectral measurements of cyanidin-3-(2''-*trans*-sinapoyl)-sophoroside-5-glucoside (Peak B), cyanidin-3-(6''-*trans*-sinapoyl)-sophoroside-5-glucoside (*Cy-trans-sin*), and cyanidin-(6''-*trans*-sinapoyl)-(2''-*trans*-sinapoyl)-sophoroside-5-glucoside (*Cy-trans-sin-sin*) in 0.01% HCl in H₂O in 380 – 700 nm range. Standardization was done at pH 1 (spectra not shown).

pH for typical ACNs to express their color (Ahmadiani et al., 2016). Albeit, its absorbance at pH 4 was still less than its absorbance at 1, by approximately 50% less. In addition, their

absorbance was still at its standardized absorbance of 2 in pH 2 and even higher in pH 8. This is a notable but not uncommon behavior, considering that pH 1 is the pH in which ACN tend to exist as a positive flavylum ion and therefore is a favorable condition for it to strongly express its color (Giusti & Wrolstad, 2003).

Most often, acylated ACNs exhibit bathochromic shift and hyperchromic effect in comparison to their non-acylated aglycones (Giusti & Wrolstad, 2003). However, in specific pHs between pH 4 – 5, even acylated ACN often minimally absorb due to the pH-dependent transition of the flavylum chromophore to a colorless chalcone (Basílio et al., 2016). This spectral behavior was also observed in *Cy-trans-sin*, in which the regioisomer of Peak B drastically decreased in absorbance in pH 4 and pH 6 to 0.23 ± 0.1 and 0.16 ± 0.14 , respectively (Fig 5.1). However, Peak B deviated from this trend, though both had similar $\lambda_{vis-max}$ at all of the pHs tested (Table 5.2). A distinguishing characteristic of Peak B is the position of its acylating group on C_{2''} of the second glycosyl group, glucose. The position of acylation has been discussed to potentially contribute to non-covalent stacking of the chromophore and the copigment, thereby causing greater molecular stability and resistance to hydration, which is a critical reaction that ACNs undergo in neutral pHs (Pina, 2014).

Comparing the two *trans*-mono-acylated Cy to *trans*-di-acylated Cy, bathochromic shift of approximately 10 – 15 nm was observed from from *Cy-trans-sin* and Peak B to *Cy-trans-sin-sin*. This was an expected trend that have known to occur when ACN chromophore

increases in acylations, due to changes in polarity and increase in hydrophobic interactions of the medium (Dangles et al., 1993; Giusti & Wrolstad, 2003b; Yoshida et al., 1992). The red shift of the *trans*-diacylated Cy indicates a slight change in color, which will be further discussed in *Colorimetric Characteristics of Trans-Sinapic Acylated Cyanidin Isolates*.

The amount of absorbance retention varied greatly, with Cy-sin-sin retaining the most pigment absorption, followed by Peak B, then Cy-sin when comparing between each other within each pH. It was expected for diacylated Cy-sin-sin to resist degradation the most, but it was unexpected for the pigment to stay intact for over 42 days in 4 °C. After degradation calculations (1), Cy-sin-sin had a 101% absorbance retention. Though it is unlikely that a hyperchromic shift was observed after 42 days, it does represent how truly stable diacylated and diglycosylated cyanidins are. Even in alkaline pHs, in which ACNs typically lose their structural integrity into a chalcone that undergoes further tautomerization and isomerization reactions, Cy-sin-sin was able to retain ~77% of absorbance when calculated with respect to the absorbance at pH 1 (Alejo-Armijo et al., 2019; Rakić & Ulrih, 2021). Peak B's retention of absorbance at low-acidic/neutral and alkaline pH is a promising finding for its application in food products that ACNs are often difficult to perform.

Table 5.2 Cyanidins *trans*- and *cis*-acylated with sinapic acid and their mixtures at absorbance values of their respective λ_{max} and the retention of the absorbance over storage in the dark at 4 °C. (n = 3, duplicate plating per replicate)

* % retention of absorbance after 42 days of storage for *cis*-acylated and *cis-trans* mixtures were not indicated in this table because it has not been 42 days since the date of initial color expression

Anthocyanin	pH 2	pH 4	pH 6	pH 8
	Absorbance at $\lambda_{vis-max}$			
Peak B	1.95±0.05 (526 nm)	0.94±0.09 (529 nm)	0.61±0.02 (545 nm)	2.20±0.10 (606 nm)
Cy- <i>trans</i> -sin	2.18±0.99 (525 nm)	0.34±0.16 (528 nm)	0.24±0.14 (547 nm)	2.50±1.00 (606 nm)
Cy- <i>cis</i> -sin	2.38±0.04 (521 nm)	1.97±0.06 (521 nm)	1.55±0.05 (523 nm)	1.76±0.12 (581 nm)
Mixture of Cy-sin isomers	1.73±0.03 (519 nm)	0.88±0.14 (518 nm)	0.60±0.11 (532 nm)	1.99±0.09 (602 nm)
Cy- <i>trans</i> -sin-sin	2.18±0.22 (539 nm)	1.49±0.28 (546 nm)	1.41±0.01 (557 nm)	2.30±0.32 (614 nm)
Cy- <i>cis</i> -sin-sin	1.97±0.06 (521 nm)	0.97±0.28 (527 nm)	1.03±0.02 (549 nm)	2.59±0.03 (613 nm)
Mixture of Cy-sin-sin isomers	1.92±0.19 (521 nm)	1.49±0.19 (523 nm)	0.87±0.12 (539 nm)	1.57±0.14 (592 nm)
	% Retention of Absorbance after 42 Days of Storage in 4C			
Peak B	99.05±0.05	55.45±0.09	31.75±0.02	28.91±0.10
Cy- <i>trans</i> -sin	61.43±0.78	16.14±0.22	12.56±0.22	21.52±0.26
Cy- <i>trans</i> -sin-sin	101.32±0.10	76.99±0.33	75.66±0.12	76.55±0.24

Table 5.3 CIELAB (Commission International de l'Eclairage and L*, a*, b*) values of *trans*- and *cis*-sinapic acylated cyanidins under pH 2, 4, 6, and 8 (n = 3, duplicate plating, 380 – 700 nm at 1 nm and 5 nm increment measurements converted to colorimetry values)

Pigment	pH 2			pH 4			pH 6			pH 8		
	L*	C* _{ab}	h* _{ab}	L*	C* _{ab}	h* _{ab}	L*	C* _{ab}	h* _{ab}	L*	C* _{ab}	h* _{ab}
Peak B	59.6 ±2.8	68.2 ±2.5	2.8 ±1.8	68.6 ±14.8	44.8 ±25.2	341.8 ±3.6	72.2 ±15.3	29.3 ±21.8	323.8 ±9.7	46.7 ±5.7	47.6 ±3.0	252.3 ±8.5
Cy- <i>trans</i> -sin	64.2 ±7.0	62.1 ±12.2	0.9 ±7.9	85.8 ±0.9	15.2 ±2.3	343.9 ±0.9	88.8 ±0.5	5.2 ±0.3	329.4 ±1.1	43.4 ±1.4	51.3 ±0.5	255.0 ±1.1
Mixture of Cy-sin isomers	57.2 ±3.5	56.8 ±3.5	12.0 ±0.4	68.3 ±6.5	33.4 ±1.8	3.4 ±0.7	71.6 ±5.8	19.5 ±0.6	354.1 ±1.5	38.9 ±2.6	38.9 ±0.8	253.0 ±1.4
Cy- <i>cis</i> -sin	55.2 ±0.2	67.1 ±0.7	15.5 ±1.3	52.6 ±1.3	61.3 ±0.8	5.4 ±1.1	52.8 ±1.8	56.8 ±0.9	355.0 ±0.1	25.1 ±2.4	24.7 ±0.7	299.0 ±2.8
Cy- <i>trans</i> -sin-sin	49.3 ±2.5	73.6 ±1.2	350.2 ±1.2	48.7 ±4.9	68.3 ±4.8	332.0 ±0.6	44.8 ±2.7	61.5 ±2.3	314.7 ±0.8	42.7 ±2.5	47.8 ±0.3	247.0 ±3.2
Mixture of Cy-sin-sin isomers	48.5 ±7.1	60.2 ±5.5	1.7 ±1.1	49.3 ±7.7	53.5 ±5.4	353.4 ±0.8	56.4 ±5.1	38.4 1.1	334.5 ±1.1	32.0 ±3.7	35.7 ±1.6	286.8 ±4.4
Cy- <i>cis</i> -sin-sin	46.4 ±1.6	62.2 ±1.3	352.1 ±0.9	59.8 ±6.9	50.7 ±9.3	339.4 ±0.7	49.2 ±0.8	45.3 ±0.4	316.7 ±0.1	33.8 ±1.8	42.9 ±1.0	243.2 ±1.0

5.4.2. Colorimetric Characteristics of *Trans*-Sinapic Acylated Cyanidin Isolates

The three *trans*-sinapic acylated cyanidins' initial color expressions exhibited colorimetric differences across most of the pHs (2, 4, and 6); though expectedly, some differences were greater than others. First, when comparing *trans*-acylated Peak B and Cy-sin in pH 2, the two compounds' L^* , C^*_{ab} , h^*_{ab} were similar to each other, though Peak B was slightly darker in color and less saturated in chroma. This finding was expected and in congruence with the two mono-acylated isolates' spectral patterns in pH 2, in which the absorbance at their $\lambda_{vis-max}$ were similar with nearly congruent unimodal shapes (Fig 5.1). In comparison, in pH 2, *Cy-trans-sin-sin* displayed an even darker color with decreased L^* compared to *Cy-sin* and Peak B. Additionally, the C^*_{ab} value was $\sim 10^\circ$ greater for the di-acylated pigment,

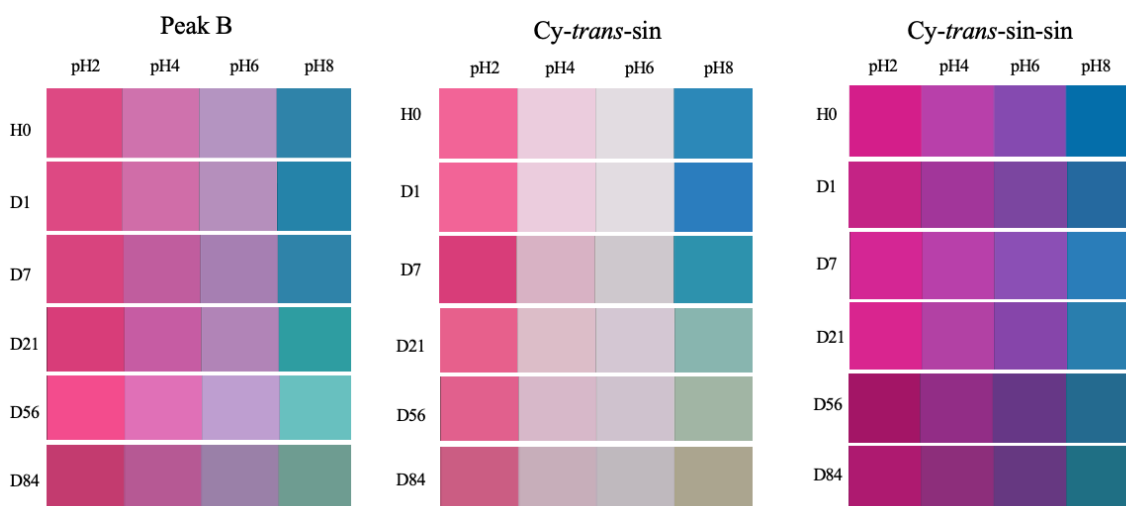


Figure 5.2

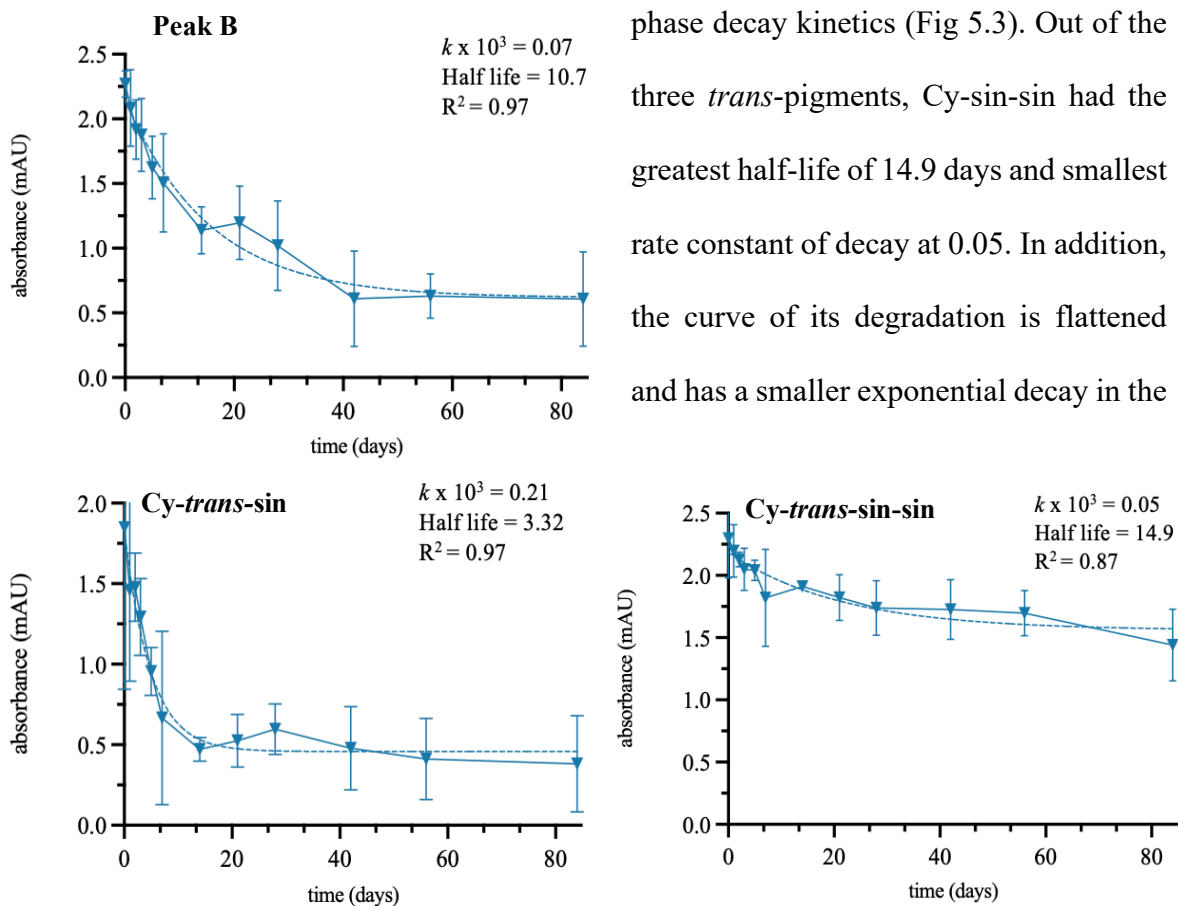
Color swatches of cyanidin-3-(2''- *trans*-sinapoyl)-sophoroside-5-glucoside (Peak B), cyanidin-3-(6''- *trans*-sinapoyl)-sophoroside-5-glucoside (*Cy-trans-sin*), and cyanidin-(6''-*trans*-sinapoyl)-(2''-*trans*-sinapoyl)-sophoroside-5-glucoside (*Cy-trans-sin-sin*) in pH 2, 4, 6, and 8 over the course of 84 days in 4 °C storage, in the dark.

and 10° less for h^*_{ab} , indicating a greater color intensity and pink hue with purple undertones. Converting these L^* , C^*_{ab} , h^*_{ab} values to color representations show that Peak B and *Cy-trans-sin* have similar hues in pH 2, but the bathochromic shift observed in *Cy-trans-sin-sin*'s $\lambda_{vis-max}$ was evident in the diacylated pigment's difference in hue (Fig 5.2).

In pH 4 and pH 6, *Cy-trans-sin* bleaches drastically more than Peak B, as Peak B was able to retain a pink in pH 4 and a dark lavender in pH 6. Although, *Cy-trans-sin* did not become completely colorless as many ACNs would in pH 4 or 6 – pHs in which ACNs often hydrate and become colorless hemiketals (Castañeda-Ovando et al., 2009; Cooper-Driver, 2001) – since *Cy-trans-sin* remained its baby pink hue with h^*_{ab} of 343.9° , though with low C^*_{ab} and high L^* . In comparison, Peak B with just one difference in glycosyl acylation position retained its C^*_{ab} at 44.8° and L^* at 68.6 . *Cy-trans-sin-sin* also did not bleach in near-neutral pHs, with an even higher C^*_{ab} value of 68.3° in pH 4 and 61.5° in pH 6, respectively. The diacylated *Cy*'s ability to exhibit high chroma in both pH 4 and 6 was previously observed from red cabbage (Ahmadiani et al., 2016). In pH 8, all three *trans*-acylated *Cy* had similarities in L^* value, C^*_{ab} value, and h^*_{ab} as well; though a slight decrease in L^* value and h^*_{ab} value were observed in *Cy-trans-sin-sin*, compared to the other mono-*trans*-acylated isolates. Both increase in acylation and pH has been associated with bathochromic shift, which is representative of more presence of the quinoidal blue chromophore (Alejo-Armijo et al., 2019).

5.4.3. Analysis of *Trans*-Isolates' Color Stabilities by Degradation Kinetics and Half Lives Calculations

Degradation of the three *trans*-sinapic acylated Cy varied greatly from each other, as their differences in acylation patterns play a role in the rate of their degradation. The half-life calculations were based on the absorbance at $\lambda_{vis-max}$ for up to 84 days of storage in the dark, under 4 °C. The greatest decrease in absorbance over time was observed in pH 8, in which Peak B, Cy-sin, and Cy-sin-sin all exhibited greatest R² values when fitted to one



phase decay kinetics (Fig 5.3). Out of the three *trans*-pigments, Cy-sin-sin had the greatest half-life of 14.9 days and smallest rate constant of decay at 0.05. In addition, the curve of its degradation is flattened and has a smaller exponential decay in the

Figure 5.3 Degradation kinetics of Peak B, Cy-*trans*-sin, and Cy-*trans*-sin-sin at pH 8, fitted to one phase decay as best fit under nonlinear regression with significance at $p < 0.05$.

beginning of the storage period, in comparison to Peak B and Cy-sin. This was to be expected, since diacylated pigments have been known to have greater chemical stability than monoacylated counterparts (Chandrajith et al., 2022; C. C. Chen et al., 2019). However, this finding could suggest that that number of acylations may play a bigger role than position of acyl groups in alkaline pH. Or another potential interpretation is that diacylated Cy includes acylation on the second glycosylation, so it was the most stable during storage. The second glycosyl acylation could play a pivotal role in stabilizing the chromophore, and thus imparting greater influence on the intramolecular copigmentation. Peak B's increased half-life and decreased rate constant in comparison to *Cy-trans-sin*'s was an additional evidence that the glycosyl acylation on the second C₃ sugar results in greater chemical stability of the chromophore. The degradation curve shows that both mono-acylated cyanidins eventually reach a plateau around ~0.5 mAU but the rate in which Cy-sin decreases in absorbance until day 20 was greater than that of Peak. With that said, first order degradation kinetics that takes approximately 20 days or more to reach a plateau is still an extraordinary performance for ACNs in pH 8. Most often, non-acylated ACNs, such as cyanidin aglycones or glucosides, are more prone to greater degradation in alkaline pHs (Giusti & Wrolstad, 2003). This makes application of all three *trans*-isolates quite favorable for refrigerated storage conditions that needs blue colors in pH 8, such as pan-coated confectionaries.

In pH 2, 4, and 6, the decrease in absorbance over time was not considerable enough to sufficiently model degradation kinetics. This is not to be confused with the results found

in Table 5.2, because the % absorbance retention was calculated as a function of the initial absorbance at pH 1, rather than calculating the final absorbances with respect to the initial absorbances at pH 2, 4, 6. The change in colorimetric representation in pH 2, 4, and 6 over 84 days also supports this, as minimal changes in hue were observed. There was potentially some browning, which led to the overall darkening of the color swatch, but the hue itself did not change. This makes application of all three *trans*-isolates favorable for the said pHs, which can apply for juices, dairy products, or crackers/biscuits.

5.4.4. Spectrophotometric Characteristics of *Cis*-Isolate and *Cis-Trans* Equilibrated Mixtures of Sinapic Acylated Cyanidins

Cy-cis-sin and *Cy-sin* isomeric mixture's spectral readings resulted in stark differences for all pHs tested. In pH 2, *Cy-cis*-sin exhibited 37% greater absorbance than *Cy-sin* isomeric mixture with no considerable shifts in their $\lambda_{vis-max}$ (Table 5.2). Considering the composition of *Cy-sin* isomeric mixture, which consisted of 40% more of the *trans*-isomer than in *Cy-cis*-sin, the 37% increase in absorbance was reasonable. When comparing both pigment samples to their control, *Cy-trans*-sin, the mixture absorbed 2.1 fold more intense and the *cis*-isolate absorbed 2.8 fold more. In pH 4, *Cy-cis*-sin performed even better than in pH 2, at ~8.6-fold increase in absorbance intensity compared to *Cy-trans*-sin and ~3.8-fold increase for *Cy-sin* isomeric mixture. Though, this increase is not substantial considering that the mono-acylated isomeric mixture absorbed in a linear pattern at 0.5 mAU rather than unimodal as observed in *Cy-cis*-sin (Fig 5.4). Similar trends of increase in absorbance at $\lambda_{vis-max}$ for the isomeric mixture and *Cy-cis*-sin was observed for pH 6,

but not pH 8. *Cis*-isomers' greater intensity of absorption at select pHs were in congruence with precedent literature, which have stated that *cis*-acylated pigments may have greater protection against hydration than *trans*-acylated pigments, due to the planarity of aglycone-copigment stacking (George et al., 2001; La & Giusti, 2022; Sigurdson et al., 2018). Though shifts in spectral patterns were not observed in pH 2, both pH 4 and pH 6 exhibited hypsochromic shift from the *trans*-isolate to *cis*-isolate—a bigger shift was observed in pH 6 than at pH 4. In pH 8, Cy-*cis*-sin displayed a quite broad spectrum at its $\lambda_{vis-max}$. In addition, it also absorbed greater than 1 in the near UV region—380 nm. Increased

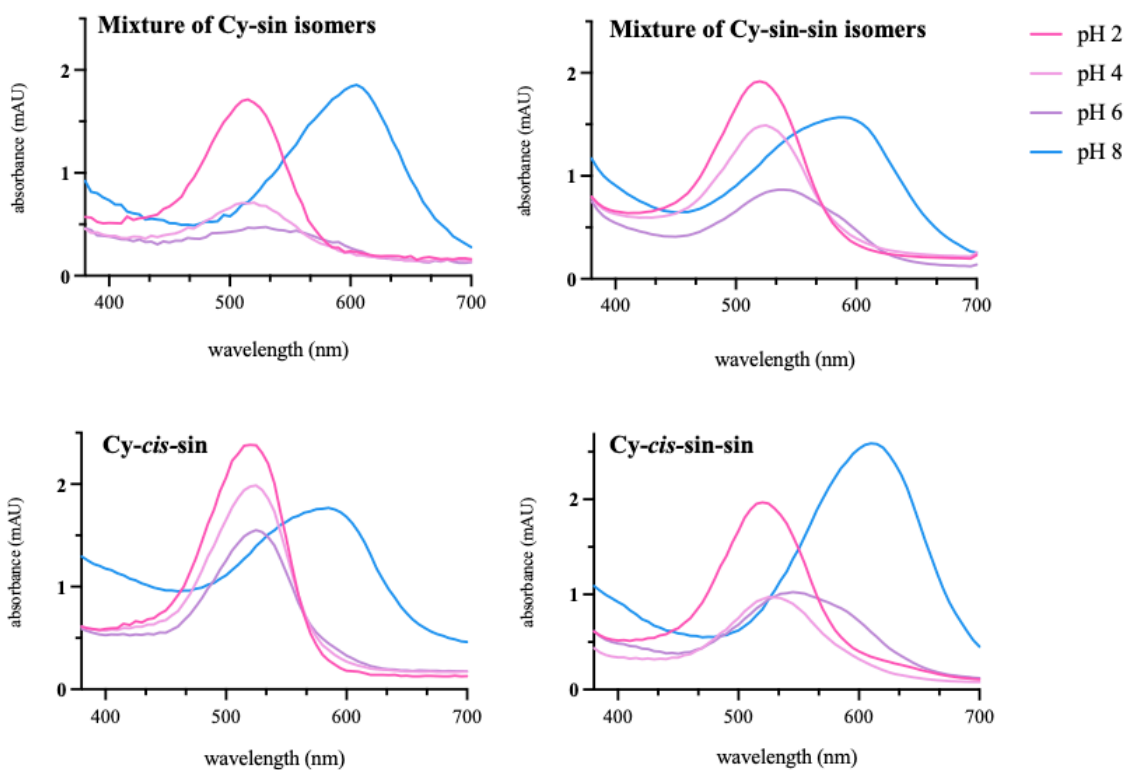


Figure 5.4 Spectral measurements of *cis*-isolates and mixtures of *cis-trans* isomers of mono- and di-acylated Cy in 380 – 700 nm after 1 h of equilibration. Standardization was done at pH 1 (spectra not shown).

absorbance in a broad range could indicate that there is greater collision of solvent and solute ($\text{Na}_2\text{HPO}_4 + \text{NaH}_2\text{PO}_4$ buffer in pH 8 and *cis*-Cy) (Mastrodomenico et al., 2012). As expected, Cy-sin isomeric mixture's each of the four pH spectral patterns were between Cy-*trans*-sin and Cy-*cis*-sin. Although the mixture contains approximately half (53.7%) of the *trans*-isomer, the mixture's spectral characteristics were more a lot more similar to the *trans*-isomer than the *cis*-isomer. In pH 2, the isomeric mixture had a hyperchromic shift compared to the *trans*-isolate, but much less than the *cis*-isolate—which absorbed nearly 1 mAU. Similarly, in pH 4 and pH 6, Cy-sin isomeric mixture exhibited approximately 2 fold greater in absorbance than Cy-*trans*-sin, though this hyperchromic shift was miniscule compared to what was observed in Cy-*cis*-sin.

Comparison of diacylated Cy with *cis* and *trans*-isomers showed differences in all of the four pHs tested. In pH 2, Cy-*cis*-sin-sin had both hypochromic and hypsochromic shift compared to its *trans*-isomer. This behavior was deviated from the trend of *cis*-isomers in pH 2. In the case of mono-acylated Cy with sinapic acid and mono-acylated Dp with *p*-coumaric acid, *cis*-isomeric configuration of both compounds showed increase in tinctorial strength in highly acidic pH, such as pH 2 (Sigurdson et al., 2018). One possible explanation is that diacylation already increases the absorbance intensity compared to monoacylation that the isomeric differences do not make as much of an impact. The difference between Cy-*cis*-sin and Cy-*trans*-sin were even more noticeable in pH 4 and pH 6, in which the *trans*-isomer displayed hyperchromic shift by 1.5 fold in both pHs. In contrast, Cy-*cis*-sin absorbed more in pH 8 and had a broader spectral peak near the

$\lambda_{vis-max}$, which could impact the hue of the pigment. Rather unexpectedly, Cy-sin-sin isomeric mixture's absorbance were not in-between the *cis*- and *trans*-isomer, as it was composed of 32% *cis* and 56% *trans*. In pH 2, the isomeric mixture was nearly identical to Cy-*cis*-sin in absorbance and spectral shape, while in pH 4, it was closer in absorbance with Cy-*trans*-sin. This finding was rather unexpected, since most logical sense would point toward the mixture reacting more like *trans*-than *cis*- across all pHs. As the pH increased to 6 and 8, the isomeric mixture displayed a hypsochromic and hypochromic shift than both *cis*- and *trans*-isomer. The decrease in lambda max and the absorbance at the lambda max was also surprising finding. This behavior suggests that favorable isomeric configuration may highly depend on pH, and sometimes not necessarily in a linear trend.

5.4.5. Colorimetric Characteristics of *Cis*-Isolate and *Cis-Trans* Equilibrated Mixtures of Sinapic Acylated Cyanidins

The CIE $L^* c^*_{ab} h^*_{ab}$ values of Cy-*cis*-sin, Cy-sin isomeric mixture, Cy-*cis*-sin-sin, and Cy-sin-sin isomeric mixtures were detailed in Table 5.3. Visual depiction of the colorimetry data were presented as color swatches in Figure 5.5. Overall, both *cis*- and *trans*-isomers of Cy-sin and Cy-sin-sin resulted in ΔE well above 5—which is indicative of the numerical value that signifies a total color difference that can be detected by untrained consumers' eyes. The exact ΔE values representing differences between *cis*-, *trans*-, and a mixture of the two isomers were presented in Table 5.4. The difference in colorimetric values were greater for *cis*- and *trans*-isomers of Cy-sin than Cy-sin-sin. The smaller difference (yet still distinct) of diacylated Cy may be attributed to the lack of isomerization of the sinapic

acid on the second glycosylation. Thus, structurally, it does not make as big of a difference on the final color characteristics as a singular acylation would when it isomerizes. The mixture of *cis*- and *trans*-isomers of Cy-sin were more similar to Cy-*cis*-sin in pH 2, but Cy-*trans*-sin in pH 4, 6, and 8. *Cis*-acylated ACNs have been known to have higher intensity in highly acidic pH when compared to their *trans*-counterparts, while *trans*-acylated ACNs perform more intensely around pH 6 (Sigurdson et al., 2018). On the other hand, mixture of Cy-sin-sin isomers varied less from *cis*-acylated isolate than Cy-*trans*-sin-sin in all pHs tested. It is difficult to make an inference regarding the tinctorial strength of *trans*- compared to *cis*- in this comparison because the composition of the *trans*-isomer is greater than *cis*- in diacylated Cy. However, this finding allows for the claim that if a darker and greener hue of Cy-*cis*-sin-sin is desired, isomerizing *trans*-isolate may lead to distinguishable difference in color but may not be similar to the *cis*-isolate.

Across all of the pHs tested, Cy-*cis*-sin had lower L^* values than its *trans*-counterpart, indicating a darker color. In addition, the *cis*-isomer exhibited an increase in chroma, especially in pH 4 and 6, in which the *trans*-isomer nearly bleached in. This behavior is on trend with the literature on the behavior of *cis*-acylated ACN and its reduced likelihood of hydration due to the planar stacking of the chromophore and the copigment (George et al., 2001). In application, increase in C^*_{ab} and decrease in L^* is favorable in food colorants, as this represents more saturated pigment, and therefore, requires less to be used. Cy-*cis*-sin's hue increased $\sim 40^\circ$ in pH 2, 4, 6, and 8, which was evident in the hypsochromic shift found in their spectral patterns. Cy-*cis*-sin had a redder hue in acidic pH and blue-purple in pH

rather than pink and blue in acidic and alkaline conditions of Cy-*trans*-sin, respectively. This may be attributed to *cis*-Cy's ability to form a stronger non-covalent bond with the flavylum ion in acidic pHs (George et al., 2001).

Table 5.4. Delta E of the *cis*- and *trans*-isomers of mono- and di-acylated Cy compared to each other and the isomeric mixture.

pH	ΔE of <i>trans</i> - vs. <i>cis</i> -		ΔE of <i>trans</i> - vs. mixture of isomers		ΔE of <i>cis</i> - vs. mixture of isomers	
	Cy-sin	Cy-sin-sin	Cy-sin	Cy-sin-sin	Cy-sin	Cy-sin-sin
pH 2	20.5±11.4	11.9±0.2	17.3±7.8	20.5±5.9	11.8±2.7	12.0±1.2
pH 4	57.9±2.0	20.2±6.5	26.7±5.4	28.0±4.1	32.7±1.3	17.2±6.7
pH 6	63.5±0.8	19.8±1.4	23.0±4.2	32.5±4.5	41.4±2.5	17.7±0.5
pH 8	42.2±1.1	11.6±3.7	13.6±1.2	32.6±4.4	31.0±2.3	28.3±0.9

On the contrary, Cy-*cis*-sin-sin did not consistently present brighter/darker colors as Cy-*cis*-sin did. Cy-*cis*-sin-sin was darker in pH 2, lighter in pH 4 and pH 6, then darker in pH 8. In chroma, the *cis*-isomer was less saturated than *trans*- in pH 2, 4, 6, and 8, while the two isomers performed similarly in hue. Based on these values, there was no clear trend in the behavior that Cy-*cis*-sin-sin undergoes. Though the *cis*-isomer showed favorable darker colors in some pHs, many of them were also duller than the *trans*-isomer. The inexplicable findings may be an experimental error stemming from some of the insoluble particles that were found in the *cis*-concentrates. The same experimental procedures were performed on

both forms of isomers, thus further examination and confirmation of *cis*-isomers' solubility and expression should be explored.

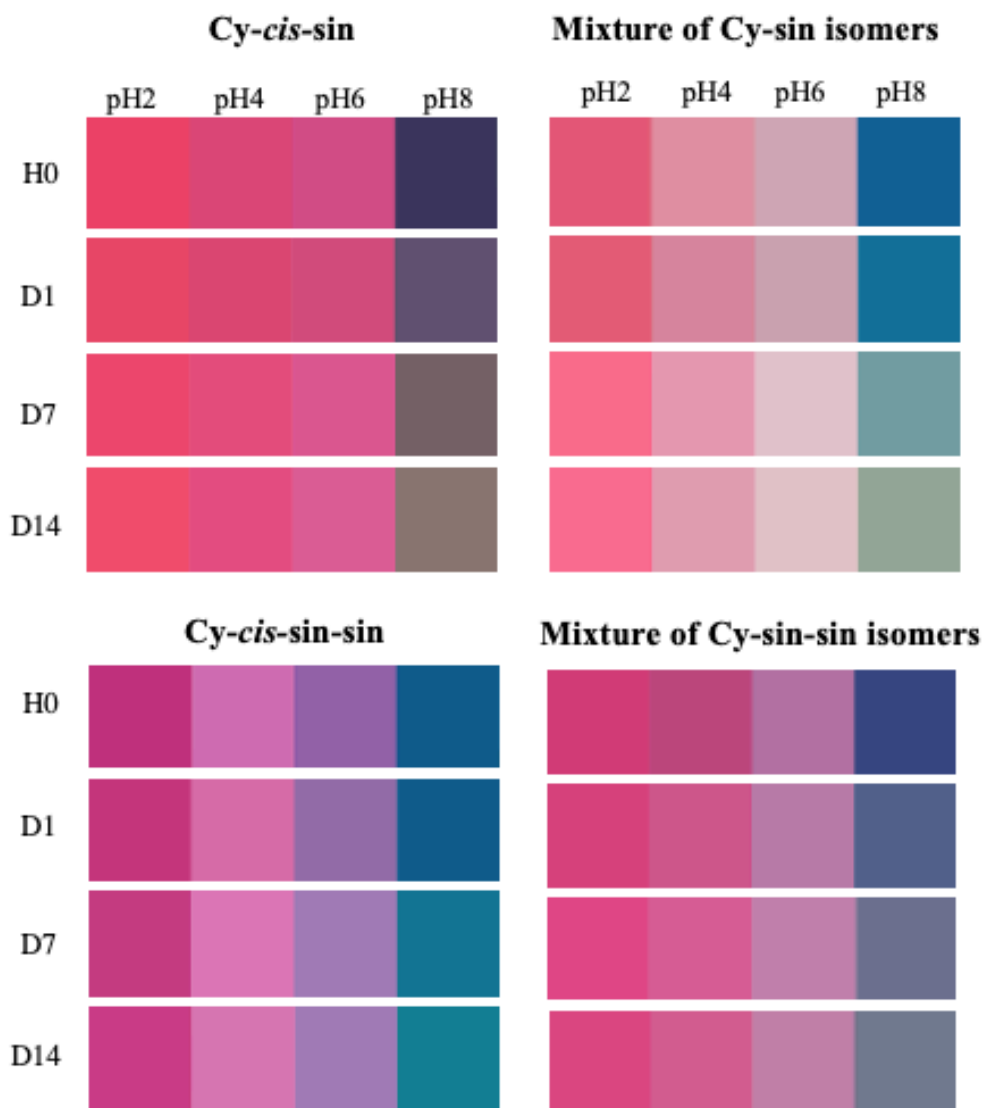


Figure 5.5 Color expression and stability of *Cy-cis-sin*, mixture of *Cy-sin* isomers, *Cy-cis-sin-sin*, and mixture of *Cy-sin-sin* isomers after 1 h of equilibration in the dark (H0) and up to 14 days of storage in 4 °C (n = 3).

5.4.6. Degradation Kinetics and Half Lives Calculations of *Cis*-Isolates and Mixture

Pigment stability of *cis*-isolates and the mixtures of *cis-trans* isomers were determined by the decrease in absorbance at λ_{max} after 14 days of storage in the dark at 4 °C. Kinetic fitting of degradation of pigments at pH 8 could be constructed, but not for pH 2, 4, and 6, since not enough degradation had occurred within the 14 days. *Cy-cis-sin* and mixture of *Cy-sin* isomers showed ample degradation within 14 days, but the di-acylated counterparts

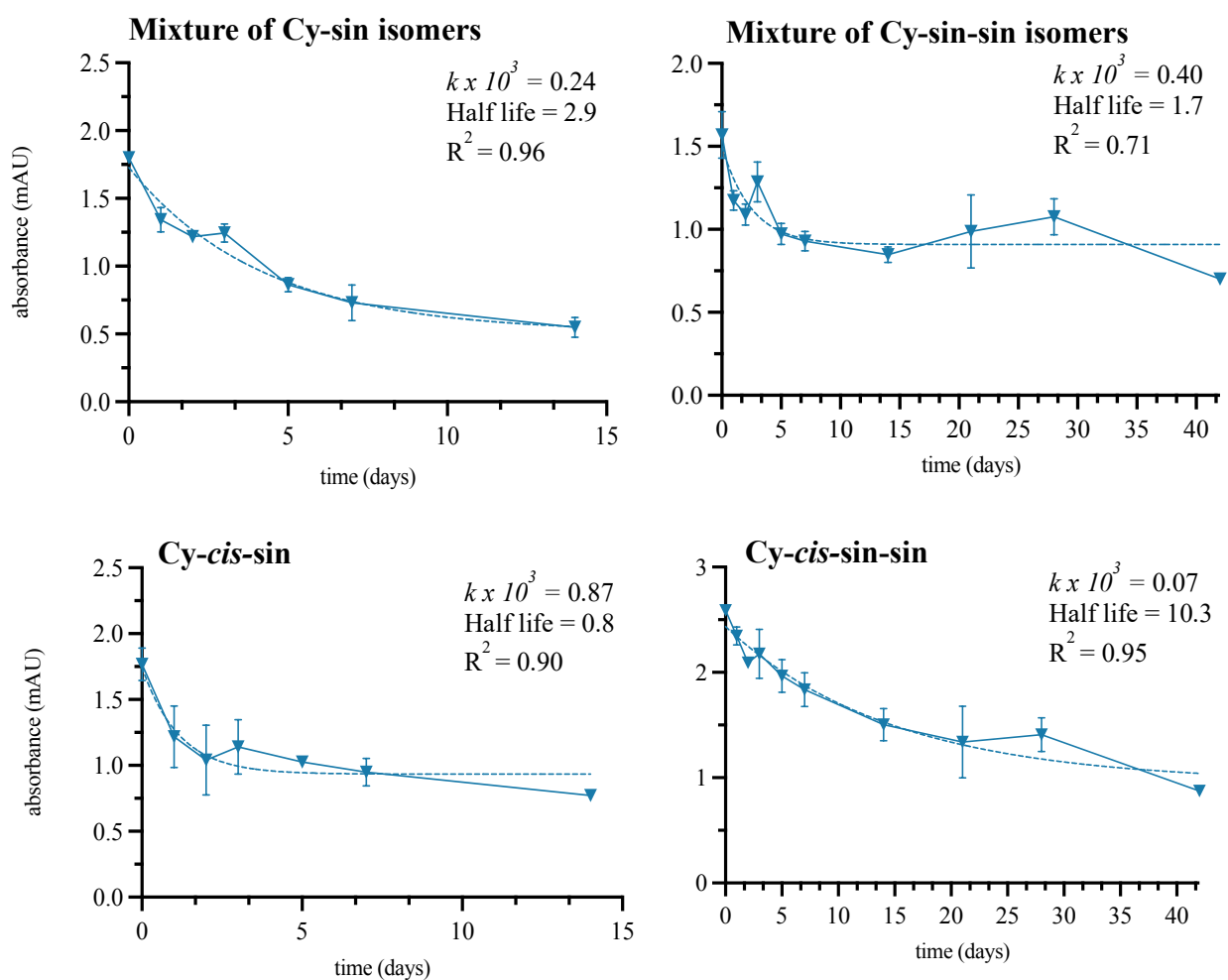


Figure 5.6 Degradation of *cis*-isolate and mixtures of *cis-trans* isomers best fitted under one phase decay and line after 14 days of storage in the dark at 4 C.

did not—which was to be expected, given the higher stability of diacylated Cy (Fig 5.6). Though best-fit analyses of the di-acylated Cy concluded that the collected data fit linear regression over one-phase decay, based on the trend and understanding of ACN degradation, these analyses are most likely inconclusive without the full 42 days of storage. The pigments will continue to be stored up to 42 days and their measurements will be added to the current set of data.

5.5. Conclusions

Chemistry of isomers have been long studied for their difference in reactivity and characteristics. *Cis*-, *trans*-, and photostationary mixture of *cis-trans* isomers of Cy acylated with sinapic acids expressed different spectroscopic and colorimetric properties. Cy-*cis*-sin had greater absorbance in pHs 4, and 6 in comparison to Cy-*trans*-sin, which nearly bleached at an absorbance below 0.5 mAU. The *cis*-isomer of diacylated Cy did not express this behavior, but had greater absorbance with broader spectral shape in pH 8. The mixture of the mono-sinapoylated Cy resulted in the expected behavior that was in between *cis-trans* isomers. However, di-sinapoylated Cy deviated from the expected. In addition, Cy-*cis*-sin exhibited a faster rate of degradation in pH 8 than Cy-*trans*-sin but differences were not observed between *cis*- and *trans*-isomers of diacylated Cy. This finding suggests that isomeric differences are not necessarily consistent and number of acylation can affect their final reactivity.

Chapter 6. Overall Conclusion and Future Research

Ultraviolet and visible energies excited *cis*-acylated delphinidins and *trans*-acylated delphinidins to varying extent of isomerizations and photostationary equilibria. Ultraviolet energy induced more photoisomerization of *cis*-to-*trans* photoreaction, while visible energy was more favorable for the reverse reaction, from *trans*-to-*cis*. The resulting color difference of the two delphinidin isomers were the most distinguishable at pH 1 and pH 8. When comparing the two isomers, *cis*-chromophore exhibited greater color intensity and stability after 25 h of storage in the dark, at 20 °C and in pH 1. In pH 8, the *cis*-isomer had a green-blue hue compared to the cyan-blue hue of the *trans*-counterpart. In addition, when the semi-crude mixture composed of both isomers (80% *trans* and 14% *cis*) were irradiated, the color of the resulting photoproducts did not vary based on the varying radiant energies.

Variation in the position, number, and type of glycosyl acylation substitution also affected the photoreactivity of acylated anthocyanins (ACNs), specifically, acylated cyanidin (Cy). Position of the acylation made the greatest impact on the extent of photoisomerization, in which C₂'-acylation on the second glycosylation did not produce its *cis*-photoproduct. Monoacylated Cy yielded a greater amount of the *cis*-photoproduct in comparison to diacylated Cy, though this may be related to the lack of photoisomerization on C₂', since diacylated Cy's second acylation is found on C₂' of the second glycosylation, though its

regioisomer at C₆' acylation did. Lastly, the type of hydroxycinnamic acid influenced the amount of Cy isomerization, with *p*-coumaric acid producing its isomer most readily, followed by sinapic acid, then ferulic acid.

Cis-, *trans*-, and photostationary mixture of *cis-trans* isomers of Cy acylated with sinapic acids expressed different spectroscopic and colorimetric properties. Cy-*cis*-sin had greater absorbance in pHs 4, and 6 in comparison to Cy-*trans*-sin, which nearly bleached as typical ACN often behave. The *cis*-isomer of diacylated Cy did not express this behavior, but had greater absorbance with broader spectral shape in pH 8. The mixture of the mono-sinapoylated Cy resulted in the expected behavior that was in-between *cis-trans* isomers. However, di-sinapoylated Cy deviated from this trend, in which the mixture of the two diacylated isomers did not exhibit behavior that laid in-between the two isolates. In addition, *cis*-isomer of monoacylated Cy exhibited a faster rate of degradation in pH 8 (first order kinetics) than its *trans*-counterpart. The same trend was also observed in diacylated Cy, suggesting that isomeric differences are not make as big of an impact as the number of acylation increases.

Overall, radiant energy impacted the direction of reversible *cis-trans* isomerization. However, all radiant energies were able to induce the excitation, though some were more optimal than others in producing greater extent of the photoreaction. Though the type of excitation energy required different exposure times to reach their respective photoequilibria, the photostationary state were within the same range from each other—

suggesting the racemic mixture to be stable anywhere from 40:60 (*cis:trans*) to 60:40 (*cis:trans*). The resulting chemical characteristics of the isomers were highly dependent on their stereochemical configuration. ACN expression, retention of color, and rate of degradation were impacted by isomeric folding in the 3-dimensional space. These findings offer methods to manipulate and control conditions for desired pigment characteristics, further expanding ACN usage in broader food applications.

With this, there is still much more work to be done in understanding the photoisomerization of hydroxycinnamic acylated ACNs. Given that the substrate of a chemical reaction affects its product greatly, ACNs with hydroxycinnamic acylations on C₇ of the A ring or C_{3'} of the B ring could show different reactivity from the acylation on C₃ glycosides. Though these complex substitution variations are often found in flowers, edible flowers are a plant source that should not be overlooked. In addition, a deeper study into the difference in intramolecular copigmentation of the sinapoylated cyanidin regioisomers and their respective isomeric configurations would offer even further understanding, manipulation, and application for color diversification of ACN as food colorants.

Bibliography

- Adelman, R. M. (2004). Neighborhood Opportunities, Race, and Class: The Black Middle Class and Residential Segregation. *City & Community*, 3(1), 43–63.
- Ahmadiani, N., Robbins, R. J., Collins, T. M., & Giusti, M. M. (2014). Anthocyanins contents, profiles, and color characteristics of red cabbage extracts from different cultivars and maturity stages. *Journal of Agricultural and Food Chemistry*, 62(30), 7524–7531. <https://doi.org/10.1021/jf501991q>
- Ahmadiani, N., Robbins, R. J., Collins, T. M., & Giusti, M. M. (2016). Molar absorptivity (ϵ) and spectral characteristics of cyanidin-based anthocyanins from red cabbage. *Food Chemistry*, 197, 900–906. <https://doi.org/10.1016/j.foodchem.2015.11.032>
- Alejo-Armijo, A., Parola, A. J., & Pina, F. (2019). pH-Dependent Multistate System Generated by a Synthetic Furanoflavylium Compound: An Ancestor of the Anthocyanin Multistate of Chemical Species. *ACS Omega*, 4, 4091–4100. <https://doi.org/10.1021/acsomega.8b03696>
- Alimahomed-Wilson, J., & Massimo, F. S. (2020). A struggle for bodies and souls: Amazon management and union strategies in France and Italy. In *The Cost of Free Shipping* (pp. 129–144). <https://about.jstor.org/terms>
- Amchova, P., Kotolova, H., & Ruda-Kucerova, J. (2015). Health safety issues of synthetic food colorants. *Regulatory Toxicology and Pharmacology : RTP*, 73(3), 914–922. <https://doi.org/10.1016/J.YRTPH.2015.09.026>
- Andersen, Ø. M., & Fossen, T. (1995). Anthocyanins with an unusual acylation pattern from stem of *Allium victorialis*. *Phytochemistry*, 40(6), 1809–1812. [https://doi.org/10.1016/0031-9422\(95\)90025-Q](https://doi.org/10.1016/0031-9422(95)90025-Q)
- Anliker, R. (1979). Ecotoxicology of dyestuffs—a joint effort by industry. *Ecotoxicology and Environmental Safety*, 3(1), 59–74. [https://doi.org/10.1016/0147-6513\(79\)90060-5](https://doi.org/10.1016/0147-6513(79)90060-5)
- Anliker, R., Moser, P., & Poppinger, D. (1988). Bioaccumulation of dyestuffs and organic pigments in fish. Relationships to hydrophobicity and steric factors. *Chemosphere*, 17(8), 1631–1644. [https://doi.org/10.1016/0045-6535\(88\)90212-3](https://doi.org/10.1016/0045-6535(88)90212-3)

- Bakowska-Barczak, A. (2005). Acylated anthocyanins as stable, natural food colorants : A review. *Polish Journal of Food and Nutrition Sciences*, *14*(2), 107–116.
- Baregheh, A., Rowley, J., & Sambrook, S. (2009). Towards a multidisciplinary definition of innovation. *Management Decision*, *47*(8), 1323–1339. <https://doi.org/10.1108/00251740910984578>
- Basílio, N., & Pina, F. (2016). Chemistry and photochemistry of anthocyanins and related compounds: A thermodynamic and kinetic approach. *Molecules*, *21*(11). <https://doi.org/10.3390/molecules21111502>
- Mansour, H., Houas, I., Montassar, F., Ghedira, K., Barillier, D., Mosrati, R., & Chekir-Ghedira, L. (2012). Alteration of in vitro and acute in vivo toxicity of textile dyeing wastewater after chemical and biological remediation. *Environmental Science and Pollution Research*, *19*(7), 2634–2643. <https://doi.org/10.1007/S11356-012-0802-7>
- Bharagava, R. N., Saxena, G., Mulla, S. I., & Patel, D. K. (2018). Characterization and Identification of Recalcitrant Organic Pollutants (ROPs) in Tannery Wastewater and Its Phytotoxicity Evaluation for Environmental Safety. *Archives of Environmental Contamination and Toxicology*, *75*(2), 259–272. <https://doi.org/10.1007/S00244-017-0490-X>
- Blando, F., Calabriso, N., Berland, H., Maiorano, G., Gerardi, C., Carluccio, M. A., & Andersen, Ø. M. (2018). Radical Scavenging and Anti-Inflammatory Activities of Representative Anthocyanin Groupings from Pigment-Rich Fruits and Vegetables. *International Journal of Molecular Sciences*, *19*(1), 169. <https://doi.org/10.3390/IJMS19010169>
- Block, J. P., Scribner, R. A., & Desalvo, K. B. (2004). Fast food, race/ethnicity, and income: A geographic analysis. *American Journal of Preventive Medicine*, *27*(3), 211–217. <https://doi.org/10.1016/J.AMEPRE.2004.06.007>
- Blumenthal, D., Campbell, E. G., Anderson, M. S., Causino, N., & Louis, K. S. (1997). Withholding Research Results in Academic Life Science: Evidence From a National Survey of Faculty. *JAMA*, *277*(15), 1224–1228. <https://doi.org/10.1001/JAMA.1997.03540390054035>
- Bogahawaththa, D., Buckow, R., Chandrapala, J., & Vasiljevic, T. (2018). Comparison between thermal pasteurization and high pressure processing of bovine skim milk in relation to denaturation and immunogenicity of native milk proteins. *Innovative Food Science & Emerging Technologies*, *47*, 301–308. <https://doi.org/10.1016/J.IFSET.2018.03.016>

- Boulton, R. (2001). The copigmentation of anthocyanins and its role in the color of red wine: A critical review. *American Journal of Enology and Viticulture*, 52(2), 67–87. <https://doi.org/10.1002/9780470988558>
- Brandt, K., & Barrangou, R. (2019). Applications of CRISPR Technologies Across the Food Supply Chain. *Annual Review of Food Science and Technology*, 10, 133–150. <https://doi.org/10.1146/annurev-food-032818>
- Brouillard, R., & Lang, J. (1990). The hemiacetal-cis-chalcone equilibrium of malvin, a natural anthocyanin. *Canadian Journal of Chemistry*, 68, 755–761. www.nrcresearchpress.com
- Brouillard, R., Mazza, G., Saad, Z., Albrecht-Gary, A. M., & Cheminat, A. (1989). The Copigmentation Reaction of Anthocyanins: A Microprobe for the Structural Study of Aqueous Solutions. *Journal of American Chemical Society*, 111(7), 2604–2610.
- Brown, M. A., de Vito, S. C., & Devito, S. C. (1993). Critical Reviews in Environmental Science and Technology Predicting azo dye toxicity Predicting Azo Dye Toxicity. *Critical Reviews in Environmental Science and Technology*, 23(3), 249–324. <https://doi.org/10.1080/10643389309388453>
- Burdge, R. J. (2015). *The Concepts, Process and Methods of Social Impact Assessment*. University Press of Colorado.
- Burdge, R. J., & Robertson, R. A. (1990). Social impact assessment and the public involvement process. *Environmental Impact Assessment Review*, 10(1–2), 81–90. [https://doi.org/10.1016/0195-9255\(90\)90008-N](https://doi.org/10.1016/0195-9255(90)90008-N)
- Burdock, G. A. (1997). *Encyclopedia of Food & Color Additives*. CRC Press, First Edition, 1-3153. <https://doi.org/10.1201/9781498711081>
- Carocho, M., Barreiro, M. F., Morales, P., & Ferreira, I. C. F. R. (2014). Adding molecules to food, pros and cons: A review on synthetic and natural food additives. *Comprehensive Reviews in Food Science and Food Safety*, 13(4), 377–399. <https://doi.org/10.1111/1541-4337.12065>
- Carolan, M. (2016). The sociology of food and agriculture: Second edition. *The Sociology of Food and Agriculture: Second Edition*, 1–348. <https://doi.org/10.4324/9781315670935/SOCIOLOGY-FOOD-AGRICULTURE-MICHAEL-CAROLAN>
- Carr, J. A., D’Odorico, P., Suweis, S., & Seekell, D. A. (2016). What commodities and countries impact inequality in the global food system? *Environmental Research Letters*, 11(9), 095013. <https://doi.org/10.1088/1748-9326/11/9/095013>

- Castañeda-Ovando, A., Pacheco-Hernández, M. de L., Páez-Hernández, M. E., Rodríguez, J. A., & Galán-Vidal, C. A. (2009). Chemical studies of anthocyanins: A review. *Food Chemistry*, 113(4), 859–871. <https://doi.org/10.1016/j.foodchem.2008.09.001>
- Chandrajith, G., Gamage, V., Lim, Y. Y., Choo, W. S. (2022). Sources and relative stabilities of acylated and nonacylated anthocyanins in beverage systems. *Journal of Food Science and Technology*, 59(3), 831–845. <https://doi.org/10.1007/s13197-021-05054-z>
- Chassaing, S., Lefevre, D., Jacquet, R., Jourdes, M., Ducasse, L., Galland, S., Grelard, A., Saucier, C., Teissedre, P. L., Dangles, O., & Quideau, S. (2010). Physicochemical Studies of New Anthocyano-Ellagitannin Hybrid Pigments: About the Origin of the Influence of Oak C-Glycosidic Ellagitannins on Wine Color. *European Journal of Organic Chemistry*, 1, 55–63. <https://doi.org/10.1002/EJOC.200901133>
- Chen, C. C., Lin, C., Chen, M. H., & Chiang, P. Y. (2019). Stability and Quality of Anthocyanin in Purple Sweet Potato Extracts. *Foods*, 8(9), 393. <https://doi.org/10.3390/FOODS8090393>
- Chen, E. (2004). Why Socioeconomic Status Affects the Health of Children A Psychosocial Perspective, *Current Directions in Psychological Science*, 13(3), 112—115.
- Chen, E., Matthews, K. A., & Boyce, W. T. (2002). Socioeconomic differences in children's health: How and why do these relationships change with age? *Psychological Bulletin*, 128(2), 295. <https://doi.org/10.1037/0033-2909.128.2.295>
- Cooper-Driver, G. A. (2001). Contributions of Jeffrey Harborne and co-workers to the study of anthocyanins. *Phytochemistry*, 56(3), 229–236. [https://doi.org/10.1016/S0031-9422\(00\)00455-6](https://doi.org/10.1016/S0031-9422(00)00455-6)
- Cortez, R., Luna-Vital, D. A., Margulis, D., & Gonzalez de Mejia, E. (2017). Natural Pigments: Stabilization Methods of Anthocyanins for Food Applications. *Comprehensive Reviews in Food Science and Food Safety*, 16(1), 180–198. <https://doi.org/10.1111/1541-4337.12244>
- Dangles, O., Saito, N., & Brouillard, R. (1993). Anthocyanin intramolecular copigment effect. *Phytochemistry*, 34(1), 119–124. [https://doi.org/10.1016/S0031-9422\(00\)90792-1](https://doi.org/10.1016/S0031-9422(00)90792-1)
- Davies, A. J., & Mazza, G. (1993). Copigmentation of Simple and Acylated Anthocyanins with Colorless Phenolic Compounds The influence of pH and structure and concentration of copigment and pigment on the copigmentation. *Journal of*

Agricultural and Food Chemistry, 41, 716–720.
<https://pubs.acs.org/sharingguidelines>

- de Campos Ventura-Camargo, B., & Marin-Maroles, M. A. (2013). Azo Dyes: Characterization and Toxicity— A Review. *Textiles and Light Industrial Science and Technology*, 2(2), 85–102.
https://www.researchgate.net/publication/282815745_Azo_Dyes_Characterization_and_Toxicity-_A_Review
- Denish, P. R., Fenger, J.-A., Powers, R., Sigurdson, G. T., Grisanti, L., Guggenheim, K. G., Laporte, S., Li, J., Kondo, T., Magistrato, A., Moloney, M. P., Riley, M., Rusishvili, M., Ahmadiani, N., Baroni, S., Dangles, O., Giusti, M., Collins, T. M., Didzbalis, J., ... Robbins, R. J. (2021). Discovery of a natural cyan blue: A unique food-sourced anthocyanin could replace synthetic brilliant blue. *Science Advances*, 7(7): 1–8. <https://www.science.org>
- Diau, E. W. G. (2004). A New Trans-to-Cis Photoisomerization Mechanism of Azobenzene on the S 1(n,π*) Surface. *Journal of Physical Chemistry A*, 108(6), 950–956.
<https://doi.org/10.1021/JP031149A/ASSET/IMAGES/LARGE/JP031149AH00002.JPEG>
- E. Gläßgen, W., Wray, V., Strack, D., W. Metzger, J., & U. Seitz, H. (1992). Anthocyanins from cell suspension cultures of *Daucus carota*. *Phytochemistry*, 31(5), 1593–1601.
[https://doi.org/10.1016/0031-9422\(92\)83113-D](https://doi.org/10.1016/0031-9422(92)83113-D)
- Eiro, M. J., & Heinonen, M. (2002). Anthocyanin Color Behavior and Stability during Storage: Effect of Intermolecular Copigmentation. *Journal of Agricultural and Food Chemistry*, 50(25), 7461–7466. <https://doi.org/10.1021/JF0258306>
- Eshuis, J., & Stuiver, M. (2005). Learning in context through conflict and alignment: Farmers and scientists in search of sustainable agriculture. *Agriculture and Human Values*, 22(2), 137–148. <https://doi.org/10.1007/s10460-004-8274-0>
- Essabbar, D., Zolghadri, M., & Zrikem, M. (2020). A framework to model power imbalance in supply chains: Situational analysis. *Asia Pacific Management Review*, 25(3), 156–165. <https://doi.org/10.1016/J.APMRV.2019.09.001>
- Fan-Chiang, H. J., & Wrolstad, R. E. (2005). Anthocyanin pigment composition of blackberries. *Journal of Food Science*, 70(3), C198–C202.
<https://doi.org/10.1111/J.1365-2621.2005.TB07125.X>

- Farr, J. E., Sigurdson, G. T., & Giusti, M. M. (2019). Stereochemistry and glycosidic linkages of C3-glycosylations affected the reactivity of cyanidin derivatives. *Food Chemistry*, 278, 443–451. <https://doi.org/10.1016/J.FOODCHEM.2018.11.076>
- Feldmann, M. P., Morris, M. L., & Hoisington, D. (2000). Genetically modified organisms: why all the controversy? *Choices. The Magazine of Food, Farm, and Resources Issues*, No. 1, 8–12. <https://www.cabdirect.org/cabdirect/abstract/20001810786>
- Fenger, J. A., Sigurdson, G. T., Robbins, R. J., Collins, T. M., Giusti, M. M., & Dangles, O. (2021). Acylated anthocyanins from red cabbage and purple sweet potato can bind metal ions and produce stable blue colors. *International Journal of Molecular Sciences*, 22(9), 4551. <https://doi.org/10.3390/ijms22094551>
- Ferreira Da Silva, P., Lima, J. C., Freitas, A. A., Shimizu, K., Maçanita, A. L., & Quina, F. H. (2005). Charge-Transfer Complexation as a General Phenomenon in the Copigmentation of Anthocyanins. *The Journal of Physical Chemistry A.*, 109(32), 7329–7338. <https://doi.org/10.1021/jp052106s>
- Figueiredo, P., George, F., Tatsuzawa, F., Toki, K., Saito, N., & Brouillard, R. (1999). New features of intramolecular copigmentation by acylated anthocyanins. *Phytochemistry*, 51(1), 125–132. [https://doi.org/10.1016/S0031-9422\(98\)00685-2](https://doi.org/10.1016/S0031-9422(98)00685-2)
- Freidberg, S. (2004). *French Beans and Food Scares: Culture and Commerce in an Anxious Age*. Oxford University Press.
- Fuß, W. (2012). Hula-twist cis–trans isomerization: The role of internal forces and the origin of regioselectivity. *Journal of Photochemistry and Photobiology A: Chemistry*, 237, 53–63. <https://doi.org/10.1016/J.JPHOTOCHEM.2012.01.019>
- Gago, S., Basílio, N., Moro, A. J., & Pina, F. (2015). Flavylium based dual photochromism: addressing cis-trans isomerization and ring opening-closure by different light inputs. *Chemical Communications*, 51, 7349. <https://doi.org/10.1039/c5cc01677k>
- Galland, S., Mora, N., Abert-Vian, M., Rakotomanomana, N., & Dangles, O. (2007). Chemical Synthesis of Hydroxycinnamic Acid Glucosides and Evaluation of Their Ability To Stabilize Natural Colors via Anthocyanin Copigmentation. *Journal of Agricultural and Food Chemistry*, 55(18), 7575–7579. <https://doi.org/10.1021/jf071205v>
- García-Beneytez, E., Revilla, E., & Cabello, F. (2002). Anthocyanin pattern of several red grape cultivars and wines made from them. *European Food Research and Technology*, 215(1), 32–37. <https://doi.org/10.1007/S00217-002-0526-X>

- Gavara, R., Gago, S., Noémi Jordã, N., & Pina, F. (2014). *4'-Carboxy-7-hydroxyflavylium. A Multistate System Involving Twelve Species Reversibly Interconverted by pH and Light Stimuli*. *Journal of Physical Chemistry A*, 118(26), 4723–4731. <https://doi.org/10.1021/jp503790z>
- George, F., Figueiredo, P., Toki, K., Tatsuzawa, F., Saito, N., & Brouillard, R. (2001). Influence of trans-cis isomerisation of coumaric acid substituents on colour variance and stabilisation in anthocyanins. *Phytochemistry*, 57(5), 791–795. [https://doi.org/10.1016/S0031-9422\(01\)00105-4](https://doi.org/10.1016/S0031-9422(01)00105-4)
- Gérard, V., Ay, E., Morlet-Savary, F., Graff, B., Galopin, C., Ogren, T., Mutilangi, W., & Lalevée, J. (2019). Thermal and Photochemical Stability of Anthocyanins from Black Carrot, Grape Juice, and Purple Sweet Potato in Model Beverages in the Presence of Ascorbic Acid. *Journal of Agricultural and Food Chemistry*, 67(19), 5647–5660. https://doi.org/10.1021/ACS.JAFC.9B01672/ASSET/IMAGES/LARGE/JF-2019-01672E_0011.JPEG
- Gesch, C. B., Hammond, S. M., & Hampson, S. E. (2002). Influence of supplementary vitamins, minerals, and essential fatty acids on the antisocial behaviour of young adult prisoners. *British Journal of Psychiatry*, 181, 22–28.
- Giusti, M. M., Rodríguez-Saona, L. E., & Wrolstad, R. E. (1999). Molar Absorptivity and Color Characteristics of Acylated and Non-Acylated Pelargonidin-Based Anthocyanins. *Journal of Agricultural and Food Chemistry*, 47(11), 4631–4637. <https://doi.org/10.1021/jf981271k>
- Giusti, M. M., & Wrolstad, R. E. (2001). Characterization and Measurement of Anthocyanins by UV-visible Spectroscopy. In *Handbook of Food Analytical Chemistry*, 2, 19–31. <https://doi.org/10.1002/0471709085.ch18>
- Giusti, M. M., & Wrolstad, R. E. (2003). Acylated anthocyanins from edible sources and their applications in food systems. *Biochemical Engineering Journal*, 14(3), 217–225. [https://doi.org/10.1016/S1369-703X\(02\)00221-8](https://doi.org/10.1016/S1369-703X(02)00221-8)
- Glenna, L. L., Tooker, J., Welsh, J. R., & Ervin, D. (2015). Intellectual Property, Scientific Independence, and the Efficacy and Environmental Impacts of Genetically Engineered Crops. *Rural Sociology*, 80(2), 147–172. <https://doi.org/10.1111/RUSO.12062>
- Glover, D. (2010). The corporate shaping of GM crops as a technology for the poor. *The Journal of Peasant Studies*, 37(1), 67–90. <https://doi.org/10.1080/03066150903498754>

- Goletti, F., & Wolff, C. (1999). The Impact of Postharvest Research. *International Food Policy Research Institute*, 202, 467–4439.
- Goto, T., Kondo, T., Kawai, T., & Tamura, H. (1984). Structure of cinerarin, a tetraacylated anthocyanin isolated from the blue garden cineraria, *Senecio cruentus*. *Tetrahedron Letters*, 25(52), 6021–6024. [https://doi.org/10.1016/S0040-4039\(01\)81749-4](https://doi.org/10.1016/S0040-4039(01)81749-4)
- Gottlieb, R. (2009). Where We Live, Work, Play . . . and Eat: Expanding the Environmental Justice Agenda. *Environmental Justice*, 2(1), 7–8. <https://doi.org/10.1089/ENV.2009.0001>
- Gould, K. S. (2004). Nature's Swiss Army Knife: The Diverse Protective Roles of Anthocyanins in Leaves. *Journal of Biomedicine and Biotechnology*, 2004(5), 314. <https://doi.org/10.1155/S1110724304406147>
- Hamm, M. W., & Bellows, A. C. (2003). Community Food Security and Nutrition Educators. *Journal of Nutrition Education and Behavior*, 35(1), 37–43. https://www.academia.edu/5589948/Community_Food_Security_and_Nutrition_Educators
- Hasselberg, M., Vaez, M., & Lucie Laflamme. (2005). Socioeconomic aspects of the circumstances and consequences of car crashes among young adults. *Social Science & Medicine*, 60(2), 287–295. <https://doi.org/10.1016/J.SOCSCIMED.2004.05.006>
- Hayashi, K., Shinagawa, H., Suzuk, A., & Tsuku, A. (1998). Photo-Isomerization of the Nasunin, the Major Eggplant Anthocyanins. *Food Science and Technology International, Tokyo*, 4(1), 25–28.
- He, J., & Giusti, M. M. (2010). Anthocyanins: Natural Colorants with Health-Promoting Properties. *Annual Review of Food Science and Technology*, 1(1), 163–187. <https://doi.org/10.1146/annurev.food.080708.100754>
- Hodges, R. J., Buzby, J. C., & Bennett, B. (2011). Postharvest losses and waste in developed and less developed countries: opportunities to improve resource use*. *The Journal of Agricultural Science*, 149(S1), 37–45. <https://doi.org/10.1017/S0021859610000936>
- Horspool, W., Lenci, F. CRC Handbook of Organic Photochemistry and Photobiology, Volumes 1 & 2. (2003). *CRC Handbook of Organic Photochemistry and Photobiology, Volumes 1 & 2*. <https://doi.org/10.1201/9780203495902>

- Hoshino, T., Matsumoto, U., Gotot, T., & Harada, N. (1982). Evidence for the Self-association of Anthocyanins IV. PMR Spectroscopic Evidence for the Vertical Stacking of Anthocyanin Molecules. *Tetrahedron Letters*, 23(4), 433–436.
- Hottenrott, H., & Thorwarth, S. (2011). Industry Funding of University Research and Scientific Productivity. *Kyklos*, 64(4), 534–555. <https://doi.org/10.1111/J.1467-6435.2011.00519.X>
- Ichiyanagi, T., Kashiwada, Y., Shida, Y., Ikeshiro, Y., Kaneyuki, T., And, #, & Konishi, T. (2005). *Nasunin from Eggplant Consists of Cis–Trans Isomers of Delphinidin 3-[4-(p-Coumaroyl)-L-rhamnosyl (1f6)glucopyranoside]-5-glucopyranoside*. <https://doi.org/10.1021/jf051841y>
- Jeyaraj, E. J., Lim, Y. Y., & Choo, W. S. (2021). Extraction methods of butterfly pea (*Clitoria ternatea*) flower and biological activities of its phytochemicals. *Journal of Food Science and Technology*, 58(6), 2054–2067. <https://doi.org/10.1007/S13197-020-04745-3/TABLES/2>
- Kloppenburg, J. Ralph. (2004). *First the seed: the political economy of plant biotechnology, 1492-2000*. University of Wisconsin Press.
- Koster, A., Penninx, B. W. J. H., Bosma, H., Kempen, G. I. J. M., Newman, A. B., Rubin, S. M., Satterfield, S., Atkinson, H. H., Ayonayon, H. N., Rosano, C., Yaffe, K., Harris, T. B., Rooks, R. N., van Eijk, J. T., & Kritchevsky, S. B. (2005). Socioeconomic differences in cognitive decline and the role of biomedical factors. *Annals of Epidemiology*, 15(8), 564–571. <https://doi.org/10.1016/J.ANNEPIDEM.2005.02.008>
- La, E. H., & Giusti, M. M. (2022). Ultraviolet–Visible Excitation of cis- and trans-p-Coumaric Acylated Delphinidins and Their Resulting Photochromic Characteristics. *ACS Food Science & Technology*, 2(5), 878–887. <https://doi.org/10.1021/ACSFOODSCITECH.2C00028>
- Leydet, Y., Batat, P., Jonusauskas, G., Denisov, S., Lima, J. C., Parola, A. J., McClenaghan, N. D., & Pina, F. (2013). Impact of water on the cis-trans photoisomerization of hydroxychalcones. *Journal of Physical Chemistry A*, 117(20), 4167–4173. <https://doi.org/10.1021/jp402761j>
- Lin, Y. J., Lee, A., Teng, L. S., & Lin, H. T. (2002). Effect of experimental factors on nitrobenzaldehyde photoisomerization. *Chemosphere*, 48(1), 1–8. [https://doi.org/10.1016/S0045-6535\(02\)00077-2](https://doi.org/10.1016/S0045-6535(02)00077-2)
- Liu, X. M., Jin, X. Y., Zhang, Z. X., Wang, J., & Bai, F. Q. (2018). Theoretical study on the reaction mechanism of the thermal: Cis-trans isomerization of fluorine-substituted

- azobenzene derivatives. *RSC Advances*, 8(21), 11580–11588. <https://doi.org/10.1039/c8ra01132j>
- Lobao, L., & Meyer, K. (2003). The Great Agricultural Transition: Crisis, Change, and Social Consequences of Twentieth Century US Farming. *Annals of the Entomological Society of America*, 27, 103–124. <https://doi.org/10.1146/ANNUREV.SOC.27.1.103>
- Lohachoompol, V., Srzednicki, G., & Craske, J. (2004). The Change of Total Anthocyanins in Blueberries and Their Antioxidant Effect After Drying and Freezing. *Journal of Biomedicine and Biotechnology*, 2004(5), 248. <https://doi.org/10.1155/S1110724304406123>
- Lopes-Da-Silva, F., de Pascual-Teresa, S., Rivas-Gonzalo, J., & Santos-Buelga, C. (2001). Identification of anthocyanin pigments in strawberry (cv Camarosa) by LC using DAD and ESI-MS detection. *European Food Research and Technology*, 214(3), 248–253. <https://doi.org/10.1007/S00217-001-0434-5>
- Louis, K. S., Jones, L. M., Anderson, M. S., Blumenthal, D., & Campbell, E. G. (2001). Entrepreneurship, Secrecy, and Productivity: A Comparison of Clinical and Non-Clinical Life Sciences Faculty. *The Journal of Technology Transfer*, 26(3), 233–245.
- Lui, B. F., Tierce, N. T., Tong, F., Sroda, M. M., Lu, H., Read De Alaniz, J., & Bardeen, C. J. (2019). Unusual concentration dependence of the photoisomerization reaction in donor-acceptor Stenhouse adducts. *Photochemical & Photobiological Sciences*, 18, 1587. <https://doi.org/10.1039/c9pp00130a>
- Malien-Aubert, C., Dangles, O., & Amiot, M. J. (2001). Color Stability of Commercial Anthocyanin-Based Extracts in Relation to the Phenolic Composition. Protective Effects by Intra- and Intermolecular Copigmentation. *Journal of Food and Agricultural Chemistry*, 49(1), 170–176. <https://doi.org/10.1021/jf000791o>
- Mansour, K. A., Fahmy Moustafa, S., Abdelkhalik, S. M., & Brigida, S. (2021). High-Resolution UPLC-MS Profiling of Anthocyanins and Flavonols of Red Cabbage (*Brassica oleracea* L. var. *capitata* f. *rubra* DC.) Cultivated in Egypt and Evaluation of Their Biological Activity. <https://doi.org/10.3390/molecules26247567>
- Marmion, D. M. (1991). Handbook of U.S. Colorants: Foods, Drugs, Cosmetics, and Medical Devices, 3rd Edition. Wiley, 592. <https://www.wiley.com/en-us/Handbook+of+U+S+Colorants%3A+Foods%2C+Drugs%2C+Cosmetics%2C+and+Medical+Devices%2C+3rd+Edition-p-9780471500742>
- Massey, D. S. (2001). America Becoming: Residential Segregation and Neighborhood Conditions in U.S. Metropolitan Areas. *America Becoming: Racial Trends and Their*

- Consequences. In *America Becoming: Vol. I*. National Academies Press.
<https://doi.org/10.17226/9599>
- Mastrodomenico, A., Gorayeb, M., & Paz, J. L. (2012). Collisional Effect of the Solvent on the Optical Responses of a Two Level System. *Journal of Nonlinear Optical Physics & Materials*, 17(2), 213–224. <https://doi.org/10.1142/S0218863508004056>
- Matsufuji, H., Kido, H., Misawa, H., Yaguchi, J., Otsuki, T., Chino, M., Takeda, M., & Yamagata, K. (2007). Stability to Light, Heat, and Hydrogen Peroxide at Different pH Values and DPPH Radical Scavenging Activity of Acylated Anthocyanins from Red Radish Extract. *Journal of Agricultural and Food Chemistry*, 55, 3692–3701. <https://doi.org/10.1021/jf063598o>
- Mayo-Wilson, E., Imdad, A., Herzer, K., Yakoob, M. Y., & Bhutta, Z. A. (2011). Vitamin A supplements for preventing mortality, illness, and blindness in children aged under 5: Systematic review and meta-analysis. *BMJ*, 343(7822). <https://doi.org/10.1136/bmj.d5094>
- Mazza, G., & Brouillard, R. (1987). Recent developments in the stabilization of anthocyanins in food products. *Food Chemistry*, 25(3), 207–225. [https://doi.org/10.1016/0308-8146\(87\)90147-6](https://doi.org/10.1016/0308-8146(87)90147-6)
- McCann, D., et al. (2007). Food additives and hyperactive behavior in 3-year-old and 8/9-year-old children in the community: a randomized, double blinded, placebo-controlled trial. *Lancet*, 370(9598), 1560–1567.
- Merino, E., & Ribagorda, M. (2012). Control over molecular motion using the cis-trans photoisomerization of the azo group. *Beilstein Journal of Organic Chemistry*, 8, 1071–1090. <https://doi.org/10.3762/bjoc.8.119>
- Mori, M., Kondo, T., Toki, K., & Yoshida, K. (2006). Structure of anthocyanin from the blue petals of *Phacelia campanularia* and its blue flower color development. *Phytochemistry*, 67(6), 622–629. <https://doi.org/10.1016/J.PHYTOCHEM.2005.12.024>
- Motta, R. (2014). Social Disputes over GMOs: An Overview. *Sociology Compass*, 8(12), 1360–1376. <https://doi.org/10.1111/SOC4.12229>
- Muntean, M.-V., Marian, O., Barbieru, V., Cătușescu, G. M., Ranta, O., Drocas, I., & Terhes, S. (2016). High Pressure Processing in Food Industry – Characteristics and Applications. *Agriculture and Agricultural Science Procedia*, 10, 377–383. <https://doi.org/10.1016/J.AASPRO.2016.09.077>

- Mulliken, S. (1916). A Method for the Identification of Pure Organic Compounds by a Systematic Analytical Procedure Based on Physical Properties and Chemical Reactions. First Edition. John Wiley & Sons, Inc.
- O’Dea, J. A., & Caputi, P. (2001). Association between socioeconomic status, weight, age and gender, and the body image and weight control practices of 6- to 19-year-old children and adolescents. *Health Education Research*, 16(5), 521–532. <https://doi.org/10.1093/HER/16.5.521>
- O’neill, C., Hawkes, F. R., Hawkes, D. L., Lourenço, N. D., Pinheiro, H. M., & Delée, W. (1999). *Review Colour in textile effluents-sources, measurement, discharge consents and simulation: a review*. [https://doi.org/10.1002/\(SICI\)1097-4660\(199911\)74:11](https://doi.org/10.1002/(SICI)1097-4660(199911)74:11)
- Ormond, K. E., Mortlock, D. P., Scholes, D. T., Bombard, Y., Brody, L. C., Faucett, W. A., Garrison, N. A., Hercher, L., Isasi, R., Middleton, A., Musunuru, K., Shriner, D., Virani, A., & Young, C. E. (2017). Human Germline Genome Editing. *American Journal of Human Genetics*, 101(2), 167–176. <https://doi.org/10.1016/J.AJHG.2017.06.012>
- Palloni, A. (2001). Diffusion in Sociological Analysis. In *Diffusion Processes and Fertility Transition: Selected Perspectives*. National Academies Press (US). <https://www.ncbi.nlm.nih.gov/books/NBK223857/>
- Pina, F. (2014). Chemical Applications of Anthocyanins and Related Compounds. A Source of Bioinspiration. *Journal of Agriculture and Food Chemistry*, 62(29), 6885–6897. <https://doi.org/10.1021/jf404869m>
- Pina, F., Melo, M. J., Ce’sar, C., Laia, A. T., Parola, A. J., & Lima, J. C. (2012). Chemistry and applications of flavylum compounds: a handful of colours. *Chemical Society Reviews*, 41, 869–908. <https://doi.org/10.1039/c1cs15126f>
- Protti, S., Ravelli, D., & Fagnoni, M. (2019). Wavelength dependence and wavelength selectivity in photochemical reactions. *Photochemical and Photobiological Sciences*, 18, 2094. <https://doi.org/10.1039/c8pp00512e>
- Pulido, L. (2015). *Geographies of race and ethnicity*. 39(6), 809–817. <https://doi.org/10.1177/0309132514563008>
- Quant, M., Hamrin, A., Lennartson, A., Erhart, P., & Moth-Poulsen, K. (2019). Solvent Effects on the Absorption Profile, Kinetic Stability, and Photoisomerization Process of the Norbornadiene–Quadricyclanes System Scheme 1. Photoinduced Isomerization and Back-Conversion of the Norbornadiene and Quadricyclane Systems. *Journal of Physical Chemistry C*, 123, 9. <https://doi.org/10.1021/acs.jpcc.9b02111>

- Rakić, V., & Ulrih, N. P. (2021). Influence of pH on color variation and stability of cyanidin and cyanidin 3-O- β -glucopyranoside in aqueous solution. *CyTA-Journal of Food*, 19(1), 174–182. <https://doi.org/10.1080/19476337.2021.1874539>
- Rasberry, C. N., Slade, S., Lohrmann, D. K., & Valois, R. F. (2015). Lessons Learned From the Whole Child and Coordinated School Health Approaches. *Journal of School Health*, 85(11), 759–765. <https://doi.org/10.1111/josh.12307>
- Robinson, T., McMullan, G., Marchant, R., & Nigam, P. (2001). Remediation of dyes in textile effluent: a critical review on current treatment technologies with a proposed alternative. *Bioresource Technology*, 77(3), 247–255. [https://doi.org/10.1016/S0960-8524\(00\)00080-8](https://doi.org/10.1016/S0960-8524(00)00080-8)
- Rodrigues, R. F., da Silva, P. F., Shimizu, K., Freitas, A. A., Kovalenko, S. A., Ernsting, N. P., Quina, F. H., & Maçanita, A. (2009). Ultrafast Internal Conversion in a Model Anthocyanin–Polyphenol Complex: Implications for the Biological Role of Anthocyanins in Vegetative Tissues of Plants. *Chemistry – A European Journal*, 15(6), 1397–1402. <https://doi.org/10.1002/CHEM.200801207>
- Rodriguez-Saona, L. E., & Wrolstad, R. E. (2001). *Current Protocols in Food Analytical Chemistry* (p. F1.1.1-F1.1.11). John Wiley & Sons, Inc.
- Rótolo, G. C., Francis, C., Craviotto, R. M., Viglia, S., Pereyra, A., & Ulgiati, S. (2015). Time to re-think the GMO revolution in agriculture. *Ecological Informatics*, 26(P1), 35–49. <https://doi.org/10.1016/j.ecoinf.2014.05.002>
- Sadilova, E., Stintzing, F. C., & Carle, R. (2006). Anthocyanins, Colour and Antioxidant Properties of Eggplant (*Solanum melongena* L.) and Violet Pepper (*Capsicum annuum* L.) Peel Extracts. *Zeitschrift für Naturforschung C*, (61c), 527-535.
- Saito, N., Tatsuzawa, F., Yazaki, Y., Shigihara, A., & Honda, T. (2007). 7-Polyacylated delphinidin 3,7-diglucosides from the blue flowers of *Leschenaultia* cv. Violet Lena. *Phytochemistry*, 68(5), 673–679. <https://doi.org/10.1016/J.PHYTOCHEM.2006.11.012>
- Sakata, K., Saito, N., & Honda, T. (2006). Ab initio study of molecular structures and excited states in anthocyanidins. *Tetrahedron*, 62, 3721–3731. <https://doi.org/10.1016/j.tet.2006.01.081>
- Saltiel, J., D'Agostino, J. T. (1971). Separation of Viscosity and Temperature Effects on the Singlet Pathway to Stilbene Photoisomerization. *Journal of American Chemical Society*, 94(18), 1265. <https://pubs.acs.org/doi/pdf/10.1021/ja00773a031>

- Saluk, J., Bijak, M., Kołodziejczyk-Czepas, J., Posmyk, M. M., Janas, K. M., & Wachowicz, B. (2012). Anthocyanins from red cabbage extract — evidence of protective effects on blood platelets. *Central European Journal of Biology*, 7(4), 655–663. <https://doi.org/10.2478/S11535-012-0057-9>
- Sari, F. (2016). The Copigmentation Effect of Different Phenolic Acids on *Berberis crataegina* Anthocyanins. *Journal of Food Processing and Preservation*, 40(3), 422–430. <https://doi.org/10.1111/jfpp.12619>
- Schultz, T., Quenneville, J., Levine, B., Toniolo, A., Martínez, T. J., Lochbrunner, S., Schmitt, M., Shaffer, J. P., Zgierski, M. Z., & Stolow, A. (2003). Mechanism and Dynamics of Azobenzene Photoisomerization. *Journal of American Chemical Society*, 125, 44. <https://doi.org/10.1021/ja021363x>
- Selig, M. J., Celli, G. B., Tan, C., La, E., Mills, E., Webley, A. D., Padilla-Zakour, O. I., & Abbaspourrad, A. (2018). High pressure processing of beet extract complexed with anionic polysaccharides enhances red color thermal stability at low pH. *Food Hydrocolloids*, 80, 292–297. <https://doi.org/10.1016/j.foodhyd.2018.01.025>
- Selwyn, B. (2015). Commodity chains, creative destruction and global inequality a class analysis on JSTOR. *Journal of Economic Geography*, 15, 253–274. https://www.jstor.org/stable/26159326#metadata_info_tab_contents
- Sigurdson, G. T., & Giusti, M. M. (2014). Bathochromic and hyperchromic effects of aluminum salt complexation by anthocyanins from edible sources for blue color development. *Journal of Agricultural and Food Chemistry*, 62(29), 6955–6965. <https://doi.org/10.1021/jf405145r>
- Sigurdson, G. T., Robbins, R. J., Collins, T. M., & Giusti, M. M. (2019). Molar absorptivities (ϵ) and spectral and colorimetric characteristics of purple sweet potato anthocyanins. *Food Chemistry*, 271, 497–504. <https://doi.org/10.1016/j.foodchem.2018.07.096>
- Sigurdson, G. T., Tang, P., & Giusti, M. M. (2017). Natural Colorants: Food Colorants from Natural Sources. *Annual Review of Food Science and Technology*, 8(1), 261–280. <https://doi.org/10.1146/annurev-food-030216-025923>
- Sigurdson, G. T., Tang, P., & Giusti, M. M. (2018). Cis-trans configuration of coumaric acid acylation affects the spectral and colorimetric properties of anthocyanins. *Molecules*, 23(3), 598. <https://doi.org/10.3390/molecules23030598>
- Silva, V. O., Freitas, A. A., Maçanita, A. L., & Quina, F. H. (2016). Chemistry and photochemistry of natural plant pigments: the anthocyanins. *Journal of Physical Organic Chemistry*, 29(11), 594–599. <https://doi.org/10.1002/poc.3534>

- Singh, P., Roy, T. K., Kanupriya, C., Tripathi, P. C., Kumar, P., & Shivashankara, K. S. (2022). Evaluation of bioactive constituents of *Garcinia indica* (kokum) as a potential source of hydroxycitric acid, anthocyanin, and phenolic compounds. *LWT*, *156*, 112999. <https://doi.org/10.1016/J.LWT.2021.112999>
- Song, B. J., Sapper, T. N., Burtch, C. E., Brimmer, K., Goldschmidt, M., & Ferruzzi, M. G. (2013). *Photo-and Thermodegradation of Anthocyanins from Grape and Purple Sweet Potato in Model Beverage Systems*. <https://doi.org/10.1021/jf3044007>
- Starfield, B., & Shi, L. (2002). Policy relevant determinants of health: An international perspective. *Health Policy*, *60*(3), 201–218. [https://doi.org/10.1016/S0168-8510\(01\)00208-1](https://doi.org/10.1016/S0168-8510(01)00208-1)
- Stintzing, F. C., Stintzing, A. S., Carle, R., Frei, B., & Wrolstad, R. E. (2002). Color and Antioxidant Properties of Cyanidin-Based Anthocyanin Pigments. *Journal of Agricultural and Food Chemistry*, *50*, 6172–6181. <https://doi.org/10.1021/jf0204811>
- Sveiby, K.-E., Gripenberg, P., Segercrantz, B., Eriksson, A., & Aminoff, A. (2009). Unintended and Undesirable Consequences of Innovation. *XXISPIM Conference on The Future of Innovation*, 21–24.6.
- Takeoka, G. R., Dao, L. T., Full, G. H., Wong, R. Y., Harden, L. A., Edwards, R. H., & Berrios, J. D. J. (1997). Characterization of Black Bean (*Phaseolus vulgaris* L.) Anthocyanins. *Journal of Agricultural and Food Chemistry*, *45*(9), 3395–3400. <https://doi.org/10.1021/JF970264D/ASSET/IMAGES/LARGE/JF970264DF00005.JPEG>
- Tang, P. (2018). *Petunidin Derivatives from Black Goji and Purple Potato as Promising Natural Colorants, and Their Co-pigmentation with Metals and Isoflavones*. The Ohio State University, Doctor of Philosophy Dissertation.
- Tatsuzawa, F. (2019). Acylated pelargonidin glycosides from the red-purple flowers of *Iberis umbellata* L. and the red flowers of *Erysimum × cheiri* (L.) Crantz (Brassicaceae). *Phytochemistry*, *159*, 108–118. <https://doi.org/10.1016/J.PHYTOCHEM.2018.12.010>
- Taylor, D. E., & Ard, K. J. (2015a). Detroit’s food justice and food systems. *Focus*, *32*(1). <https://www.irp.wisc.edu/publications/focus/pdfs/foc321c.pdf>
- Taylor, D. E., & Ard, K. J. (2015b). Food Availability and the Food Desert Frame in Detroit: An Overview of the City’s Food System. *Environmental Practice*, *17*(2), 102–133. <https://doi.org/10.1017/S1466046614000544>

- Terahara, N., Saito, N., Honda, T., Toki, K., & Osajima, Y. (1989). Structure of ternatin D1, an acylated anthocyanin from *Clitoria ternatea* flowers. *Tetrahedron Letters*, 30(39), 5305–5308. [https://doi.org/10.1016/S0040-4039\(01\)93771-2](https://doi.org/10.1016/S0040-4039(01)93771-2)
- Thompson, J., & Scoones, I. (2009). Addressing the dynamics of agri-food systems: an emerging agenda for social science research. *Environmental Science & Policy*, 12(4), 386–397. <https://doi.org/10.1016/j.envsci.2009.03.001>
- Thyberg, K. L., & Tonjes, D. J. (2016). Drivers of Food Wastage and their Implications for Sustainable Policy Development. *Technology & Society Faculty Publications*, 106, 110–123. <https://doi.org/dx.doi.org/10.1016/j.resconrec.2015.11.016>
- Toki, K., Saito, N., Ueda, T., Chibana, T., Shigihara, A., & Honda, T. (1994). Malvidin 3-glucoside-5-glucoside sulphates from *Babiana stricta*. *Phytochemistry*, 37(3), 885–887. [https://doi.org/10.1016/S0031-9422\(00\)90377-7](https://doi.org/10.1016/S0031-9422(00)90377-7)
- Trouillas, P., Sancho-García, J. C., de Freitas, V., Gierschner, J., Otyepka, M., & Dangles, O. (2016). Stabilizing and Modulating Color by Copigmentation: Insights from Theory and Experiment. *Chemical Reviews*, 116(9), 4937–4982. <https://doi.org/10.1021/acs.chemrev.5b00507>
- Turner, L. B., Mueller-Harvey, I., & McAllan, A. B. (1993). Light-induced isomerization and dimerization of cinnamic acid derivatives in cell walls. *Phytochemistry*, 33(4), 791–796. [https://doi.org/10.1016/0031-9422\(93\)85276-W](https://doi.org/10.1016/0031-9422(93)85276-W)
- Turro, N. J., Ramamurthy, V., Cherry, W., & Farneth, W. (1978). The Effect of Wavelength on Organic Photoreactions in Solution. Reactions from Upper Excited States. *Chemical Reviews*, 78(2), 125–145. <https://pubs.acs.org/doi/10.1021/cr60312a003>
- Vidana Gamage, G. C., Lim, Y. Y., & Choo, W. S. (2022). Sources and relative stabilities of acylated and nonacylated anthocyanins in beverage systems. *Journal of Food Science and Technology*, 59(3), 831–845. <https://doi.org/10.1007/S13197-021-05054-Z/FIGURES/5>
- Waldeck, D. H. (1991a). Photoisomerization Dynamics of Stilbenes. In *Chem. Rev* (Vol. 91). <https://pubs.acs.org/sharingguidelines>
- Wallace, T. C., & Giusti, M. M. (2015). Anthocyanins. *Advances in Nutrition*, 6(5), 620–622. <https://doi.org/10.3945/an.115.009233>
- Waltz, E. (2016). Gene-edited CRISPR mushroom escapes US regulation. *Nature News*, 293.

https://www.nature.com/news/polopoly_fs/1.19754!/menu/main/topColumns/topLeftColumn/pdf/nature.2016.19754.pdf

- Wardle, J., Jarvis, M. J., Steggle, N., Sutton, S., Williamson, S., Farrimond, H., Cartwright, M., & Simon, A. E. (2003). Socioeconomic disparities in cancer-risk behaviors in adolescence: baseline results from the Health and Behaviour in Teenagers Study (HABITS). *Preventive Medicine*, 36(6), 721–730. [https://doi.org/10.1016/S0091-7435\(03\)00047-1](https://doi.org/10.1016/S0091-7435(03)00047-1)
- Weisburger, J. H. (2002). Comments on the history and importance of aromatic and heterocyclic amines in public health. *Mutation Research/Fundamental and Molecular Mechanisms of Mutagenesis*, 506–507, 9–20. [https://doi.org/10.1016/S0027-5107\(02\)00147-1](https://doi.org/10.1016/S0027-5107(02)00147-1)
- Wield, D., Chataway, J., & Bolo, M. (2010). *Issues in the Political Economy of Agricultural Biotechnology*. <https://doi.org/10.1111/j.1471-0366.2010.00274.x>
- Wiles, N. J., Northstone, K., Emmett, P., & Lewis, G. (2009). ‘Junk food’ diet and childhood behavioural problems: results from the ALSPAC cohort. *European Journal of Clinical Nutrition*, 63, 491–498. <https://doi.org/10.1038/sj.ejcn.1602967>
- Wu, X., Beecher, G. R., Holden, J. M., Haytowitz, D. B., Gebhardt, S. E., & Prior, R. L. (2006). *Concentrations of Anthocyanins in Common Foods in the United States and Estimation of Normal Consumption*. 54, 4069–4075. <https://doi.org/10.1021/jf0603001>
- Yoshida, K., Kondo, T., & Goto, T. (1992). Intramolecular stacking conformation of gentiodelphin, a diacylated anthocyanin from *Gentiana makinoi*. *Tetrahedron*, 48(21), 4313–4326. [https://doi.org/10.1016/S0040-4020\(01\)80442-7](https://doi.org/10.1016/S0040-4020(01)80442-7)
- Yoshida, K., Kondo, T., Kameda, K., & Goto, T. (1990). Structure of Anthocyanins Isolated from Purple Leaves of *Perilla ocimoides* L. var. *crispa* Benth and Their Isomerization by Irradiation of Light. *Agricultural and Biological Chemistry*, 54(7), 1745–1751.
- Yoshida, K., Okuno, R., Kameda, K., & Kondo, T. (2002). Prevention of UV-light induced E,Z-isomerization of caffeoyl residues in the diacylated anthocyanin, gentiodelphin, by intramolecular stacking. *Tetrahedron Letters*, 43(35), 6181–6184. [https://doi.org/10.1016/S0040-4039\(02\)01319-9](https://doi.org/10.1016/S0040-4039(02)01319-9)
- Yoshida, K., Okuno, R., Kameda, K., Mori, M., & Kondo, T. (2003). Influence of E,Z-isomerization and stability of acylated anthocyanins under the UV irradiation. *Biochemical Engineering Journal*, 14(3), 163–169. [https://doi.org/10.1016/S1369-703X\(02\)00217-6](https://doi.org/10.1016/S1369-703X(02)00217-6)

- Zhao, C. L., Chen, Z. J., Bai, X. S., Ding, C., Long, T. J., Wei, F. G., & Miao, K. R. (2014). Structure-activity relationships of anthocyanidin glycosylation. *Molecular Diversity*, 18(3), 687–700. <https://doi.org/10.1007/S11030-014-9520-Z/TABLES/2>
- Zhao, C. L., Wen, G. S., Mao, Z. C., Xu, S. Z., Liu, Z. J., Zhao, M. F., & Lin, C. (2015). Molecular structures of the stem tuber anthocyanins of colored potatoes and their coloring effects on the tubers. *Natural Product Communications*, 10(3), 461–466. <https://doi.org/10.1177/1934578X1501000322>
- Zhao, C. L., Yu, Y. Q., Chen, Z. J., Wen, G. S., Wei, F. G., Zheng, Q., Wang, C. de, & Xiao, X. L. (2017). Stability-increasing effects of anthocyanin glycosyl acylation. *Food Chemistry*, 214, 119–128. <https://doi.org/10.1016/j.foodchem.2016.07.073>
- Zheng, J., Ding, C., Wang, L., Li, G., Shi, J., Li, H., Wang, H., & Suo, Y. (2011). Anthocyanins composition and antioxidant activity of wild *Lycium ruthenicum* Murr. from Qinghai-Tibet Plateau. *Food Chemistry*, 126, 859–865. <https://doi.org/10.1016/j.foodchem.2010.11.052>
- Zhou, Y. (2021). Comparing the biochemical compositions of fruits from the *Sambucus* species and the color expression of their anthocyanin extracts as modulated by UV irradiation. The Ohio State University, Doctor of Philosophy Dissertation.
- Zhou, Y., Gao, Y. G., & Giusti, M. M. (2020). Accumulation of anthocyanins and other phytochemicals in american elderberry cultivars during fruit ripening and its impact on color expression. *Plants*, 9(12), 1–14. <https://doi.org/10.3390/plants9121721>
- Zimmerman, A. A., Orlando, C. M., Gianni, M. H. (1969). Concentration Effects in Photochemical cis-trans Isomerization. A Study of Difurylethylene and Dithienylethylene. *The Journal of Organic Chemistry*, 34(1), 73–77.

